THE OPTICAL POLARIZATION OF QUASI-STELLAR AND BL LACERTAE OBJECTS

by

Richard Lee Moore

A Dissertation Submitted to the Faculty of the

DEPARTMENT OF ASTRONOMY

In Partial Fulfillment of the Requirements
For the Degree of

DOCTOR OF PHILOSOPHY

In the Graduate College

THE UNIVERSITY OF ARIZONA

1 9 8 1

MOORE, RICHARD LEE

THE OPTICAL POLARIZATION OF QUASI-STELLAR AND BL LACERTAE OBJECTS

The University of Arizona PH.D. 1981

PLEASE NOTE:

In all cases this material has been filmed in the best possible way from the available copy. Problems encountered with this document have been identified here with a check mark ✓.

1. Glossy photographs or pages _____
2. Colored illustrations, paper or print _____
3. Photographs with dark background _____
4. Illustrations are poor copy _____
5. Pages with black marks, not original copy _____
6. Print shows through as there is text on both sides of page _____
7. Indistinct, broken or small print on several pages _____
8. Print exceeds margin requirements _____
9. Tightly bound copy with print lost in spine _____
10. Computer printout pages with indistinct print ✓
11. Page(s) _____ lacking when material received, and not available from school or author.
12. Page(s) _____ seem to be missing in numbering only as text follows.
13. Two pages numbered _____. Text follows.
14. Curling and wrinkled pages _____
15. Other _____

University
Microfilms
International

THE OPTICAL POLARIZATION OF QUASI-STELLAR AND BL LACERTAE OBJECTS

by

Richard Lee Moore

A Dissertation Submitted to the Faculty of the

DEPARTMENT OF ASTRONOMY

In Partial Fulfillment of the Requirements
For the Degree of

DOCTOR OF PHILOSOPHY

In the Graduate College

THE UNIVERSITY OF ARIZONA

1 9 8 1

THE UNIVERSITY OF ARIZONA
GRADUATE COLLEGE

As members of the Final Examination Committee, we certify that we have read the dissertation prepared by Richard Lee Moore

entitled "The Optical Polarization of Quasi-Stellar and BL Lacertae Objects"

and recommend that it be accepted as fulfilling the dissertation requirement for the Degree of Doctor of Philosophy.

Henry J. Stockton	Jan 9 1981 Date
P. A. Strittmatter	Jan 9, 1981 Date
Ray J. Weymann	Jan 9, 1981 Date
Lawrence Aller	Jan 9, 1981 Date
J. N. P. Angel	Jan 9 81 Date

Final approval and acceptance of this dissertation is contingent upon the candidate's submission of the final copy of the dissertation to the Graduate College.

I hereby certify that I have read this dissertation prepared under my direction and recommend that it be accepted as fulfilling the dissertation requirement.

J. N. P. Angel	1/13/81
Dissertation Director	Date

STATEMENT BY AUTHOR

This dissertation has been submitted in partial fulfillment of requirements for an advanced degree at The University of Arizona and is deposited in the University Library to be made available to borrowers under rules of the Library.

Brief quotations from this dissertation are allowable without special permission, provided that accurate acknowledgment of source is made. Requests for permission for extended quotation from or reproduction of this manuscript in whole or in part may be granted by the head of the major department or the Dean of the Graduate College when in his judgment the proposed use of the material is in the interests of scholarship. In all other instances, however, permission must be obtained from the author.

SIGNED: Richard L. Moore

ACKNOWLEDGMENTS

I sit here and think about all the people who have been teachers and friends during these last four years, and realize there are many people who have contributed to my personal and professional growth during this arduous process. Although it is often difficult to identify the ways in which these people have contributed to me, I feel their influence and I want to take this opportunity to thank them.

I want to sincerely thank my advisor, Roger Angel, for all he has taught me. I consider Roger to be primarily responsible for my making the crucial transition from an astronomy graduate student to an astronomer. It has been a pleasure to work with Roger. His genuine enthusiasm, extensive knowledge, and insightful ideas have been inspiring and motivating.

I would also like to thank Pete Stockman, with whom I have collaborated on much of the QSO polarimetry research. We have spent innumerable hours together discussing this research; he has generously shared his observations and ideas. His help is greatly appreciated.

I have benefitted from interactions with nearly all the Steward Observatory faculty. I would make special mention of Andrezj Pacholczyk, Peter Strittmatter, Ray Weymann, and Bob Williams; their teaching and interest in my research have been of great help. I would note that this project would have been impossible without continued support of the telescope scheduling committee, who have allotted generous amounts of time.

The camaraderie among my fellow graduate students has been a constant source of scientific exchange and personal support. I have enjoyed numerous talks with Joe Davila, Brad Peterson, and Gary Schmidt. I would particularly like to thank Mark Adams; I value highly his friendship and all the support he has given me.

I am indebted to several friends for reminding me that astronomy is not all there is to life. The times I have shared with Ann Leenhouts, Roberta Matteson, David Quantz, Alice Tocco and others are invaluable.

Finally, I give special thanks to my wife, Nancy Henricks. She has devotedly helped me while I have written this dissertation - patiently tolerating my preoccupation, calmly listening to my ravings, and cooking excellent dinners. Most important, the love and support she has given me the last two years have awakened in me the long-lost inner smile. To Nan, I dedicate this work.

TABLE OF CONTENTS

TABLE OF CONTENTS--Continued

LIST OF ILLUSTRATIONS

LIST OF ILLUSTRATIONS--Continued

LIST OF ILLUSTRATIONS--Continued

LIST OF TABLES

ABSTRACT

In this dissertation, I examine the optical linear polarization of quasi-stellar objects (QSOs) and BL Lacertae objects. I present extensive polarimetric observations of a large sample of QSOs, systematically analyze the correlations between polarization and other properties of QSOs, compare the properties of QSOs and BL Lac objects, and discuss the implications of these results for theoretical models.

The large high-accuracy polarization survey which is presented establishes that the majority of radio-loud QSOs ($\sim$ 85%) and essentially all radio-quiet QSOs have low polarization ($P < 2\%$), and that there is a discontinuity in the distribution of polarization between these QSOs and the rare highly polarized ($P > 3\%$) QSOs. A physical distinction between "normal" low polarization QSOs and highly polarized QSOs (HPQs) is apparent not only in the polarization distribution, but also in the polarimetric variability and wavelength dependence. Normal QSOs exhibit little evidence of polarimetric variability over time scales of years, and the polarization appears to increase at shorter wavelengths. In contrast, the HPQs show strong rapid ($\tau \sim$ days) variability and the polarization is more nearly wavelength independent.

Systematic analyses of the correlations between polarization and other properties of QSOs also indicate a physical distinction between normal QSOs and HPQs. It is shown that high polarization is correlated with rapid, large-amplitude photometric variability, relatively steep,

smooth optical/infrared continua, a high ratio of X-ray to optical emission, compact radio structure, and extreme properties such as low-frequency variability and superluminal expansion. Other correlation analyses demonstrate that normal QSOs and HPQs are still related phenomena; the distributions of redshift, optical luminosity, and emission line equivalent width are similar for normal QSOs and HPQs.

The characteristics established for the class of HPQs clearly demonstrate that HPQs and BL Lac objects are intimately related. However, HPQs also exhibit some properties (e.g. strong emission lines) characteristic of normal QSOs. Thus, the HPQs represent a crucial link between the QSO and BL Lac phenomena.

The origins of the optical polarized emission in BL Lac objects, HPQs, and normal QSOs are examined. The high, wavelength-independent polarization and power law energy distribution observed in HPQs and BL Lac objects suggest that the continuum is synchrotron radiation. Scattering in an asymmetric geometry may be responsible for the polarization of normal QSOs.

I discuss the implications of these results for two types of theoretical models. In the first model, it is assumed that the emission is isotropic and not relativistically enhanced. This implies that the tremendous luminosities ($L \leqslant 10^{15} L_{\odot}$) from the rapidly variable HPQs (and BL Lac objects) are produced in a central engine only light-days across. In normal QSOs, this central emission must be obscured and reprocessed by surrounding material. Theoretical constraints concerning the central engine are presented, and it is shown that rapid reacceleration of electrons to relativistic energies is required.

Although the "isotropic" model described above cannot be ruled out, the characteristics of the HPQs suggest an alternative "anisotropic" model in which the variable highly polarized emission is produced in a jet oriented along our line-of-sight. Relativistic enhancement of this emission eases restrictions imposed by the high apparent luminosity and rapid variability of HPQs and BL Lac objects. In normal QSOs, the jet is oriented away from us and only the isotropic component of QSO emission (e.g. low polarization continuum and emission lines) is visible. This model readily accounts for many of the observed properties of normal QSOs, HPQs, and BL Lac objects. However, two important predictions of this model, that the HPQs should be systematically more luminous and have weaker emission lines than normal QSOs, are not supported by my results.

CHAPTER I

INTRODUCTION

A. Historical Perspective

Soon after the identification of strong radio sources with high redshift quasi-stellar objects (QSOs), optical polarization measurements were made to search for nonthermal optical emission. The first QSOs identified, 3CR 48 and 3CR 273, were observed to have low but significant linear polarization (Matthews and Sandage 1963, Whiteoak 1966, see also Liller 1969). Within a few years Kinman and collaborators discovered high polarization ($P > 10\%$) and rapid variability in the QSOs 3C 446 (Kinman, Lamla, and Wirtanen 1966), 3C 279 (Kinman 1967), and 3CR 345 (Kinman et al. 1968); Visvanathan (1968) also discovered high polarization in 3CR 454.3. Three small polarization surveys of bright QSOs were made during the late 1960s by Kinman (1967), Appenzeller and Hiltner (1967), and Visvanathan (1968); a total of thirty QSOs were surveyed. Although only the four QSOs mentioned above clearly showed high polarization, the remainder of the QSOs observed appeared to exhibit some polarization ($P \sim 1 - 4\%$). The measurements were generally not accurate enough to unambiguously measure polarizations of less than a few percent. The conclusion drawn from these early polarization observations was that QSOs exhibited some linear polarization. This was taken, together with the (approximately) power law energy distribution of the optical continuum, as support for a nonthermal origin for the emission.

Since they were discovered, the four known highly polarized QSOs have been the focus of extensive observations at both optical and radio wavelengths. Optical photometric monitoring has shown them to be "optically-violent variables (OVVs)", i.e., to exhibit rapid ($\tau \sim$ days) large amplitude ($\Delta m \geq 2$ mag) variability (see references in Grandi and Tifft 1974). The optical polarization and energy distribution of these objects was comprehensively studied by Visvanathan (1973). He concluded that the energy distributions are relatively steep power laws (see also Oke, Neugebauer, and Becklin 1970) and are rapidly variable. The polarization is also rapidly variable and is roughly wavelength independent. Radio observations have revealed that these objects are all compact, flat spectrum, variable sources (see references in Moore and Stockman 1981). Two of these QSOs, 3C 279 and 3CR 345, have exhibited superluminal expansion in their radio structure (e.g., Cohen et al. 1977). Another of these objects, 3CR 454.3, is a low-frequency radio variable (Hunstead 1972). Clearly, the unusual nature of these QSOs involves not only their high optical polarization, but also nearly every observable quantity.

Another class of objects, the BL Lacertae objects, was discovered soon after QSOs were identified (see Stein, O'Dell, and Strittmatter 1976). The distinguishing feature of BL Lac objects is the lack of emission lines in the optical spectrum. High optical polarization was first observed in BL Lac objects by Visvanathan (1969); subsequent polarimetry has shown that high variable polarization is a common property of all BL Lac objects (e.g. Strittmatter et al. 1972,

Kinman 1976, Angel et al. 1978, and references in Angel and Stockman 1980). Generally, BL Lac objects exhibit a number of other common properties: rapid, large amplitude photometric variability, steep power law optical continua, flat variable radio spectra, and compact radio structure (Stein, O'Dell and Strittmatter 1976, Angel and Stockman 1980).

It is readily apparent from this general description that the continuum properties of BL Lac objects are strikingly similar to the properties of the known highly polarized QSOs. The highly polarized QSOs share properties of both QSOs and BL Lac objects, and represent the strongest evidence for a relationship between the two phenomena.

Observations of the highly polarized objects (both QSOs and BL Lac objects) are of profound theoretical significance. If the variability time scale is comparable to the light-travel time across the emission region, these rapidly variable objects allow us the closest look at the compact ($\sim$ light-days) central energy source. The dimensions probed by optical variability studies are several orders of magnitude smaller than those observed with VLBI measurements. A basic theoretical problem presented by these objects is to explain how the apparently tremendous luminosities ($L \lesssim 10^{15}\ L_\odot$) are produced in a volume of dimensions $\lesssim 10^{-3}$ pc. Clearly the rapid variability, as well as other extreme properties such as superluminal expansion, strain "conservative" source models; numerous explanations have been proposed including noncosmological redshifts, nonisotropic emission, and bulk relativistic motion.

The optical polarization has played a significant role in establishing the connection between QSOs and BL Lac objects, and in suggesting that the optical continua of these objects may be synchrotron emission. By the late 1970s, a fairly simple picture had emerged of the polarization characteristics of QSOs and BL Lac objects. Some QSOs and all BL Lac objects are highly polarized and variable; these objects share numerous other continuum properties. The remainder of QSOs have lower polarization.

Although this simple picture of the optical polarization of QSOs and BL Lac objects is (as we will show here) basically correct, it is far from complete. Very few QSOs had been observed polarimetrically; at the time this project was initiated, polarization measurements were available for only 35 QSOs (Burbidge, Crowne, and Smith 1977). In addition most of these measurements were subject to strong instrumental effects and were generally not accurate enough to define the polarization of QSOs unless they were highly polarized. Thus, the actual amount of polarization, even in those QSOs which had been observed, was generally unknown. Essentially nothing was known about the variability or wavelength dependence of polarization in these lower polarization QSOs. Almost no polarization measurements had been made of radio-quiet QSOs, even though they constitute the great majority of QSOs.

There was a relatively large amount of data available concerning the four known highly polarized QSOs. However, despite the observational and theoretical significance of this class of objects,

no new members of this class had been discovered since 1968. Any discussion of the general properties of this class was inherently limited by the fact that only four examples were known. Polarization surveys which had been made were neither systematic nor large enough to determine the fraction of QSOs which are highly polarized. The small number known limited the scope of questions which could be posed such as whether high polarization is correlated with redshift or luminosity. Certainly these four objects exhibit a number of properties in common aside from their high polarization. However, the nature of the correlations between high polarization and other characteristics had not been systematically examined. For example, are all OVV QSOs highly polarized? Are all highly polarized QSOs compact radio sources? Are there continuous correlations, for example, in the sense that QSOs with steeper optical continua have gradually higher polarization? The comparison of the properties of highly polarized QSOs and BL Lac objects was also limited by the small size of the class. Thus, even though extensive observations had been made, numerous questions remained.

Finally, relatively few monitoring programs were available which carefully documented the short-term variability of the rapidly variable highly polarized objects. It is crucial to determine the minimum time scales of variability as this is the only means of estimating the size of the emission region. In addition to determining the size, the nature of the variability can provide clues to the physical characteristics of the central emission region.

B. Objectives of this Study

The basic objective of this research is to examine the polarization of QSOs and BL Lac objects. This objective includes making measurements of the polarization, determining the correlations between polarization and other observed properties of these objects, and discussing the theoretical implications of these results. The majority of this research concerns the polarization of QSOs. As we will show, the polarimetric characteristics of BL Lac objects are relevant to the polarization of QSOs and these will be discussed.

The initial objective is to observationally define the general polarimetric properties of QSOs. First, the distribution of polarization for both radio-loud and radio-quiet QSOs is to be determined. These distributions were unknown except to the extent that some radio-loud QSOs are highly-polarized while others have lower polarization. We also examine the variability and wavelength dependence of polarization for both high and low polarization QSOs.

The second objective is to establish in a systematic manner the correlations between polarization and other properties of QSOs. Some of the correlations to be examined are motivated by the properties of the previously known highly polarized QSOs; however, the tests of these correlations are carried out systematically so as to establish the nature of the correlations rather than to draw *post facto* conclusions. The properties which will be discussed are the radio luminosity (only in terms of objects being radio-loud or radio-quiet), the redshift, the optical luminosity, the optical photometric variability

(both amplitude and time scale of variability), the spectral index of the optical continuum, the emission line strength (in terms of the equivalent width of Mg II), the X-ray luminosity, the ratio of optical to X-ray luminosity, and the structure of extended radio emission.

It is expected that in the course of fulfilling the two initial objectives above, additional highly polarized QSOs will be discovered. This is certainly a major objective of this research. Additional examples are necessary to establish the properties of the class. With a larger sample of highly polarized QSOs available, it is also intended to compare their properties with those of BL Lac objects.

The final observational objective is to intensively monitor the short-term polarimetric and photometric variability of selected highly polarized objects in order to determine the time scale and nature of this variability.

Completion of these observational objectives represents a major step towards understanding the nature of the polarization and its relationship to other properties of QSOs and BL Lac objects. The picture which emerges is far more complete than any previous study has presented. With this observational basis, the final objective is to discuss the theoretical implications of our results for various models of QSOs and BL Lac objects.

C. Overview of Contents

In order to accomplish the three initial observational objectives above, we have made extensive observations of a large number of QSOs. In Chapter II, the sample selection and methods of observations are described. Three samples of QSOs have been constructed; the criteria for each of these samples are specifically described in Chapter II. The first sample is comprised of all bright northern QSOs, and is designed to determine the general distribution of polarization for both radio-loud and radio-quiet QSOs. Two other QSO samples have been compiled with the intent of testing the correlations between high polarization and violent variability and steep optical continua, as suggested in the original HPQs. In total, 231 QSOs have been surveyed for their optical polarization. This represents more than a sixfold increase in the number of QSOs for which polarization measurements are available. In order to test the correlations between polarization and other properties of QSOs, we have researched the literature and compiled other relevant data concerning the QSOs in our samples; these data are also described in Chapter II.

The characteristics of the polarization of QSOs are described in Chapter III. More than 560 polarimetric observations of the 231 QSOs are presented. The typical accuracies of these measurements are $\sigma_p \sim 0.2 - 0.6\%$. Accuracies of this order are significantly better than those of previous surveys and, as we will show, are necessary to reasonably determine the polarization of most QSOs. Two or more observations have been made of 100 QSOs in order to determine the

variability of polarization. Two-color wavelength dependence measurements have been made of 26 QSOs.

The results of these measurements show that the great majority of QSOs have very low optical polarization ($P \lesssim 1\%$). The distribution of polarization is not continuous at higher polarizations ($P > 2\%$); there is a relatively clear distinction between high and low polarization QSOs. The majority of radio-loud QSOs and essentially all radio-quiet QSOs have low polarization. If the highly polarized QSOs (hereafter, HPQs) are excluded, there are no significant polarimetric differences between radio-loud and radio-quiet QSOs. Since nearly all QSOs have low polarization, we will often refer to low polarization QSOs as "normal" QSOs. The polarization of normal QSOs is generally constant over time scales of years. The polarization appears to be slightly higher at shorter wavelengths.

As a direct result of these surveys, we have discovered fourteen new QSOs which are definitely highly polarized and five possible HPQs. With the original four HPQs and three HPQs recently discovered by other authors, the number of HPQs now known is at least twenty-one (with six additional possible HPQs). This represents a dramatic increase in the size of the sample of HPQs and is, in itself, a major contribution of this research. With one exception, all of the HPQs are radio-loud QSOs. The polarimetric characteristics of the HPQs are markedly different from normal QSOs. Generally, the polarization is wavelength independent and varies dramatically over typical time scales of a few days.

The correlations between optical polarization and other properties of QSOs are presented and discussed in Chapter IV. The primary emphasis of these tests is to examine the properties of QSOs where the polarization is regarded simply as "on" (high polarization) or "off" (low polarization). The evidence for continuous correlations is also discussed. A complete summary of these results is deferred to Chapter IV; the previously suspected correlations, based on the original four HPQs, are generally confirmed.

A fundamental conclusion emerges from these extensive surveys and systematic correlation analyses. With some reservations, there are two fairly distinct types of QSOs which can be distinguished simply on the basis of their optical polarization. Normal low polarization QSOs exhibit moderate photometric variability, have relatively hard and "bumpy" optical/infrared continua, and may be either radio-loud or radio-quiet. The rare HPQs are extremely variable, have steep power law optical continua, are generally compact radio sources, and probably have a higher ratio of X-ray to optical luminosity. The physical phenomena represented by these two types of QSOs are still related. This is evidenced by the similarity of other characteristics of the two classes (e.g. the redshifts, the optical luminosities, and the emission line strengths).

The distinctive properties of the HPQs lead us into a discussion of the properties of BL Lac objects and their relationship to the HPQs. In Chapter V we discuss the polarimetric properties and other emission characteristics of BL Lac objects. These properties are compared to

the HPQs, using the much larger sample of HPQs now available. It is clear that the continua of HPQs and BL Lac objects are very similar. The HPQs, by exhibiting properties of both normal QSOs and BL Lac objects, do provide the crucial link between these two phenomena.

In Chapter VI we present two examples of intensive monitoring of rapidly variable objects. These monitoring programs provide well-documented examples of the nature and time scales of polarimetric and photometric variability. The first object, B2 1308+326, was observed during a very high luminosity phase and found to have a variability time scale of one day. This object represents one of the most extreme examples of high luminosity and rapid variability. The second monitoring program is an unprecedented worldwide effort to carefully track the variability of BL Lacertae for ten days. Both photometric and polarimetric observers, located on three continents, monitored BL Lacertae for up to 20 hours per day, thus filling in the large daily monitoring gaps which plague single telescope monitoring of objects with typical time scales of $\sim$1 day.

We conclude in Chapter VII with a discussion of the theoretical implications of the observational results obtained. The possible sources of polarized emission in normal QSOs and highly polarized objects are discussed. Several models to account for the three classes of objects (normal QSOs, HPQs, and BL Lac objects) are presented. The simplest interpretation is that the three classes have a similar central "engine", but that the rapidly variable objects are

"naked" and thus the emission from this central region is visible. In normal QSOs, the central emission is obscured, reprocessed, and depolarized. The greatest difficulty of this model is that mentioned earlier in this chapter: how the tremendous luminosity is produced (and the emission not depolarized) in the compact central engine. The theoretical constraints which can be imposed on such a model are presented. An alternative model in which our orientation with respect to a relativistic jet determines the type of object observed is also discussed. The observational predictions of these models are discussed, both in terms of the results obtained here and further observational tests.

It is important to note the collaborations which have contributed to this work and the publications in which the results have been or will be presented. Drs. H. S. Stockman and J. R. P. Angel initiated the broadband survey of bright QSOs; preliminary results of this survey have been published by Stockman and Angel (1978) and Stockman (1978). I have contributed survey, variability, and wavelength dependence observations of these objects and have analyzed the final results. All data for the bright survey QSOs and a discussion of the polarimetric properties of low polarization QSOs will be presented by Stockman, Moore, and Angel (Ap. J., in preparation). Further samples of QSOs, and the compilation and analysis of the correlation data are primarily my responsibility. The polarimetric data for these objects, all correlation data, and a discussion of the correlations will be published by Moore and Stockman (Ap. J., in preparation). A

description of the properties of the highly polarized QSOs has been published by Moore and Stockman (1981). The monitoring programs of B2 1308+326 and BL Lac are the result of large collaborations. I coordinated the monitoring of B2 1308+326, and the results have been published by Moore et al. (1980). The BL Lac program was coordinated by myself, Dr. Angel, and Dr. J. T. McGraw and the participants are listed in Chapter VI; the results will be published by Moore et al. (1981). The theory and discussion presented in the final chapter are my own responsibility (with ample credit to the references cited).

It is assumed throughout this dissertation that the redshifts of QSOs and BL Lac objects are cosmological. The Hubble constant and deceleration parameter are adopted to be $H_o = 75$ km s^{-1} Mpc^{-1} and $q_o = 0$.

CHAPTER II

OBSERVATIONAL TECHNIQUES AND DESCRIPTION OF SAMPLES

In this chapter we describe the general methods used to measure and analyze the polarization of QSOs. The polarimeter, observing method, and data reduction are described. We discuss the effect of statistical errors in the degree and position angle of polarization, the effect of local interstellar polarization, and the technique adopted to derive distributions of polarization. In addition, the samples of QSOs which have been observed are described; the criteria for each sample are delineated. Finally, we give a description of all non-polarimetric data which have been compiled concerning these QSOs.

A. Observational Method

The observations reported here were made with the Angel polarimeter, similar to the one described by Angel and Landstreet (1970). Most of the observations were made with the UAO 2.3 m telescope; a few were made with the UAO 1.54 m, UAO 0.9 m, and KPNO 4 m telescopes. The polarimeter has a high modulation efficiency (typically 80%) and very low instrumental polarization (less than 0.1%).

The polarimeter is designed to measure either circular or linear polarization. In circular mode, incoming light passes through a Pockels cell which acts as a (±) quarter-wave plate. The retardation

introduced by the Pockels cell is a function of the voltage across the crystal; this voltage is modulated rapidly ($\sim$ 100 Hz) between positive and negative voltage under computer control. The effect of the voltage modulation is that an incoming sense of circular polarization is converted alternately to one of two senses of linear polarization. Below the Pockels cell is a Wollaston prism to diverge the orthogonal senses of linear polarization to two photomultiplier tubes (PMTs). The Pockels cell, Wollaston prism, and PMTs are fixed with respect to each other. This implies that each of the PMTs, while always viewing the same sense of linear polarization from the Wollaston prism, is measuring the amount of light in alternate senses of circular polarization above the Pockels cell. This design minimizes instrumental polarization. The computer synchronizes the voltage modulation with the PMT outputs and sums the counts corresponding to the two senses of incoming circular polarization for both independent PMTs. The rapid modulation and simultaneous measurements of both senses of polarization minimizes guiding and seeing errors. The uncertainty of the measurements is generally limited by photon counting statistics.

The linear polarization Stokes parameters Q or U are measured by inserting an achromatic quarter-wave plate above the Pockels cell. The quarter-wave plate converts incoming linear polarization to circular polarization as seen by the Pockels cell; the remainder of the instrument operates identically as it does when measuring incoming circular polarization. The entire polarimeter is rotated with respect to the sky. The Stokes parameter Q is measured at 0°, 90°, 180° and

270° (relative to an arbitrary orientation), while U is measured at 45°, 135°, 225° and 315°. The redundancy in using four positions for each parameter further reduces instrumental polarization.

The photomultiplier tubes used for these observations (RCA 31034A) have GaAs photocathodes. The wavelength response is approximately constant from 3200 Å (the atmospheric cut-off) to 8600 Å. The survey and variability measurements are made unfiltered in order to maximize the signal-to-noise. The effective wavelength is $\sim$0.6 μm with a bandpass of $\sim$0.5 μm. Some of the observations are made with filters; these filters and the bandpasses they correspond to will be described in the footnotes to Table 2.

The typical observing sequence consists of a 5 - 10 minute integration of the object (+ sky) followed by an identical measurement of the adjacent sky background. In most cases, a 4" aperture is used. The relatively slow sky-chopping does introduce some uncertainty because of possible sky variability; this uncertainty is more significant for very faint objects ($V \geq 18$) where the QSO signal is a fraction of the sky background signal. Repeated object/sky observations are sometimes made to improve the accuracy without slowing the rate of sky-chopping. The instrumental modulation efficiency is calibrated several times each night by inserting a Nicol prism above the polarimeter (producing completely linearly-polarized light) and measuring the polarization. The typical efficiency for unfiltered measurements is 80%; it is slightly higher for filtered measurements. The orientation

of the polarimeter with respect to the sky is also determined each night by observing standard stars with known position angles of interstellar polarization.

The results of each integration (for linear polarization measurements) are the count rate (photons/sec) and the normalized (percentage) Stokes parameters Q and U. The unnormalized Stokes parameters for the sky measurement are subtracted from those of the object (+ sky) measurement, and the result is then renormalized. Thus, the rate, Q, and U (normalized) are derived for the object. The percentage polarization P and position angle θ are calculated by

$$\begin{aligned} P &= (Q^2 + U^2)^{\frac{1}{2}} \\ \theta &= \tfrac{1}{2} \tan^{-1}\left(\frac{U}{Q}\right) \quad . \end{aligned} \tag{1}$$

The errors of the Stokes parameters Q and U are derived from photon statistics, this being a reasonable estimate of the true uncertainty. For equal integration times for Q and U, the errors in P and θ are

$$\begin{aligned} \sigma_P &\approx \sigma_Q \sim \sigma_U \\ \sigma_\theta &= \tfrac{1}{2} \frac{\sigma_P}{P} = \frac{180^\circ}{2\pi} \frac{\sigma_P}{P} \end{aligned} \tag{2}$$

The only further reduction of the derived polarization is to divide P and σ_P by the instrumental modulation efficiency. The position angle θ is corrected by adding a fixed angle (determined nightly from standard

stars) to account for the orientation of the polarimeter with respect to the sky. No correction is made for instrumental polarization; it has been measured to be <0.1%.

The photon rate is indicative of the brightness of the object. The aperture normally used (4") is usually larger than the seeing disk, but is too small for accurate photometric measurements. This sacrifice of some photometric accuracy is made because the reduced sky background greatly improves the polarimetric accuracy. We have calibrated the observed unfiltered count rates against the V magnitude for a large number of QSOs; the dispersion in this calibration is $\sim$ 0.4 magnitudes. At least some of this dispersion is due to color differences among the QSOs. Thus, small deviations of the derived broadband magnitudes from the V magnitude cannot be considered reliable. However, large deviations ($\geq$ 1 mag) or significant scatter among repeated observations of the same QSO are indicative of variability.

There are two important factors which must be taken into account when evaluating the polarization measurements. First, while the Stokes parameters Q and U do have normal error distributions, P and θ do not. The degree of polarization P is a positive definite quantity and there is a statistical bias towards the measured polarization being greater than the true polarization. The general formula for the probability of measuring a polarization in the interval (x,x+dx), if the true polarization is ξ, can be derived from the relationship between polarization and the normally distributed Stokes parameters, and is

$$P(x|\xi)dx = \frac{X}{2\pi\sigma_x^2} \exp\left[-\frac{x^2+\xi^2}{2\sigma_x^2}\right] dx \int_0^{2\pi} \exp\left[\frac{x\xi}{\sigma_x^2}\cos\theta\right] d\theta \qquad (3)$$

For the case of unpolarized light ($\xi = 0$), the probability is

$$P(x|0)dx = \frac{x}{\sigma_x^2} \exp\left[-\frac{x^2}{2\sigma_x^2}\right] dx \qquad (4)$$

Equation [4] illustrates the bias towards overestimating the true polarization; the most likely measurement of unpolarized light is $x = \sigma_x$. For unpolarized light, the probability of obtaining a measurement $x \geq 2\ \sigma_x$ is 13%; the probability of measuring $x \geq 3\sigma_x$ is 1%. Thus, a $2-3\sigma$ result is required before an individual measurement can be regarded as a likely detection. The bias towards overestimating the true polarization decreases as ξ/σ_x increases.

The nature of the errors in the degree of polarization must be kept in mind with regard to the position angle errors. The uncertainty of the position angle is 28°.6 (σ_P/P). However, a measurement of $P \leq 2\sigma_P$ is not clear evidence of a detection and therefore the formal position angle error is not meaningful unless $\sigma_\theta \leq 15°$.

The second important factor in evaluating the polarization measurements is the role of local interstellar polarization. Ideally, the Stokes parameters of interstellar polarization in any direction could be subtracted from the observed Stokes parameters. However, high galactic latitude interstellar polarization is not well known (and is

beyond the scope of this paper to determine). Most of the QSOs observed are at high latitudes where the interstellar polarization is small; however, it cannot be ignored since the polarization of most QSOs is very low ($P < 1\%$). A general method of estimating the contribution of interstellar polarization is required.

The maximum interstellar polarization can be determined if the interstellar reddening is known. Hiltner (1956) found that the ratio of interstellar polarization to visual extinction has a relatively flat distribution up to a maximum of $P_{IS}(\%)/A_V(\text{mag}) = 2.76$. Since $A_V = 3\ E(B-V)$ (Allen 1973), $P_{IS}(\%) < 8.28\ E(B-V)$. High latitude interstellar reddening is better known than polarization. Specific reddening laws and the technique used to estimate the contribution of interstellar polarization will be discussed in detail below. It is important to keep in mind that this method gives only the maximum degree of interstellar polarization, not the actual degree or position angle; for any individual object, the effect of interstellar polarization is not known.

B. Distributions of Polarization

Frequently in this dissertation we are interested in determining the distribution of polarization for various samples. Histograms of the observed polarization are misleading because of both the range of uncertainties and the statistical bias towards overestimating the true polarization. A statistical method is required which deconvolves the effects of individual measurement errors, using the probability function associated with polarization (Eq. [3]). An algorithm ideally suited to this purpose is described by Lucy (1974) and is adopted here.

The same algorithm is also used to statistically estimate the contribution of local interstellar polarization. A comparison distribution of polarization can be derived which represents the distribution if objects had no intrinsic polarization and only local interstellar polarization were present. The intrinsic polarization of the objects can be estimated by a comparison of the two distributions.

1. The Lucy Algorithm

The algorithm described by Lucy (1974) is an iterative scheme to deconvolve sampling effects with a known probability function. The underlying distribution is iteratively approximated, using the set of observed values and the probability function associated with selecting those observed values. The discrete, heterogeneous version of the Lucy algorithm (his Eqns. [16 - 18]) is used. The desired underlying distribution, the probability of an object having a true polarization in the interval $(\xi,\xi + d\xi)$, is denoted by $\chi(\xi)\, d\xi$. The function of observed values is

$$\tilde{\phi}(x) = \frac{1}{N} \sum_{n=1}^{N} \delta(x - x_n) \quad , \tag{5}$$

where x_n is the observed polarization for each of N objects in the sample. The probability of measuring a polarization in the interval $(x_n, x_n + dx)$ is $P_n(x_n|\xi)$, given in Equation [3]. With this notation, the iterative scheme to calculate $\chi(\xi)$ is

$$\phi_n^r(x_n) = \int \chi^r(\xi)\ P_n(x_n|\xi)\ d\xi \tag{6}$$

$$Q_n^r(\xi \mid x_n) = \chi^r(\xi)\ \frac{P_n(x_n|\xi)}{\phi_n^r(x_n)} \tag{7}$$

$$\chi^{r+1}(\xi) = \frac{1}{N} \sum_{n=1}^{N} Q_n^r(\xi|x_n) \quad . \tag{8}$$

To avoid possible bias, the initial estimate for $\chi^\circ(\xi)$ is always taken here to be a constant distribution.

For any sample of observations, this method can be applied to determine the underlying distribution of true polarization, corrected for the effect of measurement errors. An example of the results of this algorithm is given in Figure 1. This figure shows a histogram of observed polarization values for a sample of 137 bright QSOs (to be discussed below) with typical measurement errors of $\sigma_p \sim 0.2 - 0.4\%$. Overlying the histogram is the distribution of polarization derived by the Lucy technique and normalized to the same area. The most notable effect is the shift to lower polarizations in the Lucy distribution, particularly at low values of P; this is the expected correction for the statistical bias in observed polarization. Another quality of the derived distribution, which will be apparent throughout this dissertation, is that the distribution is very smooth. This can be misleading, particularly when the sample contains a small number of observations. The smoothness is an artifact of the technique and is

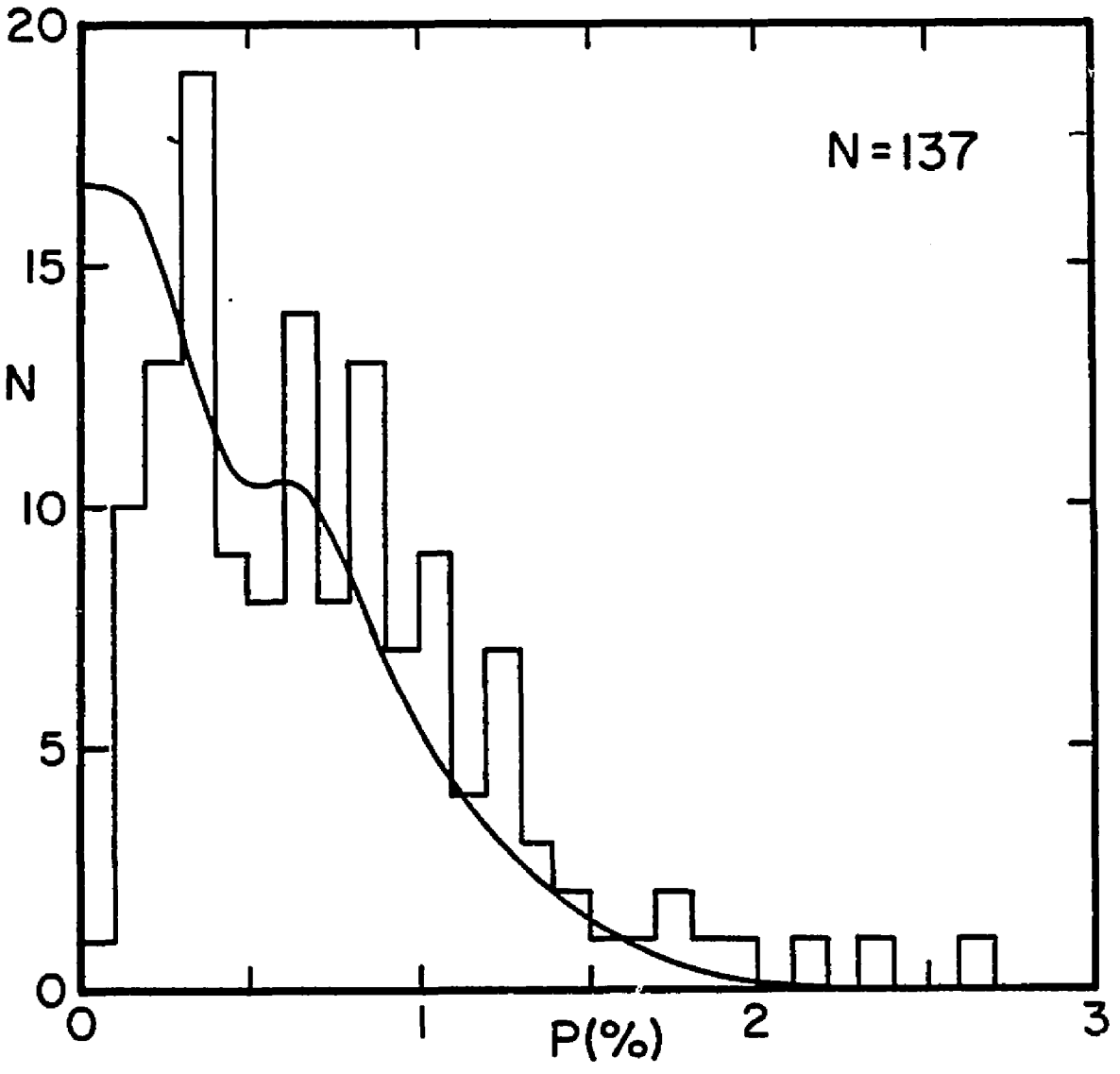

Figure 1. Histogram and probability distribution of polarization for the bright QSO sample.

indicative of a well-determined distribution. It is important to bear in mind the actual number of observations used to derive each distribution; this number will be given for all distributions.

There is a choice of which iteration to adopt to represent the underlying distribution. The method quickly approximates the underlying distribution then slowly converges to the best fit of the data points (corrected for the error distribution). The primary effect here of additional iterations is to amplify the significance of the observations with the smallest errors (normally the brightest objects). This is illustrated in Figure 2, which shows the first, third, fifth, tenth, and twentieth iterations of the same sample as in Figure 1. The peaks near 0% and 0.6% become more significant with further iterations because there are several accurate measurements near these values; many other measurements with larger errors can be consistent with these values. This preference for the values of the well-measured (brighter) objects is not desired, so the number of iterations used to derive the distributions is small. We have chosen to consistently adopt the third iteration to represent the underlying distribution.

2. Local Interstellar Polarization

We have shown that the maximum degree of interstellar polarization for any object can be derived from the reddening in its direction. Three independent reddening laws have been tested and are described here. The first is from Holmberg (1974), which gives the color excess as a function of galactic latitude, $E(B-V) = 0.052 \csc|b|$. The second

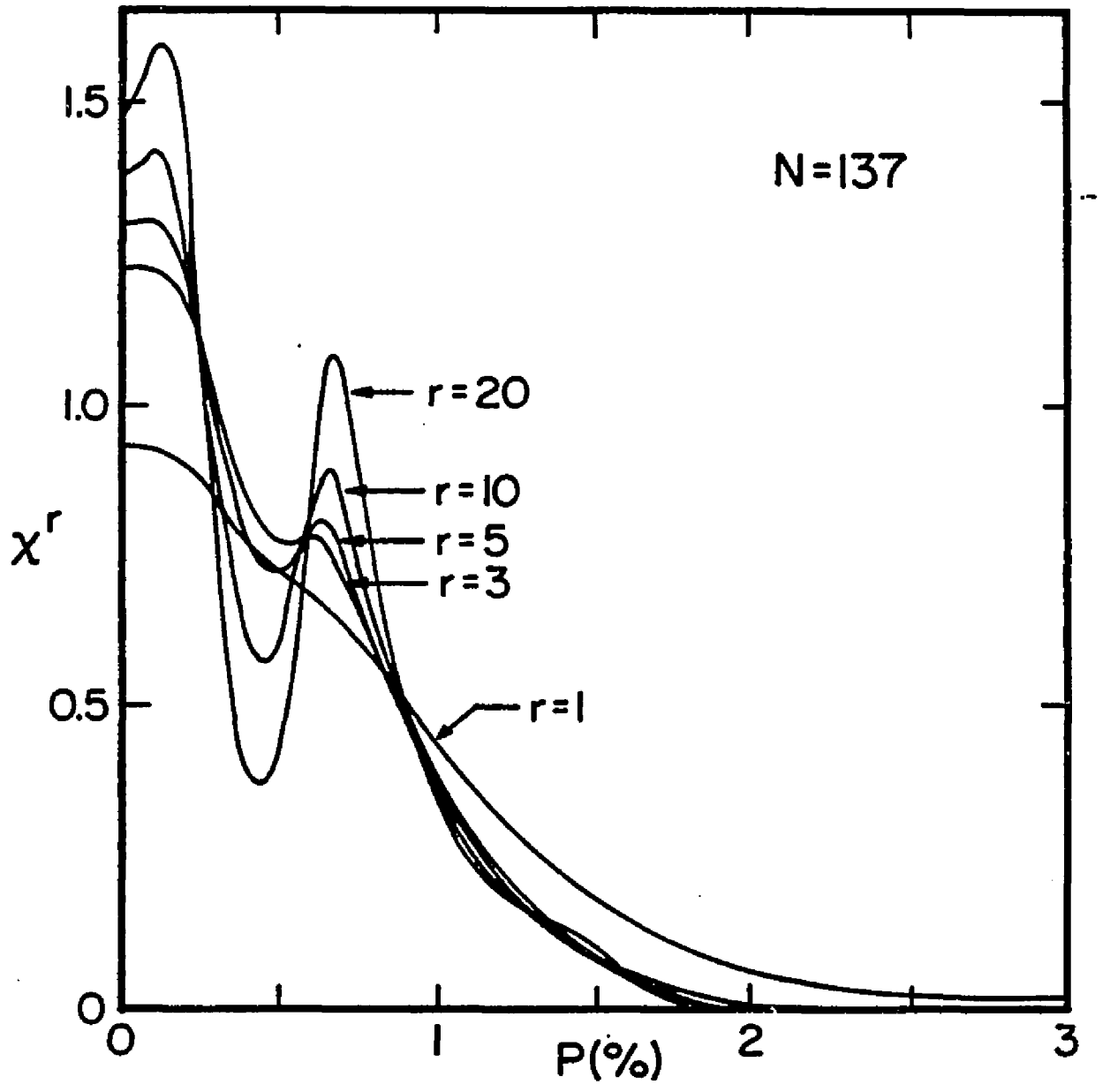

Figure 2. The effects of successive iterations of the Lucy algorithm.

Iterations r=1, 3, 5, 10, and 20 are shown. The significance of the accurate polarization measurements is amplified with further iterations.

(Sandage 1973) is also a function of latitude only; there is no reddening for $|b| > 50°$, and $E(B-V) = 0.033\ (\csc|b| - 1)$ for $|b| \leq 50°$. The third law tested is from Burstein and Heiles (1978) and the reddening is a function of both latitude and longitude. This method (their Eqn. [4]) uses the neutral hydrogen column density and a measure of the gas-to-dust ratio in each direction to estimate the reddening.

In order to estimate the contribution of interstellar polarization to a derived polarization distribution, we first generate a set of pseudo-measurements which statistically represent what we would observe if the sample of QSOs had no intrinsic polarization. The pseudo-measurements are constructed in the following way. The distribution of P_{IS}/A_V from Hiltner (1956) is approximated with a flat distribution. Therefore, after the maximum interstellar polarization for each object is calculated by one of the reddening laws above, it is multiplied by a random number between zero and one. We then construct artificial Stokes parameters Q and U which would yield the resultant polarization, superimpose noise appropriate to the error of the measurement, and then calculate the final polarization from the revised Q and U values. The last step is necessary to transform a "true" polarization to a polarization one would expect to measure. A pseudo-measurement is generated in this manner for each object in the sample. These values and the observed statistical errors are then deconvolved in the same way as the original data with the Lucy algorithm to derive the comparison distribution of interstellar polarization. The

deviation between this distribution and the distribution derived from the measured values is then an estimate of the intrinsic polarization of the sample.

In (a) of Figure 3, three interstellar polarization distributions are given, using the reddening laws above, for the same sample of QSOs as was shown in Figures 1 and 2. In addition to the interstellar distributions, a delta function distribution is shown for comparison; this distribution is derived similarly to the interstellar simulations except that the initial polarization (before adding noise) is zero. The delta function distribution represents the limiting resolution of the Lucy technique with this set of observations. It is clear that the Sandage law (S) and the Burstein and Heiles law (BH) give similar results and that these distributions are nearly the same as the delta function distribution (i.e., there is very little interstellar polarization for this sample). The Holmberg law (H) gives a substantially higher estimate of the amount of interstellar polarization. There are two arguments that the Holmberg law gives an overestimate of the true interstellar polarization. The first argument is that it predicts higher values of interstellar polarization near the galactic poles than are observed (Markannen 1978). The second argument is that the interstellar distributions derived using this law are comparable to the distributions derived from actual measurements of low polarization QSOs; this would imply that these QSOs have almost no intrinsic polarization. However, a strong correlation is present between the measured position angle of optical polarization and the position

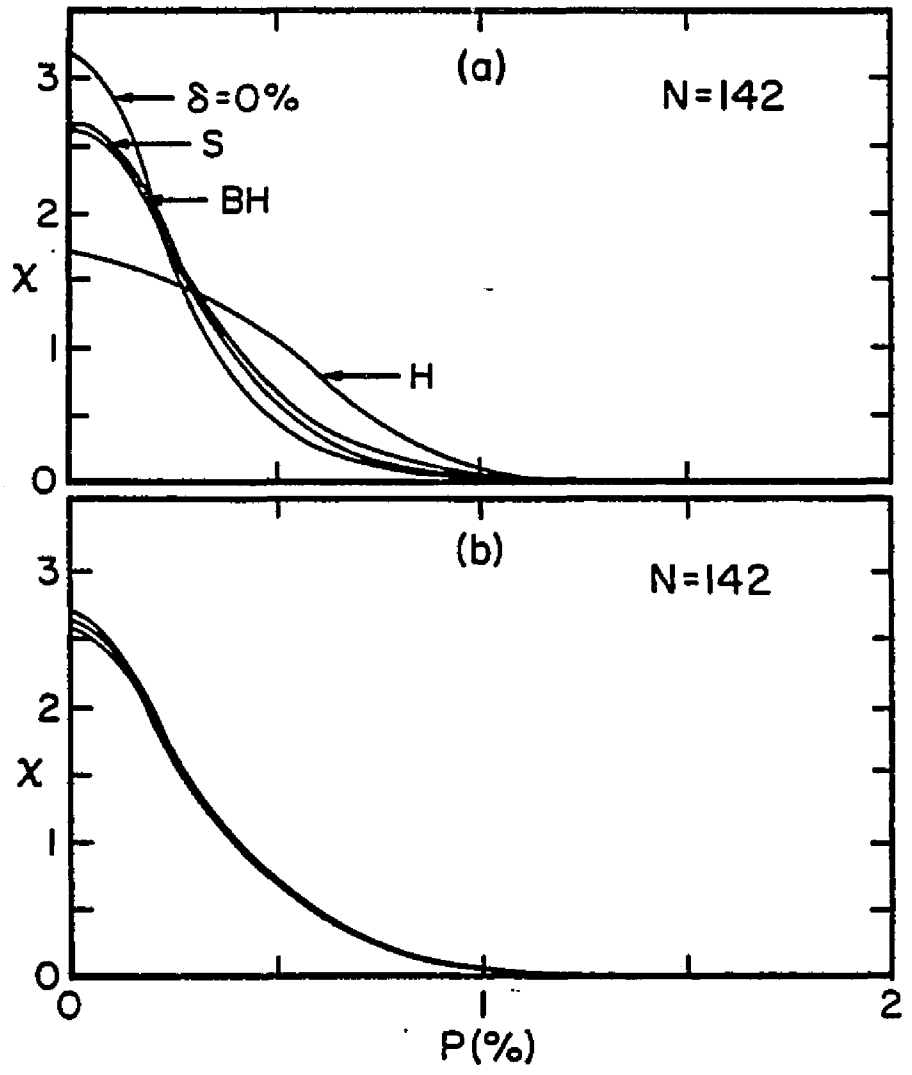

Figure 3. Probability distributions of polarization for local interstellar polarization.

a. Distributions derived using the reddening laws of Holmberg (1974, "H"), Sandage (1973, "S"), and Burstein and Heiles (1978, "BH"). A distribution derived for a delta function is also shown.

b. Three independent probability distributions using the reddening law of Burstein and Heiles (1978).

angle of extended radio structure in low polarization QSOs (Stockman, Angel, and Miley 1978). This correlation implies that the measured optical polarization is predominantly intrinsic polarization, contrary to the interstellar polarization simulations using the Holmberg law. We have chosen to adopt the Burstein and Heiles law for all derivations of the interstellar polarization.

The distributions derived for interstellar polarization are statistical simulations; repeated simulations for the same sample of objects will differ. Random number generators are used to construct the set of pseudo-measurements both in the transformation from the maximum interstellar polarization and in the noise generator. An example of three independent simulations of the interstellar polarization for the bright QSO sample is given in (b) of Figure 3. The three derived distributions for this large sample (N = 142) agree quite well. It is important to remember, particularly for samples which are small and/or include low latitude objects, that the interstellar simulations are only statistical estimates.

C. Samples of QSOs

1. Sample Criteria

The selection of QSOs for the polarization survey is based on several criteria. There are three primary samples; the purpose and criteria for each sample are specifically described here. Nearly all of the QSOs have been selected from the catalog of Burbidge, Crowne, and Smith (1977, hereafter BCS); those QSOs which are not in BCS are listed in the recent updated catalog by Hewitt and Burbidge (1980).

The largest sample is the "bright QSO" survey. All QSOs listed in BCS with V $\leq$17 and δ >-20° are included in this survey (142 QSOs). These limits are chosen because accurate measurements are readily obtainable with the UAO 2.3 m telescope. This survey is used primarily to determine the general distribution of polarization among radio-quiet and radio-loud QSOs. The survey is an "unbiased" magnitude-limited sample, in that objects are chosen (from the catalog) without regard to any property except their brightness and declination. However, the sample is "unbiased" only to the extent that the catalog of BCS is unbiased; numerous selection effects are present in the BCS catalog, which is simply a catalog of all QSOs known at that time. The primary selection effect of concern here is that the majority of QSOs in the catalog are radio-selected QSOs even though only $\sim$10% of QSOs are radio-loud (Sramek and Weedman 1978, 1980; Smith and Wright 1980). To counter this selection effect, we have included a few additional optically-selected QSOs which are slightly fainter than seventeenth magnitude in this sample; nevertheless two-thirds of the sample are radio-selected QSOs.

The second sample of QSOs is the "variability" sample, which consists of all QSOs with V < 18 and δ > -20°, for which any kind of variability information was available in the literature as of late 1977 (109 QSOs). Prior to this survey it was known that the four highly polarized QSOs were optically-violent variables; however, this correlation had not been examined in a systematic way. The purpose

of this sample is to determine the relationship between the photometric variability and polarization of QSOs. It is important to note that this is not a survey of photometric OVVs; all QSOs meeting the above criteria which have been monitored for variability, whether or not they have exhibited variability, are included. A few QSOs of particular interest fainter than V = 18 have also been included. We parametrize the photometric variability by the maximum amplitude and minimum time scale of variability exhibited in the monitoring available; in many cases the monitoring is deemed insufficient to reasonably determine the time scale of variability and only the amplitude is given. A primary source for much of this information is the compilation of variability data by Grandi and Tifft (1974) and the references therein. As more recent monitoring data have become available, some of the descriptive parameters have been updated and some new objects included.

While there is a great deal of variability information compiled for this sample, the information cannot be regarded as representative of all QSOs; there are strong selection effects and marked inhomogeneity present in the variability data. For example, researchers tend to continue monitoring those QSOs which have already exhibited strong variability. Many QSOs are originally chosen for monitoring on the basis of radio variability or a flat radio spectrum (e.g. Folsom et al. 1971). Some of these data are based on historical light curves from the Harvard archives; these light curves are published with a bias towards those QSOs which show extreme variability (M. Liller, private communication, 1979).

Few optically-selected QSOs have been monitored. Finally, the frequency, baseline, and accuracy of the monitoring of the QSOs in this sample are very inhomogenous. This inhomogeneity has a direct impact on the parameters used to describe the photometric variability; the maximum amplitude of variability can only increase with additional observations and the minimum time scale observable is dependent on the frequency of monitoring. A more systematic examination of the relationship between variability and polarization requires that a large unbiased sample of QSOs be monitored uniformly; such a sample is not presently available.

The final sample is compiled in order to examine the correlation between the polarization and optical continuum spectral index of QSOs. This "spectrophotometry" sample consists of all QSOs with $V < 18$ and $\delta > -20°$ for which multichannel spectrophotometry is available in the literature (114 QSOs). The optical spectral index α_{OPT} (defined as $f_\nu \alpha \nu^{-\alpha}$) is used to describe the continuum energy distribution; the power law index is a convenient parameter to approximate the energy distribution but does not imply that the energy distribution is a true power law. As in the variability sample, objects are generally chosen without regard to the value of α. The one exception to this is that a few steep spectrum QSOs fainter than $V = 18$ are included, since few of these are known.

There is considerable overlap between the three QSO samples described above; a total of 220 objects are represented. Eleven additional QSOs of special interest are also included in the general survey. Thus, polarimetric observations of 231 QSOs are to be presented.

2. Description of Information Compiled

In this section we describe the non-polarimetric data which are compiled for the 231 QSOs in the general polarization survey. The intent is to correlate the polarization with other properties of QSOs. For example, samples have been specifically constructed to test the correlations of polarization with photometric variability and with optical spectral index. We can examine additional correlations by compiling data concerning other properties of those QSOs in the general survey.

All non-polarimetric information regarding the general survey QSOs is compiled in Table 1 (p. 38). The first ten columns give general information common to all the QSOs. The coordinate designation, survey name, V magnitude, and redshift (z) are taken from BCS or Hewitt and Burbidge (1980). The galactic latitude (b^{II}) and maximum degree of interstellar polarization (P_{ISM}) are listed in columns five and six. The maximum interstellar polarization is calculated using the Burstein and Heiles (1978, their Equation [4]) reddening law; this value is used as input for all interstellar polarization simulations as described in § II.B.2.

There are three general classifications assigned to all QSOs to define various subsets of the general survey. The first classification in column 7 ("O/R") is whether a QSO is optically-selected ("O") or radio-selected ("R"). This classification is made from the original identification references in BCS. While this designation is based only on the selection technique, we will <u>assume</u> in our discussion

that the optically-selected QSOs are radio-quiet and the radio-selected QSO are radio-loud. Radio measurements of these optically-selected QSOs are generally not available to test this assumption; however, only $\sim$ 10% of optically-selected QSOs are radio-loud (Sramek and Weedman 1978, 1980; Smith and Wright 1980). The second classification ("BS") is whether a QSO is in the "bright QSO" sample; if so, an "X" appears in column 8. Finally, we distinguish in column 9 ("HPQ") those QSOs which are highly polarized. As will be justified in §III, the general criteria adopted for a QSO to be highly polarized are that $P > 3\%$ and that $P/\sigma_P > 3$. If only one measurement satisfies these criteria, the QSO is designated a possible ("P") HPQ; if two or more measurements meet the criteria, the QSO is considered a definite ("D") HPQ. (No entry in this column implies that no measurements fulfilled these criteria.) The second aspect of the HPQ classification is whether the first measurement of the QSO meets the high polarization criteria. If it does, the suffix "-1" is shown; otherwise, the suffix ">1" is assigned.

The final quantity given for all survey QSOs is the logarithm of the rest-frame monochromatic luminosity at 2500 Å ($\log L_{OPT}$). The luminosity is calculated using the V magnitude and redshift (from BCS) and assuming a power law of index α. For variable QSOs, the V magnitude from BCS is still uniformly used and is intended to be representative of the typical brightness. The calibration of Schmidt (1968) is used to calculate the V band flux; the continuum magnitude, V_C, is

approximated by V. The spectral index, if available, is taken from the following column; otherwise, $\alpha = 0.7$ is assumed (Richstone and Schmidt 1980). The formula for the monochromatic luminosity is

$$L_\nu(\nu_o) = 4\pi\left(\frac{cz}{H_o}\right)^2\left(1+\frac{z}{2}\right)^2 f_\nu(\nu_{obs})\left(\frac{\nu_o}{\nu_{obs}}\right)^{-\alpha}(1+z)^{\alpha-1} \qquad (9)$$

where $f_\nu(\nu_{obs})$ is the monochromatic flux at the effective frequency of the V band (Richstone and Schmidt 1980; Schmidt 1968).

The remainder of the data in Table 1 are taken from the literature; if there is no entry in a data column, then this information is not available. Reference codes are provided for each parameter; these codes are listed at the end of the table.

The final entries of the first "page" of the table are the optical spectral index α_{OPT} ($f_\nu \alpha \nu^{-\alpha}$) and references. Objects with an entry in this column constitute the spectrophotometry sample.

The coordinate designation and HPQ classification are repeated in columns 1 and 2 of the second "page" of Table 1. The maximum amplitude of photometric variability (Δm) and references are listed in columns 3 and 4. These QSOs constitute the variability sample. We note that when reference 0 is given, this amplitude is based on magnitude estimates from our observations. It is only included if the variability exceeds one magnitude from the BCS magnitude; the sign of the variability ($\Delta m = V_{BCS} - m$) is given for reference 0 entries. If the variability monitoring is sufficient to estimate a characteristic time scale of variability, the minimum time scale (τ) and references

are tabulated in columns 5 and 6. This time scale is a subjective estimate; the possible classifications are time scales of a day ("DY"), days ("DYS"), a week ("WK"), a month ("MT"), months ("MTS"), a year ("YR"), and years ("YRS").

The equivalent width of the Mg II emission line and references are listed in columns 7 and 8. This emission line is chosen to represent emission line strengths because its equivalent width is known for more QSOs in our sample than any other line. The equivalent width of emission lines does vary as the continuum brightness changes (Miller and French 1978, Arp et al. 1979, Netzer et al. 1979), so an average value is taken among the references listed.

A number of X-ray observations of QSOs by HEAO-B (Einstein) are now available. The X-ray data are parametrized by the monochromatic rest-frame luminosity at 2 keV (L_X) and the optical/X-ray spectral index (α_{ox}). The monochromatic luminosities are calculated from published integrated fluxes in a 0.5 - 4.5 keV restframe bandpass by assuming an energy power law of index 0.5 (Tananbaum et al. 1979). The tabulated optical and X-ray luminosities are used to calculate a power law spectral index α_{ox} which characterizes the energy distribution between 2500 Å and 2 keV. This index is a convenient parameter to represent the ratio of optical to X-ray luminosity; its use does not imply that the energy distribution is necessarily a power law.

The position angle of extended radio structure (θ_{rad}) and its uncertainty are listed with references in columns 12 and 13. The final column is the absolute difference ($|\theta|$) between this position angle of

radio structure and the average position angle of optical polarization. The latter angle is calculated by a weighted average (in Q/U space) of all broadband polarization measurements of the QSO. The uncertainty of the difference is derived from the uncertainty of both angles.

The information presented in Table 1 is a valuable compilation of data for those QSOs which are in the general polarization survey. The correlations between the properties tabulated in Table 1 and the polarization of QSOs are discussed in detail in § IV. Both the polarimetric characteristics and their relationship to other characteristics of QSOs are important clues in evaluating theoretical models.

Table 1. Compilation of Non-Polarimetric Data for QSOs Surveyed.

OBJECT	NAME	V	Z	b^{II}	P_{ISM}	O/R	BS	HPQ	L_{OPT}	α_{OPT}	REF
0003+158	PHL 658	16.40	0.450	-45	0.24	R	X		30.45	1.00	32
0007+106	III ZW 2	15.40	0.089	-51	0.53	O	X		29.41	0.66	65
0017+154	3CR 9	18.21	2.012	-47	0.26	R			31.51	1.36	29,33,35
0019+011	MCS 232	17.00	2.180	-61	0.19	O	X		32.00	.	
0024+224	NAB	16.60	1.118	-40	0.20	O	X		31.38	.	
0026+129	PG	14.78	0.142	-49	0.57	O	X		29.97	1.04	65
0038-019	PKS	18.50	1.690	-64	0.11	R			31.09	.	
0043+008	MCS 275	17.50	2.210	-62	0.03	O	X		31.82	.	
0044+030	PKS	16.00	0.624	-60	0.19	R	X		31.00	.	
0051+291	4C 29.01	17.80	1.828	-33	0.59	R			31.40	0.10	39
0054+144	PHL 909	16.70	0.171	-48	0.48	O	X		29.47	.	
0056-001	PHL 923	17.33	0.720	-63	0.16	R			30.61	.	
0058+019	PHL 938	17.16	1.955	-61	0.30	O	X		31.82	0.85	29,36
0100+130	PHL 957	16.57	2.660	-50	0.31	O	X		32.46	0.86	65
0106+013	PKS	18.39	2.107	-61	0.16	R			31.46	1.08	39
0110+297	4C 29.02	17.00	0.363	-33	0.51	R	X		30.13	0.35	39
0119-046	PKS	16.88	1.955	-66	0.34	R	X		31.91	.	
0122-003	PKS	16.70	1.070	-62	0.14	R	X		31.29	.	
0123+257	4C 25.05	17.50	2.358	-36	0.69	R			31.86	0.52	39
0130+242	4C 24.02	16.80	0.457	-37	0.73	R	X		30.36	.	
0132+205	NAB	17.50	1.782	-41	0.45	O	X		31.55	.	
0133+207	3CR 47	18.10	0.425	-41	0.38	R			29.77	.	
0134+329	3CR 48	16.20	0.367	-29	0.36	R	X		30.27	1.26	29,65
0137+060	PHL 1092	17.00	0.396	-55	0.22	O	X		30.14	.	
0137+012	PHL 1093	17.07	0.260	-59	0.06	R			29.28	2.50	34
0137-010	NAB	17.00	0.330	-61	0.04	O	X		29.96	.	
0141+339	4C 33.03	17.50	1.455	-27	0.30	R			31.32	0.70	39
0146+017	MCS 141	17.50	2.920	-58	0.05	O	X		32.17	.	
0147+089	PHL 1186	17.40	0.270	-51	0.38	O			29.42	1.50	34
0148+090	PHL 1194	17.50	0.299	-51	0.38	O			29.62	0.90	34
0159-117	3C 57	16.40	0.699	-67	0.00	R	X		30.95	.	
0202+319	DW	18.00	1.466	-28	0.49	R			31.12	.	
0205+024	NAB	15.40	0.155	-55	0.19	O	X		29.97	0.46	65
0214+108	PKS	17.00	0.408	-47	0.76	R	X		30.17	.	
0226-038	PHL 1305	16.96	2.064	-57	0.10	R	X		31.95	.	
0229+131	PKS	17.71	2.065	-43	0.76	R			31.67	0.86	39
0229+341	3CR 68.1	19.00	1.238	-24	0.36	R		D-1	30.57	5.10	37,53,65
0232-042	PHL 1377	16.46	1.436	-56	0.08	R	X		31.72	.	
0237-233	PHL 8462	16.63	2.223	-65	0.06	R			32.21	0.95	29,65
0333+321	NRAO 140	17.50	1.258	-19	2.48	R			31.15	.	
0336-019	CTA 26	18.40	0.852	-42	0.59	R		D-1	30.36	.	
0340+048	3CR 93	18.09	0.357	-38	1.22	R			29.44	1.50	53
0348+061	NAB	17.60	2.058	-35	1.30	O	X		31.69	.	
0349-146	MSH 03-19	16.22	0.614	-46	0.17	R	X		30.92	0.50	65
0350-073	3C 94	16.49	0.962	-43	0.52	R	X		31.26	0.68	65
0403-132	PKS	17.17	0.571	-43	0.22	R		D-1	30.44	.	
0405-123	PKS	14.82	0.574	-42	0.22	R	X		31.43	0.37	29,65
0409+229	3C 108	17.90	1.213	-20	1.37	R			30.96	3.00	53
0414-060	3C 110	15.00	0.781	-37	0.31	R	X		31.63	.	
0420-014	PKS	18.00	0.915	-33	0.73	R		D-1	30.60	.	

Table 1.--Continued

OBJECT	HPQ	Δm	REF	τ	REF	W_λ	REF	L_x	REF	α_{ox}	θ_{rad}	REF	$\lvert\Delta\theta\rvert$
0003+158		0.5	4	MTS	20,21	.		.		.	115+ 6	54	7+ 8
0007+106		0.6	13	.		.		.		.	.		.
0017+154		0.2	4,20	MTS	20	.		27.60	63	1.50	137+15	54	0+19
0019+011		.		.		.		.		.	.		.
0024+224		.		.		.		.		.	.		.
0026+129		.		.		.		26.57	63	1.31	.		.
0038-019		.		.		.		.		.	.		.
0043+008		.		.		.		28.04	63	1.45	.		.
0044+030		.		.		.		.		.	.		.
0051+291		1.1	0	.		.		.		.	.		.
0054+144		.		.		.		26.41	63	1.17	.		.
0056-001		0.1	4,23	.		.		.		.	.		.
0056+019		0.1	4,7	.		.		.		.	.		.
0100+130		.		.		.		<28.20	64	>1.63	.		.
0106+013		.		.		.		.		.	.		.
0110+297		-1.6	0	.		67	39	.		.	42+ 1	54	21+13
0119-046		0.2	4,23	.		.		.		.	.		.
0122-003		.		.		.		.		.	.		.
0123+257		.		.		.		.		.	.		.
0130+242		.		.		.		.		.	93+ 3	54	20+ 6
0132+205		.		.		.		.		.	.		.
0133+207		1.0	4,0	.		.		27.38	63	0.92	35+ 2	54	14+ 6
0134+329		0.4	4	YR	22	17	29,65	.		.	.		.
0137+060		.		.		.		25.96	63	1.60	.		.
0137+012		0.4	4	MT	20	.		.		.	7+20	54	12+28
0137-010		.		.		.		26.54	63	1.31	.		.
0141+339		.		.		.		.		.	.		.
0146+017		.		.		.		<27.94	63	>1.62	.		.
0147+089		.		.		.		.		.	.		.
0148+090		.		.		.		.		.	.		.
0159-117		0.8	4	MT	20,23	.		.		.	7+ 5	57	4+17
0202+319		.		.		.		.		.	.		.
0205+024		.		.		.		.		.	.		.
0214+108		1.3	0	.		.		.		.	75+ 3	54	38+ 4
0226-038		0.1	4,20	.		.		28.22	63	1.43	.		.
0229+131		0.3	4,23	.		.		.		.	.		.
0229+341	D-1	.		.		17	53,65	.		.	173+10	66	53+10
0232-042		0.3	4	YR	20,21	.		.		.	90+20	60	74+22
0237-233		0.2	4	.		.		28.82	64	1.30	.		.
0333+321		0.3	23	YRS	23	.		.		.	.		.
0336-019	D-1	0.8	23	MT	23	.		.		.	.		.
0340+048		.		.		28	53	.		.	.		.
0348+061		.		.		.		.		.	.		.
0349-146		0.1	4,20	.		73	65	.		.	166+ 1	54	3+11
0350-073		0.4	4,6	.		43	65	.		.	90+11	54	78+11
0403-132	D-1	0.8	4	YR	21	.		.		.	.		.
0405-123		0.5	4	MTS	24	33	29,65	.		.	3+10	54	39+11
0409+229		.		.		20	53	.		.	.		.
0414-060		1.3	19	MT	19	.		27.55	63	1.57	.		.
0420-014	D-1	2.8	4,41	MT	18	.		27.78	64	1.08	.		.

Table 1.--Continued

OBJECT	NAME	V	Z	b^{II}	P_{ISM}	O/R	BS	HPQ	L_{OPT}	α_{OPT}	REF
0421+019	PKS	17.50	0.689	-31	1.22	R			30.48	0.85	39
0440-003	PKS	19.22	0.850	-28	0.44	R			30.01	1.00	39
0454+039	PKS	16.50	1.345	-23	0.56	R	X		31.63	.	
0518+165	3CR 138	18.84	0.760	-11	1.14	R			30.06	.	
0538+498	3CR 147	17.80	0.545	10	1.08	R			30.14	.	
0642+449	OH 471	17.91	3.402	18	0.68	R			32.20	.	
0704+384	4C 38.20	17.50	0.579	19	0.55	R			30.40	0.13	39
0710+118	3CR 175	16.60	0.768	10	1.03	R	X		30.97	.	
0736+017	PKS	16.47	0.191	11	0.94	R	X	D>1	29.56	1.10	34
0738+313	OI 363	17.00	0.630	24	0.39	R	X		30.69	0.07	39
0740+380	3C 186	17.60	1.063	26	0.53	R			30.92	.	
0742+318	4C 31.30	16.00	0.462	25	0.40	R	X		30.75	0.35	39,65
0752+258	OI 287	17.00	0.446	25	0.31	R	X	D-1	30.26	.	
0758+143	3CR 190	20.00	1.195	22	0.17	R			30.09	3.00	53
0809+483	3CR 196	17.79	0.871	33	0.33	R			30.63	.	
0827+243	OJ 248	17.50	0.939	32	0.22	R			30.83	.	
0837-120	PKS	15.76	0.200	17	0.36	R	X		29.79	1.48	34,65
0839+616	4C 61.19	17.00	0.862	37	0.44	R	X		30.93	.	
0846+513	W1	20.00	1.860	39	0.12	R		P-1	30.78	2.23	42
0847+190	LB 8741	16.60	0.568	34	0.19	O	X		30.66	.	
0848+163	LB 8775	16.90	1.932	34	0.32	O	X		31.89	.	
0850+140	3CR 208	17.42	1.110	33	0.36	R			31.03	1.50	29
0855+143	3CR 212	19.06	1.048	35	0.17	R		P-1	30.24	3.60	53
0859-140	PKS	16.59	1.327	21	0.31	R	X		31.57	.	
0906+430	3CR 216	18.48	0.670	43	0.06	R		D-1	29.87	2.50	53
0906+015	PKS	17.50	1.018	31	0.22	R		D>1	30.91	.	
0906+484	PG	16.06	0.118	43	0.05	O	X		29.33	0.90	65
0923+392	4C 39.25	17.86	0.699	46	0.00	R			30.37	.	
0953+254	OK 290	17.46	0.712	51	0.26	R			30.55	.	
0955+326	3C 232	15.78	0.533	52	0.08	R	X		30.95	0.50	65
0957+003	PKS	17.57	0.907	41	0.12	R			30.76	.	
0958+551	MKN 132	16.00	1.758	49	0.00	R	X		32.09	0.24	65
1001+054	PG	16.38	0.161	45	0.00	O	X		29.59	0.52	65
1004+130	PKS	15.15	0.242	49	0.27	R	X		30.50	0.34	34,65
1011+250	TON 490	15.40	1.631	55	0.27	O	X		32.38	1.81	39
1012+008	PG	16.00	0.185	44	0.03	O	X		29.82	.	
1019+309	OL 333	17.00	0.238	57	0.18	R	X		29.65	.	
1020-103	OL-133	16.50	0.197	38	0.28	R	X		29.68	.	
1028+313	B2	16.71	0.177	59	0.09	R	X		29.50	.	
1038+064	4C 06.41	16.81	1.270	53	0.05	R	X		31.44	.	
1040+123	3CR 245	17.29	1.029	56	0.17	R			31.01	0.69	35,65
1048-090	3C 246	16.79	0.344	43	0.03	R	X		30.09	.	
1049+215	4C 21.28	18.50	1.300	62	0.00	R			30.79	.	
1049+616	4C 61.20	16.48	0.422	50	0.00	R	X		30.41	.	
1055-045	OS	17.00	1.430	48	0.10	O	X		31.50	.	
1055+201	PKS	17.07	1.110	63	0.00	R			31.18	.	
1058+110	4C 10.30	17.10	0.420	59	0.03	R			30.16	.	
1100+772	3CR 249.1	15.72	0.311	39	0.14	R	X		30.50	0.33	29,36,65
1103-006	PKS	15.46	0.426	52	0.31	R	X		30.83	.	
1104+167	4C 16.30	15.70	0.634	64	0.00	R	X		31.13	.	

Table 1.--Continued

OBJECT	HPQ	Δm	REF	τ	REF	W_λ	REF	L_x	REF	α_{ox}	θ_{rad}	REF	$\lvert\Delta\theta\rvert$
0421+019		.		.		.		.		.	.		.
0440-003		2.4	41	WK	41	34	39	27.48	64	0.97	.		.
0454+039		.		.		.		.		.	.		.
0518+165		1.5	4,18	WK	18	.		27.06	63	1.15	.		.
0538+498		0.5	4	MT	20	.		26.59	63	1.36	.		.
0642+449		0.3	23	.		.		28.87	63	1.28	.		.
0704+384		.		.		88	39	.		.	83+ 4	54	64+17
0710+118		0.1	4	YRS	24	.		27.00	63	1.52	59+ 5	54	9+77
0736+017	Q>1	1.0	18,0	MT	18	.		26.10	64	1.33	.		.
0738+313		0.3	23	YRS	23	24	39	.		.	.		.
0740+380		0.1	4,20	.		.		27.43	63	1.34	132+10	57	43+31
0742+318		.		.		61	39,65	.		.	125+ 2	56	68+ 5
0752+258	Q-1	.		.		.		.		.	.		.
0758+143		.		.		48	53	.		.	.		.
0809+483		0.5	4	MT	20	.		26.94	63	1.42	36+ 6	59	11+22
0827+243		.		.		.		.		.	.		.
0837-120		1.0	4	MTS	17	.		.		.	90+ 2	54	16+21
0839+616		.		.		.		.		.	.		.
0846+513	P-1	5.0	42	OYS	42	.		.		.	.		.
0847+190		.		.		.		.		.	.		.
0848+163		.		.		.		.		.	.		.
0850+140		0.1	23	.		.		27.43	63	1.38	77+10	59	29+17
0855+143	P-1	.		.		30	53	.		.	143+10	66	57+12
0859-140		.		.		.		.		.	.		.
0906+430	Q-1	.		.		95	53	.		.	.		.
0906+015	Q>1	2.2	4,41	WK	18,41	.		27.51	64	1.31	.		.
0906+484		.		.		.		.		.	.		.
0923+392		1.3	0	.		.		27.58	63	1.07	.		.
0953+254		0.5	23	MTS	23	.		.		.	.		.
0955+326		1.2	4	YRS	24	85	65	.		.	.		.
0957+003		0.2	23	.		.		.		.	110+15	60	40+41
0956+551		.		.		25	65	.		.	.		.
1001+054		.		.		.		.		.	.		.
1004+130		1.0	4	MTS	17	18	65	<25.81	63	>1.80	117+ 2	54	39+ 3
1011+250		-1.3	0	.		.		28.26	64	1.58	.		.
1012+008		.		.		.		.		.	.		.
1019+309		0.1	23	.		.		.		.	.		.
1020-103		.		.		.		.		.	.		.
1028+313		1.0	8	.		.		26.61	63	1.11	.		.
1038+064		.		.		.		.		.	.		.
1040+123		0.1	4	.		46	65	.		.	.		.
1048-090		0.1	4,20	.		.		.		.	122+ 4	54	26+10
1049+215		.		.		.		.		.	.		.
1049+616		1.6	19	MT	19	.		.		.	.		.
1055-045		.		.		.		.		.	.		.
1055+201		0.2	4,23	.		.		.		.	165+ 3	54	14+28
1058+110		1.0	4	.		.		.		.	92+10	54	21+19
1100+772		0.3	4	MT	20,21	57	29	26.89	63	1.39	98+ 3	54	27+ 8
1103-006		.		.		.		.		.	.		.
1104+167		.		.		.		.		.	129+10	55	21+14

Table 1.--Continued

OBJECT	NAME	V	Z	b^{II}	P_{ISM}	O/R	BS	HPQ	L_{OPT}	α_{OPT}	REF
1127-145	PKS	16.90	1.187	44	0.22	R	X		31.32	.	
1128+315	B2	16.00	0.289	72	0.00	R	X		30.24	.	
1137+660	3CR 263	16.32	0.652	50	0.00	R	X		30.91	.	
1146+111	MC 2	17.00	0.863	68	0.03	R	X		30.97	0.20	40
1146-037	PKS	16.40	0.341	55	0.17	R	X		30.24	.	
1148-001	PKS	17.60	1.982	59	0.04	R			31.64	.	
1150+497	4C 49.22	16.10	0.334	65	0.00	R	X	P-1	30.34	.	
1156+295	4C 29.45	15.60	0.729	78	0.00	R	X	D-1	31.29	0.93	39
1157+014	PKS	17.00	1.986	61	0.05	R	X		31.88	.	
1202+281	GQ COMAE	15.51	0.165	80	0.03	O	X		29.91	.	
1208+322	B2	16.00	0.388	80	0.05	R	X		30.52	.	
1211+334	ON 319	17.00	1.598	80	0.00	R	X		31.59	0.29	39
1213-065	OS	17.00	1.410	55	0.32	O	X		31.48	.	
1215+113	MC 2	16.50	1.396	72	0.00	R	X		31.67	.	
1217+023	PKS	16.53	0.240	64	0.10	R	X		29.83	0.80	34
1219+755	MKN 205	14.50	0.070	42	0.14	O	X		29.49	0.88	65
1222+228	TON 1530	17.00	2.051	83	0.17	O	X		31.90	0.52	39
1223+252	4C 25.40	16.00	0.268	84	0.20	R	X		30.17	*	34
1225+317	B2	15.87	2.200	83	0.09	R	X		32.43	0.50	28
1226+023	3CR 273	12.86	0.158	64	0.03	R	X		31.06	0.24	30,34,65
1229-021	PKS	16.75	1.038	60	0.12	R	X		31.23	.	
1229+204	TON 1542	15.30	0.064	82	0.17	O	X		28.90	1.47	31
1237-101	ON-162	17.50	0.753	52	0.18	R			30.59	.	
1244+324	4C 32.41	17.20	0.949	85	0.10	R			30.96	0.60	39
1246+377	BSO 1	16.98	1.241	80	0.00	O	X		31.34	.	
1246-057	OS	17.00	2.212	57	0.10	O	X		32.02	.	
1248+305	4C 30.25	17.50	1.061	87	0.06	R			30.97	0.35	39
1250+568	3CR 277.1	17.93	0.321	61	0.00	R			29.66	0.28	29
1252+119	PKS	16.64	0.871	75	0.15	R	X		31.09	.	
1253-055	3C 279	17.75	0.538	57	0.11	R		D-1	30.03	1.45	29,32,65
1257+346	B 201	16.79	1.375	83	0.00	O	X		31.53	.	
1302-102	PKS	16.10	0.286	52	0.22	R	X		30.19	.	
1304+346	B 340	16.97	0.184	82	0.00	O	X		28.92	2.60	34
1305+069	3C 281	17.02	0.599	69	0.06	R			30.55	.	
1308+326	B2	16.20	0.997	83	0.00	R		D-1	31.37	1.60	44,50
1309-056	OS	17.00	2.180	57	0.22	O	X		32.00	.	
1317+277	TON 153	15.30	1.022	84	0.07	O	X		31.80	.	
1317+520	4C 52.27	17.00	1.060	65	0.00	R	X		31.16	.	
1318+290	TON 155	16.90	1.703	83	0.00	O	X		31.71	0.35	39
1318+290	TON 156	16.40	0.549	83	0.00	O	X		30.77	0.27	39
1321+294	TON 157	16.00	0.960	83	0.00	O	X		31.45	.	
1328+254	3CR 287	17.67	1.055	81	0.00	R			30.88	.	
1328+307	3CR 286	17.25	0.849	81	0.00	R			30.85	0.30	29,35
1331+170	MC 3	16.00	2.081	76	0.00	R	X		32.34	.	
1332+552	4C 55.27	16.00	0.249	61	0.00	R	X		30.10	*	38
1333+286	RS 23	18.74	1.908	80	0.00	O			31.14	.	
1340+289	B2	16.50	0.905	79	0.00	R	X		31.19	.	
1346-036	OS	17.00	2.344	56	0.27	O	X		32.09	.	
1351+640	PG	14.84	0.088	52	0.14	O	X		29.71	0.38	39,65
1354+195	PKS	16.02	0.720	73	0.06	R	X		31.18	0.31	29

Table 1.--Continued

OBJECT	HPQ	Δm	REF	τ	REF	W_λ	REF	L_x	REF	α_{ox}	θ_{rad}	REF	$\lvert\Delta\theta\rvert$
1127-145		0.1	4	.		.		.		.	.		.
1128+315		.		.		.		.		.	178+10	56	1+14
1137+660		2.0	4	MTS	21	.		27.64	63	1.26	112+ 1	54	15+16
1146+111		.		.		27	40	.		.	.		.
1146-037		.		.		.		.		.	.		.
1148-001		0.2	4,11	.		.		.		.	.		.
1150+497	P-1	-2.0	4,2,0	MTS	24	.		.		.	75+12	54	73+15
1156+295	D-1	-2.6	4,0	MT	0	109	39	.		.	.		.
1157+014		.		.		.		.		.	.		.
1202+281		1.4	9	.		.		26.70	63	1.23	.		.
1208+322		.		.		.		.		.	3+ 5	56	15+ 6
1211+334		.		.		.		.		.	.		.
1213-065		.		.		.		.		.	.		.
1215+113		.		.		30	40	.		.	.		.
1217+023		1.2	4	MTS	17	.		27.08	63	1.05	.		.
1219+755		.		.		.		26.12	63	1.29	.		.
1222+228		0.1	4	.		.		.		.	.		.
1223+252		0.4	4	DY	14	.		26.18	63	1.53	31+ 1	54	16+10
1225+317		.		.		.		28.34	63	1.57	.		.
1226+023		0.5	4	MT	24	.		27.89	63	1.22	45+ 3	58	11+ 4
1229-021		0.5	4	YR	20	.		.		.	.		.
1229+204		0.0	4	YR	6	.		.		.	.		.
1237-101		0.4	23	YRS	23	.		26.98	63	1.39	.		.
1244+324		-1.4	0	.		46	39	.		.	43+10	56	67+26
1246+377		.		.		.		.		.	.		.
1246-057		.		.		.		<27.84	63	>1.60	.		.
1248+309		.		.		24	39	.		.	40+10	56	1+39
1250+568		.		.		83	29	26.01	64	1.40	.		.
1252+119		0.5	4,23	YRS	23	.		27.43	63	1.40	.		.
1253-055	D-1	6.7	4,10	WK	15	34	32,65	27.70	63	0.89	.		.
1257+346		.		.		.		<27.39	64	>1.59	.		.
1302-102		1.2	0	.		.		.		.	.		.
1304+346		.		.		.		.		.	.		.
1305+069		.		.		.		.		.	13+ 3	54	8+29
1308+326	D-1	5.6		DY	49	.		.		.	.		.
1309-056		.		.		.		28.11	63	1.49	.		.
1317+277		.		.		.		.		.	.		.
1317+520		.		.		.		.		.	.		.
1318+290		.		.		.		27.81	63	1.50	.		.
1318+290		.		.		36	39	<26.29	63	>1.72	.		.
1321+294		.		.		.		.		.	.		.
1328+254		0.1	4,22	.		.		.		.	.		.
1328+307		0.1	4,22	.		8	29	.		.	.		.
1331+170		.		.		.		28.00	63	1.67	.		.
1332+552		-1.9	0	.		.		.		.	141+ 1	54	32+77
1333+286		.		.		.		<27.81	63	>1.28	.		.
1340+289		.		.		.		.		.	.		.
1346-036		.		.		.		<27.98	63	>1.58	.		.
1351+640		.		.		.		24.81	63	1.88	.		.
1354+195		0.5	4	MTS	17	.		.		.	165+ 5	54	2+23

Table 1.--Continued

OBJECT	NAME	V	Z	b^{II}	P_{ISM}	O/R	BS	HPQ	L_{OPT}	α_{OPT}	REF
1356+581	4C 58.29	16.00	0.321	57	0.00	R	X		30.34	.	
1358+043	PG	16.31	0.430	62	0.10	O	X		30.58	0.26	65
1415+172	OQ 125	16.50	0.821	68	0.00	R	X		31.12	0.20	40
1416+159	MC 3	17.00	1.472	67	0.00	R	X		31.56	1.30	40
1416+067	3CR 298	16.79	1.439	61	0.04	R	X		31.59	.	
1421+330	MKN 679	16.50	1.904	69	0.00	O	X		32.03	.	
1421+122	OQ 135	16.50	1.604	64	0.05	R	X		31.83	.	
1422+202	4C 20.33	17.86	0.871	67	0.06	R			30.62	0.41	39
1423+242	4C 24.31	17.20	0.649	69	0.04	R			30.58	0.47	39
1425+267	TON 202	15.68	0.366	69	0.00	R	X		30.59	0.72	65
1453-109	MSH14-121	17.37	0.940	41	0.90	R			30.83	1.62	33
1458+718	3CR 309.1	16.78	0.905	42	0.10	R	X		31.10	0.23	29
1508-055	PKS	17.00	1.191	43	0.67	R	X		31.29	.	
1510-089	PKS	16.52	0.361	40	0.80	R	X	P>1	30.20	0.92	29,65
1511+103	MC 2	17.00	1.546	53	0.25	R	X		31.61	1.10	40
1512+370	4C 37.43	15.50	0.371	58	0.08	R	X		30.81	0.07	39,65
1517+176	MC 3	17.50	1.390	54	0.42	R			31.32	2.10	40
1517+239	LB 9612	16.40	1.901	57	0.44	O	X		32.07	.	
1522+155	MC 3	17.50	0.628	53	0.33	R		O-1	30.47	0.20	40
1523+214	LB 9707	16.90	1.924	55	0.61	O	X		31.89	.	
1525+227	LB 9743	15.30	0.253	54	0.50	O	X		30.31	.	
1542+373	4C 37.45	17.70	0.972	52	0.09	R			30.80	0.23	39
1545+210	3CR 323.1	16.69	0.264	49	0.38	R	X		29.83	0.91	29,34
1546+027	PKS	18.00	0.413	41	0.96	R		O-1	29.78	.	
1548+114	MC 2	17.00	0.436	45	0.27	R	X		30.24	.	
1556+335	GC	17.00	1.650	49	0.22	R	X		31.66	.	
1611+343	DA 406	17.50	1.401	46	0.08	R			31.29	1.10	39
1612+266	NAB	17.30	0.395	45	0.21	O	X		30.10	0.30	39
1612+261	TON 256	15.41	0.131	45	0.27	O	X		29.72	0.79	29,65
1616+177	3CR 334	16.41	0.555	41	0.49	R	X		30.77	0.30	29,65
1622+238	3CR 336	17.47	0.927	42	0.38	R		P>1	30.82	.	
1623+269	4C 26.48	17.50	0.779	43	0.28	R			30.66	0.32	39
1626+363	4C 36.28	17.50	1.254	43	0.08	R			31.14	0.12	39
1633+382	4C 38.41	18.00	1.814	42	0.00	R			31.38	.	
1634+269	4C 26.49	17.75	0.561	40	0.36	R			30.18	0.72	39
1635+119	MC 2	17.00	0.146	35	0.61	R	X		29.20	.	
1641+399	3CR 345	15.96	0.595	41	0.00	R	X	O-1	30.90	1.15	27,33,65
1704+608	3CR 351	15.28	0.371	36	0.06	R	X		30.79	0.56	29,65
1720+246	V396 HER	16.42	0.175	30	0.69	O	X		29.60	.	
1721+343	4C 34.47	16.50	0.206	32	0.41	R	X		29.96	-0.21	39
1741+279	4C 27.36	17.70	0.372	26	0.67	R			29.78	0.79	39
1745+163	MC 3	17.60	0.392	21	0.84	R			29.91	0.60	40
1828+487	3CR 380	16.81	0.692	24	0.61	R	X		30.78	0.67	29,33
1830+285	4C 28.45	17.00	0.594	16	1.46	R	X		30.61	0.23	39
1954+513	OV 591	18.50	1.230	12	0.55	R			30.72	.	
2044-168	PKS	16.90	1.943	-33	0.60	R	X		31.90	.	
2044-027	3C 422	19.50	0.942	-27	0.41	R			29.94	2.50	53
2120+168	3CR 432	17.96	1.805	-23	0.93	R			31.43	1.13	29
2126-158	PKS	17.30	3.270	-42	0.56	R			32.39	.	
2128-123	PKS	15.98	0.501	-41	0.36	R	X		30.78	.	

Table 1.--Continued

OBJECT	HPQ	Δm	REF	τ	REF	W_λ	REF	L_x	REF	α_{ox}	θ_{rad}	REF	$\lvert\Delta\theta\rvert$
1356+581		.		.		.		.		.	.		.
1358+043		.		.		22	65	.		.	.		.
1413+172		.		.		52	40	.		.	.		.
1416+129		.		.		14	40	.		.	.		.
1416+067		.		.		.		27.70	63	1.49	78+10	58	45+18
1421+330		.		.		.		.		.	.		.
1421+122		-1.3	0	.		.		.		.	.		.
1422+202		0.2	4	.		40	39	27.17	63	1.32	0+ 5	54	14+40
1423+242		.		.		39	39	.		.	29+ 4	54	11+90
1425+267		.		.		63	65	.		.	56+ 3	54	19+ 3
1458-109		.		.		.		.		.	160+ 3	54	75+ 8
1458+718		0.1	4,21	.		.		27.53	63	1.37	.		.
1508-055		.		.		.		.		.	.		.
1510-089	P>1	5.4	4,26	WK	23,26	57	65	26.96	64	1.24	.		.
1511+103		.		.		32	40	.		.	.		.
1512+370		.		.		22	39,65	.		.	110+ 2	54	16+ 4
1517+176		-1.0	0	.		18	40	.		.	.		.
1517+239		.		.		.		.		.	.		.
1522+155	O-1	-1.0	0	.		17	40	.		.	.		.
1523+214		.		.		.		.		.	.		.
1525+227		-1.1	0	.		.		.		.	.		.
1542+373		.		.		10	39	.		.	.		.
1545+210		2.0	4	MTS	17	66	29	26.96	64	1.10	21+ 1	54	9+ 3
1546+027	O-1	.		.		.		.		.	.		.
1548+114		.		.		.		.		.	.		.
1556+335		.		.		.		27.48	63	1.61	.		.
1611+343		.		.		.		.		.	.		.
1612+266		.		.		14	39	26.14	64	1.52	.		.
1612+261		0.0	4	.		.		26.19	64	1.35	.		.
1618+177		1.0	4	MTS	17	58	29,65	.		.	118+ 3	54	23+15
1622+238	P>1	-1.2	4,0	.		.		.		.	30+ 4	54	17+11
1623+269		-1.1	0	.		40	39	.		.	33+10	55	32+43
1628+303		.		.		.		.		.	38+ 6	54	81+21
1633+382		.		.		.		27.89	64	1.34	.		.
1634+269		.		.		47	39	.		.	107+ 3	54	9+10
1635+119		.		.		.		26.09	63	1.20	.		.
1641+399	O-1	2.0	4	WK	17,16	55	27,65	27.61	64	1.26	149+ 6	62	80+ 6
1704+608		1.3	4	YR	17	24	65	26.63	63	1.60	34+ 1	54	58+12
1720+246		1.0	9	.		.		25.70	63	1.50	.		.
1721+343		1.2	0	.		.		.		.	162+ 1	61	19+ 5
1741+279		.		.		68	39	.		.	.		.
1749+163		.		.		.		.		.	.		.
1828+487		0.6	4	YR	24,17	.		27.61	63	1.22	116+10	57	55+26
1830+285		.		.		87	39	.		.	.		.
1954+513		.		.		.		.		.	.		.
2044-168		.		.		.		.		.	.		.
2044-027		.		.		38	53	.		.	.		.
2120+168		0.4	4	.		.		.		.	130+ 5	59	8+13
2126-158		.		.		.		29.43	63	1.14	.		.
2128-123		0.8	4	YRS	17	.		.		.	.		.

Table 1.--Continued

OBJECT	NAME	V	Z	b^{II}	P_{ISM}	O/R	BS	HPQ	L_{OPT}	α_{OPT}	REF
2134+004	PHL 61	18.00	1.936	-36	0.57	R			31.42	0.46	39
2135-147	PHL 1657	15.53	0.200	-43	0.57	R	X		30.10	0.62	29,34,65
2141+175	PKS	15.50	0.213	-26	1.07	R	X		30.15	.	
2142+110	MC 2	17.60	0.550	-31	0.61	R			30.29	0.30	40
2145+067	PKS	16.47	0.990	-34	0.61	R	X		31.31	0.32	29,65
2156+297	4C 29.64	17.50	1.753	-20	0.80	R			31.56	1.00	39
2201+315	4C 31.63	15.47	0.297	-19	0.79	R	X		30.58	0.25	39,65
2201+171	MC 3	18.80	1.080	-30	0.61	R		P>1	30.46	.	
2208-137	PKS	17.00	0.392	-50	0.31	R	X	D-1	30.13	.	
2209+080	4C 08.64	18.50	0.484	-38	0.43	R			29.46	2.38	39
2214+350	GC	18.50	0.510	-18	1.01	R			29.79	.	
2216-038	PKS	16.38	0.901	-47	0.56	R	X		31.23	.	
2223-052	3C 446	18.39	1.404	-49	0.66	R		D-1	30.96	1.75	27,29,65
2225-055	PHL 5200	17.70	1.981	-50	0.66	Q		D-1	31.62	0.85	65
2230+114	CTA 102	17.33	1.037	-39	0.60	R		D-1	30.99	0.99	29,35
2234+282	B2	19.00	0.795	-26	0.70	R		D>1	29.88	2.67	39
2247+140	4C 14.82	17.00	0.237	-39	0.36	R	X		29.65	.	
2251+158	3CR 454.3	16.10	0.859	-38	0.59	R	X	D>1	31.25	1.31	27,29,65
2251+113	PKS	15.82	0.323	-42	0.45	R	X		30.41	0.71	29,36,65
2251+244	4C 24.61	17.80	2.328	-31	0.61	R			31.91	1.51	39
2305+187	4C 18.69	16.50	0.313	-37	0.48	R	X		30.11	.	
2308+098	4C 09.72	15.00	0.432	-46	0.34	R	X		31.03	.	
2325+269	4C 27.52	17.50	0.875	-32	0.45	R			30.76	0.52	39
2325+293	4C 29.68	17.30	1.015	-30	0.63	R			31.00	0.35	29
2328+107	MC 2	18.10	1.498	-47	0.38	R			31.13	1.00	40
2340-036	PKS	17.00	0.896	-61	0.27	R	X		30.97	.	
2344+092	PKS	15.97	0.677	-50	0.53	R	X		31.14	0.24	39
2345-167	PKS	18.00	0.600	-72	0.05	R		D-1	30.15	.	
2349-010	PG	15.60	0.174	-60	0.27	Q	X		29.92	.	
2351-154	OZ-187	17.00	2.665	-72	0.10	R	X		32.25	.	
2353+283	4C 28.59	17.80	0.731	-33	0.34	R			30.47	0.39	39

Table 1.--Continued

OBJECT	HPQ	Δm	REF	τ	REF	W_λ	REF	L_x	REF	α_{ox}	θ_{rad}	REF	$\lvert\Delta\theta\rvert$
2134+004		3.5	4,12	.		.		.		.	.		.
2135-147		1.3	4	YR	17	.		26.89	63	1.23	104+ 2	54	35+57
2141+175		.		.		.		25.87	63	1.64	.		.
2142+110		.		.		.		.		.	.		.
2145+067		0.2	4	.		42	65	.		.	.		.
2156+297		-1.8	0	.		.		.		.	.		.
2201+315		0.2	4	.		41	39,65	.		.	.		.
2201+171	P>1	0.5	52	.		15	40	.		.	.		.
2208-137	D-1	.		.		.		.		.	.		.
2209+080		-1.0	18,0	MT	18	130	39	.		.	.		.
2214+350		.		.		.		.		.	.		.
2216-038		0.2	4,11	.		.		27.46	64	1.45	.		.
2223-052	D-1	3.4	4,41	WK	21,41	.		28.64	63	0.89	.		.
2225-055	D-1	0.2	4,7	.		.		<28.18	63	>1.32	.		.
2230+114	D-1	1.0	4,0	.		55	29	27.98	63	1.16	.		.
2234+282	D>1	.		.		73	39	.		.	.		.
2247+140		.		.		.		.		.	.		.
2251+158	D>1	2.3	4,45	DYS	5	14	27,65	.		.	.		.
2251+113		0.2	4	.		50	65	.		.	155+10	54	67+10
2251+244		.		.		.		.		.	.		.
2305+187		.		.		.		.		.	.		.
2308+098		.		.		.		.		.	147+ 2	54	37+ 3
2325+269		.		.		38	39	.		.	145+10	54	75+24
2325+293		.		.		.		.		.	115+ 2	54	9+20
2328+107		.		.		37	40	.		.	.		.
2340-036		.		.		.		.		.	.		.
2344+092		0.5	4	.		.		27.43	63	1.43	.		.
2345-167	D-1	2.5	4,41	WK	18	.		26.90	64	1.25	160+12	54	1+13
2349-010		.		.		.		.		.	.		.
2351-154		-1.5	0	.		.		.		.	.		.
2353+283		.		.		51	39	.		.	50+10	55	26+14

Reference Codes (Table 1)

0 This paper

1 Stockman and Angel 1978

2 Stockman 1978

3 Moore and Stockman 1981

4 Grandi and Tifft 1974

5 Angione 1971

6 Angione 1973

7 Barbieri and Erculiani 1968

8 Battistini, Bracessi, and Formiggini 1974

9 Bond, Kron, and Spinrad 1977

10 Eachus and Liller 1975

11 Folsom et al. 1971

12 Gottlieb and Liller 1978

13 Green 1976

14 Jackisch 1971

15 Kinman 1967

16 Kinman et al. 1968

17 Lü 1972

18 McGimsey et al. 1975

19 Miller 1977

20 Peach 1969

21 Penston and Cannon 1970

22 Sandage 1966

23 Scott et al. 1976

24 Tritton and Selmes 1971

25 Weistrop 1793b

26 Liller and Liller 1975

27 Visvanathan 1973

28 Nordsieck 1976

29 Oke, Neugebauer, and Becklin 1970

30 Wampler and Oke 1967

31 Wampler 1967a

32 Oke 1967

33 Wampler 1967b

34 Baldwin 1975

35 Oke 1966

36 Wampler 1968

37 Boksenberg, Carswell, and Oke 1976

38 Hawley, Miller, and Weymann 1977

39 Richstone and Schmidt 1980

40 Smith et al. 1977

41 Pollock et al. 1979

42 Arp et al. 1979

43 Baldwin et al. 1977

44 Miller, French, and Hawley 1978

45 Usher 1975

46 Kinman 1976

47 Smith 1978

48 Gottlieb and Liller 1976

49 Moore et al. 1980

50 Puschell et al. 1979

51 Kinman et al. 1967

52 Zotov and Tapia 1979

53 Smith and Spinrad 1980

54 Miley and Hartsuijker 1978

55 Wardle and Miley 1974

56 Fanti et al. 1977 .

57 Wilkinson, Richards, and Bowden 1974

58 Anderson and Donaldson 1967

59 Hogg 1969

60 MacDonald and Miley 1971

61 Conway, Burn and Vallee 1977

62 Davis, Stannard, and Conway 1977

63 Zamorani et al. 1980

64 Ku and Helfand 1980

65 Neugebauer et al. 1979

66 Mackay 1969

CHAPTER III

CHARACTERISTICS OF QSO POLARIZATION

The polarimetric characteristics of QSOs are described in this chapter. The observations presented represent a vast improvement in both the number of QSOs observed and the accuracy of the measurements. It is now possible to accurately describe the distribution of polarization for both radio-quiet and radio-loud QSOs. An important question to be answered is whether there is a clear polarimetric distinction between low and high polarization QSOs or whether these represent extremes of a continuous distribution. It is also possible to discuss the variability and wavelength dependence of polarization for both high and low polarization QSOs.

A. Polarization Measurements

More than 560 polarization measurements of the 231 QSOs in our survey are presented in Table 2. These measurements include the initial broadband survey measurements as well as variability and wavelength dependence observations. For each QSO, the coordinate designation, survey name, and galactic latitude (b^{II}) are given. For each measurement, the date (UT), percentage polarization (P and σ_p), and position angle (θ and σ_θ) are listed. The estimated broadband magnitude (m) is tabulated for most unfiltered measurements on the UAO 2.3 m telescope.

If the observation was made with a filter, the filter code is given in the next column (FIL); the filters are described at the end of the table. Relevant notes appear in the final column. The telescope used for all measurements not made on the UAO 2.3 m are noted in this column (KPNO 4m, UAO 1.5 m, and UAO 0.9 m).

Table 2. Optical Polarization Measurements of QSOs.

OBJECT	NAME	b^{II}	DATE	P	σ_P	θ	σ_θ	m	FIL	COMMENTS
0003+158	PHL 658	-45	9/07/77	0.68	0.20	100	9	15.8		
			12/07/77	1.66	0.30	92	5		B-A	
			12/07/77	1.06	0.33	100	9		R-H	
			10/08/78	0.62	0.16	114	7	15.4		
0007+106	III ZW 2	-51	9/09/77	0.28	0.19	96	18	15.6		
0017+154	3CR 9	-47	10/08/78	1.14	0.52	137	13	17.2		
0019+011	MCS 232	-61	11/05/78	0.93	0.26	24	8			4M
			1/14/80	1.38	0.65	44	14	17.9		
0024+224	NAB	-40	9/11/77	0.63	0.29	90	14	16.5		
0026+129	PG	-49	9/09/77	0.27	0.17	83	17	15.4		
0038-019	PKS	-64	9/08/80	0.55	0.34	117	18	16.9		
0043+008	MCS 275	-62	11/05/78	0.33	0.38	103	33			4M
0044+030	PKS	-60	12/07/77	0.27	0.21	179	22	15.6		
0051+291	4C 29.01	-33	10/27/78	0.80	0.38	119	14	16.7		
0054+144	PHL 909	-48	9/12/77	0.42	0.23	18	16	16.0		
0056-001	PHL 923	-63	10/27/78	0.86	0.62	99	21	17.3		
0058+019	PHL 938	-61	9/11/77	0.78	0.40	108	15	17.0		
0100+130	PHL 957	-50	9/11/77	0.84	0.29	112	10	16.5		
0106+013	PKS	-61	8/28/79	2.15	1.11	29	15	18.2		
			9/08/80	1.87	0.84	143	13	18.3		
			12/01/80	2.60	1.34	86	14	18.8		
0110+297	4C 29.02	-33	10/27/78	2.60	1.15	63	13	18.6		
0119-046	PKS	-66	9/09/77	1.03	0.64	175	18	17.6		
0122-003	PKS	-62	8/01/78	0.45	0.57	30	36	16.8		
0123+257	4C 25.05	-36	10/27/78	1.63	0.81	140	14	17.8		
0130+242	4C 24.02	-37	9/09/77	1.70	0.52	110	9	17.5		
			10/28/78	1.74	0.58	117	9	17.2		
0132+205	NAB	-41	9/12/77	0.70	0.69	103	28	17.9		
0133+207	3CR 47	-41	9/06/80	1.62	0.36	49	6	17.0		
0134+329	3CR 48	-29	9/09/77	1.41	0.24	148	5	16.1		
			1/13/78	1.43	0.26	150	5	16.0		
			1/13/78	1.34	0.41	162	9		B-A	
			1/13/78	0.77	0.27	143	10		R-E	
			1/14/78	1.45	0.29	156	6		B-A	
			1/14/78	1.35	0.29	162	6		R-E	
			10/28/78	1.28	0.24	153	5	15.9		
			11/05/78	1.81	0.24	156	4		B-B	4M
0137+060	PHL 1092	-55	9/12/77	0.32	0.34	27	30	16.8		
0137+012	PHL 1093	-59	7/11/78	1.26	0.88	19	20	17.6		
0137-010	NAB	-61	9/11/77	0.63	0.31	154	14	16.6		
0141+339	4C 33.03	-27	10/08/78	1.99	0.43	64	6	17.0		
			10/28/78	2.23	0.50	68	6	17.1		
			10/28/78	1.42	0.61	73	12		B-A	
			10/28/78	2.08	0.67	82	9		R-E	
			10/22/79	1.08	0.44	63	11	17.5		
0146+017	MCS 141	-58	11/06/78	1.17	0.23	138	5			4M
			1/14/80	2.44	0.89	139	10	18.0		
0147+089	PHL 1186	-51	10/08/78	1.25	0.65	155	15	17.5		
0148+090	PHL 1194	-51	10/27/78	1.21	0.54	139	13	17.1		
0159-117	3C 57	-67	8/01/78	1.04	0.73	72	20	16.5		
			8/07/78	0.65	0.30	4	13	16.3		
0202+319	DW	-28	9/09/80	2.02	0.29	61	4	17.5		
			12/01/80	0.95	0.77	96	23	18.2		
0205+024	NAB	-55	9/12/77	0.72	0.17	22	7	15.5		
			10/23/79	0.65	0.21	18	9	15.7		

Table 2.--Continued

OBJECT	NAME	b^{II}	DATE	P	σ_P	θ	σ_θ	m	FIL	COMMENTS
0214+108	PKS	-47	9/09/77	1.27	0.24	102	5	16.0		
			10/28/78	1.18	0.35	116	9	15.9		
			11/27/78	1.13	0.22	121	6	15.7		
			11/27/78	1.17	0.26	116	6		B-B	
			11/27/78	1.20	0.52	134	12		R-G	
			1/13/80	1.65	0.25	114	4	16.8		
0226-038	PHL 1305	-57	9/09/77	1.20	0.53	68	13	17.4		
0229+131	PKS	-43	10/08/78	1.26	0.79	148	18	17.8		
0229+341	3CR 68.1	-24	1/17/80	7.26	1.49	39	6			4M(A)
			9/06/80	7.54	1.31	52	5	19.3		
0232-042	PHL 1377	-56	9/09/77	0.91	0.32	163	10	16.5		
0237-233	PHL 8462	-65	10/08/78	0.25	0.29	43	33	16.1		
0333+321	NRAO 140	-19	10/27/78	0.97	0.32	157	9	16.5		
			10/23/79	0.93	0.36	145	11	16.8		
			3/16/80	1.55	1.42	41	26	18.3		
			9/09/80	0.51	0.32	145	18	16.8		
0336-019	CTA 26	-42	12/23/79	19.36	2.44	22	4	19.1		
			3/15/80	4.29	0.88	105	6	17.6		
0340+048	3CR 93	-38	1/17/80	2.15	1.42	79	19			4M(A)
			9/09/80	0.27	0.76	12	79	18.7		
0348+061	NAB	-35	12/07/77	1.39	0.51	157	10	17.2		
0349-146	MSH 03-19	-46	2/12/78	0.55	0.37	164	20	16.4		
			8/07/78	1.36	0.52	163	11	16.9		
0350-073	3C 94	-43	9/12/77	1.20	0.27	24	6	16.4		
			10/26/78	1.63	0.35	8	6	16.3		
			11/03/78	1.11	0.25	1	6			4M
			11/03/78	1.75	0.47	27	8		B-B	4M
			11/03/78	0.92	1.38	38	43		R-G	4M
			11/03/78	2.01	1.33	7	19		R-I	4M
			11/04/78	1.06	0.51	19	14		R-G	4M
			1/13/80	1.67	0.24	14	4	16.7		
0403-132	PKS	-43	1/13/78	3.90	0.61	3	4	17.2		
			1/14/78	3.82	0.50	4	4	16.8		
			1/14/78	4.31	0.54	6	4		B-A	
			1/14/78	3.66	0.47	179	4		R-E	
			10/08/78	0.32	0.89	156	81	18.0		
			11/26/78	0.95	0.54	15	16	17.4		
			10/23/79	3.38	0.54	172	5	17.2		
			1/14/80	0.37	0.83	140	64	17.9		
			3/17/80	1.21	1.30	44	31	18.1		
			9/08/80	1.41	0.73	126	15	18.1		
0405-123	PKS	-42	2/10/78	0.83	0.16	136	5	15.1		
			10/27/78	0.34	0.16	142	14	14.5		
			1/13/80	0.50	0.16	160	9	15.3		
0409+229	3C 108	-20	1/17/80	1.80	1.06	142	17			4M(A)
			9/09/80	2.04	0.49	132	7	18.5		
0414-060	3C 110	-37	12/07/77	0.78	0.22	146	8	15.9		
			10/27/78	0.92	0.36	141	11	15.9		
0420-014	PKS	-33	10/08/78	19.98	0.43	176	1	16.6		
			10/26/78	20.19	1.26	149	2			(B)
			10/27/78	17.08	0.50	155	1	16.5		
			10/27/78	16.52	0.66	157	1		B-A	
			10/27/78	16.86	0.46	151	1		R-E	
			10/28/78	18.91	0.49	153	1	16.6		
			11/26/78	10.24	0.62	150	2	17.3		
			11/24/79	18.94	0.39	150	1	16.1		
			3/15/80	17.72	0.61	161	1	17.2		

Table 2. --Continued

OBJECT	NAME	b^{II}	DATE	P	σ_P	θ	σ_θ	m	FIL	COMMENTS
0421+019	PKS	-31	10/27/78	0.26	0.35	58	38	16.5		
			10/23/79	0.36	0.60	101	47	17.4		
0440-003	PKS	-28	1/17/80	2.73	1.61	85	17			4M
			9/08/80	0.71	2.36	50	95	19.6		
0454+039	PKS	-23	12/07/77	0.32	0.28	147	25	16.3		
0516+165	3CR 138	-11	4/11/80	2.19	2.13	148	28	19.3		
0538+498	3CR 147	10	2/10/78	1.20	0.64	147	15	17.5		
			10/23/79	1.62	0.74	168	13	17.7		
0642+449	OH 471	18	12/06/77	1.67	0.88	1	15	18.1		
0704+384	4C 38.20	19	4/04/78	2.42	1.44	147	17	18.5		
0710+118	3CR 175	10	12/06/77	0.10	0.27	50	73	16.1		
0736+017	PKS	11	12/06/77	0.46	0.27	178	16	15.9		
			10/27/78	4.32	0.29	53	2	16.0		
			10/28/78	1.61	0.30	66	5	16.2		
			10/28/78	0.86	0.42	63	14		B-A	
			10/28/78	1.17	0.39	67	9		R-E	
			11/03/78	1.30	0.43	44	9			4M
			11/26/78	5.65	0.19	31	1	15.3		
			11/26/78	4.97	0.27	28	1		B-A	
			11/26/78	6.12	0.20	31	1		R-E	
			1/23/79	1.48	0.54	23	10	16.7		
			4/01/79	1.13	0.48	33	12	16.4		
			11/24/79	2.39	0.97	161	12	17.3		
			3/17/80	0.77	0.44	50	16	17.1		
			4/13/80	0.46	0.60	29	38	17.3		
0738+313	OI 363	24	12/07/77	0.19	0.23	31	34	16.0		
0740+380	3C 186	26	10/28/78	0.70	0.74	89	30	17.6		
0742+318	4C 31.30	25	12/07/77	0.58	0.18	5	8	15.5		
			11/26/78	0.58	0.17	32	8	15.1		
			1/13/80	0.64	0.16	4	7	16.0		
0752+258	OI 287	25	12/07/77	7.98	0.44	141	2	16.9		
			1/13/78	7.04	0.48	143	2	17.2		
			1/13/78	8.04	0.81	148	3		B-A	
			1/13/78	7.90	0.43	144	1		R-E	
			2/10/78	8.17	0.48	142	2	17.1		
			10/27/78	7.98	0.53	144	2	17.1		
			11/03/78	8.29	1.11	143	4			4M
			4/02/79	8.43	0.56	144	2	17.0		
			10/23/79	8.00	0.64	146	2	17.4		
			1/14/80	7.80	0.57	147	2	17.5		
			12/01/80	8.49	0.73	145	2			(B)
0758+143	3CR 190	22	1/17/80	5.34	2.81	46	15			4M(A)
0809+483	3CR 196	33	10/28/78	0.74	0.57	25	22	17.5		
0827+243	OJ 248	32	11/24/79	0.13	0.60	30	90	18.0		
			4/11/80	1.53	0.80	31	15	17.9		
0837-120	PKS	17	2/10/78	0.38	0.28	74	21	16.2		
0839+616	4C 61.19	37	12/07/77	0.52	0.64	54	35	17.4		
0846+513	#1	39	1/17/80	12.88	3.19	111	7			4M(A)
0847+190	LB 8741	34	12/07/77	0.61	0.40	119	19	16.5		
0848+163	LB 8775	34	12/07/77	1.37	0.54	27	11	17.1		
0850+140	3CR 208	33	2/12/78	1.05	0.50	106	14	17.2		
0855+143	3CR 212	35	1/17/80	7.40	2.15	12	8			4M(A)
			12/01/80	5.31	2.12	30	11	19.9		
0859-140	PKS	21	11/24/79	1.07	0.65	49	17			(B)
0906+430	3CR 216	43	1/17/80	3.34	0.98	97	8			4M(A)
			3/15/80	1.50	0.55	51	10	18.3		
			4/11/80	2.24	0.76	130	10	18.3		

Table 2. --Continued

OBJECT	NAME	b^{II}	DATE	P	σ_P	θ	σ_θ	m	FIL	COMMENTS
0906+015	PKS	31	2/12/78	2.39	0.63	31	7	17.5		
			11/27/78	1.00	0.70	11	20	17.6		
			1/23/79	1.46	0.68	67	13	17.5		
			3/15/80	2.34	0.52	57	6	17.9		
			4/11/80	3.16	0.53	68	5	17.7		
			4/13/80	1.66	0.56	63	10	17.9		
			12/01/80	7.33	0.70	160	3	18.0		
0906+484	PG	43	1/13/78	1.08	0.30	148	8	16.6		
0923+392	4C 39.25	46	11/27/78	0.50	0.50	128	28	16.6		
			4/30/79	0.64	0.40	82	18	16.9		
			4/13/80	0.91	0.35	102	11	16.8		
0953+254	OK 290	51	4/04/78	0.73	0.44	91	17	17.0		
			4/11/80	2.16	0.82	55	11	17.9		
0955+326	3C 232	52	1/13/78	0.18	0.24	101	37	16.0		
			4/12/80	0.87	0.41	44	13	16.0		
0957+003	PKS	41	4/02/79	0.38	0.52	150	40	17.1		
0958+551	MKN 132	49	1/13/78	0.23	0.25	46	32	16.1		
1001+054	PG	45	2/10/78	0.77	0.22	74	8	15.9		
			4/30/79	0.25	0.34	138	39	16.6		
1004+130	PKS	49	2/12/78	0.94	0.19	87	6	15.0		
			5/26/78	0.76	0.20	67	7	15.0		
			5/28/78	1.03	0.18	50	5		B-A	
			5/28/78	0.23	0.20	55	24		R-E	
			5/29/78	1.66	0.44	53	8		B-B	
			5/29/78	0.30	0.32	105	30		R-G	
			5/30/78	0.45	0.37	39	24		B-B	
			1/23/79	0.51	0.14	77	8	14.9		
			1/13/80	0.79	0.11	77	4	15.3		
			1/17/80	1.26	0.12	62	3		B-C	4M
			1/17/80	0.43	0.14	72	11		R-G	4M
1011+250	TON 490	55	2/12/78	0.37	0.28	88	22	16.3		
			4/12/80	0.38	0.50	75	38	16.8		
1012+008	PG	44	6/08/78	0.25	0.30	118	34	16.1		
1019+309	OL 333	57	2/12/78	0.27	0.46	76	49	17.1		
1020-103	OL-133	38	5/21/79	0.58	0.24	131	12	15.8		
1028+313	B2	59	1/13/78	0.25	0.23	166	25	15.8		
1036+064	4C 06.41	53	3/04/78	0.62	0.24	149	11	16.1		
1040+123	3CR 245	56	2/12/78	0.41	0.58	172	41	17.3		
1048-090	3C 246	43	2/12/78	0.85	0.30	96	10	16.2		
1049+215	4C 21.28	62	4/14/80	1.55	1.18	36	22	18.5		
1049+616	4C 61.20	50	2/10/78	0.83	0.34	176	12	16.7		
			4/02/79	1.85	0.43	9	7	16.3		
			1/13/80	0.74	0.43	34	17	17.6		
1055-045	OS	48	3/04/78	0.84	0.54	155	18	17.3		
1055+201	PKS	63	4/04/78	0.39	0.38	151	28	16.8		
1058+110	4C 10.30	59	4/03/78	1.01	0.59	71	17	17.3		
1100+772	3CR 249.1	39	1/13/78	0.71	0.22	76	8	15.8		
			4/02/79	0.96	0.48	54	9	15.7		
1103-006	PKS	52	2/12/78	0.37	0.26	138	20	16.1		
1104+167	4C 16.30	64	3/04/78	0.56	0.21	159	11	15.7		
			4/12/80	0.70	0.36	127	15	16.1		
1127-145	PKS	44	4/02/79	1.26	0.44	23	10	16.8		
1128+315	B2	72	2/10/78	0.95	0.33	172	10	16.6		
			4/12/80	0.29	0.33	14	33	16.2		
1137+660	3CR 263	50	1/13/78	0.35	0.20	97	16	15.7		

Table 2.--Continued

OBJECT	NAME	b^{II}	DATE	P	σ_P	θ	σ_θ	m	FIL	COMMENTS
1146+111	MC 2	68	5/21/79	2.17	1.42	108	19	18.7		
1146-037	PKS	55	3/04/78	0.40	0.27	42	20	16.3		
1146-001	PKS	59	5/28/78	0.77	0.67	128	25	17.3		
			4/14/80	0.61	0.55	72	26	17.4		
1150+497	4C 49.22	65	4/04/78	3.98	0.78	142	6	17.8		
			5/12/78	1.75	0.71	179	12	18.0		
			5/28/78	0.44	1.12	6	72	18.1		
			6/08/78	1.85	1.09	91	17	18.1		
			4/02/79	1.77	1.00	21	16	17.5		
			4/30/79	1.72	0.65	147	11	17.5		
			1/14/80	0.61	0.81	28	38	18.0		
			3/15/80	0.69	0.71	109	29	17.9		
			4/14/80	0.91	0.72	112	23	17.9		
1156+295	4C 29.45	78	2/10/78	9.24	1.19	24	4	18.2		
			3/14/78	4.83	0.25	119	1	16.2		
			3/14/78	5.15	0.32	113	2		B-A	
			3/14/78	6.16	0.35	111	2		R-E	
			5/29/78	0.86	0.63	116	21	17.4		
			11/27/78	8.73	0.40	93	1	16.7		
			1/23/79	3.60	0.55	3	4	17.2		
			4/02/79	7.59	0.47	122	2	16.5		
			4/11/80	14.38	0.39	65	1	16.4		
			4/11/80	0.12	0.14					CIRC(D)
			4/12/80	9.94	0.46	68	1	16.2		
1157+014	PKS	61	3/04/78	0.91	0.61	30	19	17.4		
1202+281	GQ COMAE	80	3/04/78	0.34	0.15	162	13	15.2		
			4/12/80	0.77	0.35	177	13	16.3		
1208+322	B2	80	3/14/78	1.03	0.24	26	7	16.0		
			4/30/79	1.10	0.29	10	8	16.4		
			1/13/80	1.25	0.36	15	8	16.8		
1211+334	ON 319	80	3/14/78	0.91	0.49	143	16	17.3		
1213-065	OS	55	1/13/78	1.11	0.64	19	17	17.5		
1215+113	MC 2	72	6/09/78	0.36	0.34	72	28	16.4		
1217+023	PKS	64	4/05/78	0.18	0.28	151	45	16.3		
1219+755	MKN 205	42	4/05/78	0.35	0.16	119	13	15.2		
1222+228	TON 1530	83	6/08/78	0.84	0.24	150	8	16.0		
			4/30/79	1.07	0.28	143	8	16.1		
1223+252	4C 25.40	84	6/09/78	0.66	0.38	38	16	16.7		
			1/23/79	1.01	0.42	55	12	16.9		
1225+317	B2	83	2/10/78	0.16	0.24	150	45	16.1		
1226+023	3CR 273	64	3/04/78	0.21	0.04	52	6	12.6		
			5/29/78	0.31	0.07	58	6	12.7		
			5/29/78	0.39	0.09	42	6		B-A	
			5/29/78	0.20	0.07	55	9		R-E	
			6/03/78	0.31	0.13	58	12			1.5M
			1/14/80	0.25	0.04	58	4	12.8		
1229-021	PKS	60	4/05/78	0.10	0.53	168	90	17.1		
1229+204	TON 1542	82	4/05/78	0.61	0.12	118	6	14.8		
			5/22/79	0.60	0.15	86	7	15.2		
			5/22/79	0.40	0.22	101	16		B-B	
			5/22/79	0.55	0.22	107	11		R-G	
			3/17/80	0.46	0.15	90	9	15.2		
1237-101	ON-162	52	5/28/78	1.23	1.18	81	28	17.9		
1244+324	4C 32.41	85	5/12/78	2.16	1.82	110	24	18.6		
1246+377	BSO 1	80	2/10/78	1.71	0.58	152	10	17.4		

Table 2.--Continued

OBJECT	NAME	b^{II}	DATE	P	σ_P	θ	σ_θ	m	FIL	COMMENTS
1246-057	OS	57	4/05/78	1.87	0.31	139	5	16.3		
			4/02/79	2.10	0.34	159	5	16.5		
			4/02/79	3.77	0.64	136	5		B-B	
			4/02/79	1.46	0.44	137	9		R-G	
			1/14/80	2.06	0.29	150	4	16.6		
1248+305	4C 30.25	87	5/29/78	1.42	1.90	41	38	18.3		
1250+568	3CR 277.1	61	5/30/78	1.30	0.78	136	17	17.7		
1252+119	PKS	75	6/08/78	0.44	0.34	141	22	16.5		
1253-055	3C 279	57	3/14/78	4.04	0.69	66	5	17.6		
			5/30/78	10.60	0.39	98	1	16.6		
			1/23/79	11.75	0.32	97	1	16.1		
			4/30/79	5.44	0.73	53	4	17.5		
1257+346	B 201	83	2/10/78	0.65	0.39	46	17	16.7		
1302-102	PKS	52	5/21/79	0.18	0.15	26	24	14.9		
			4/12/80	0.08	0.18	55	67	15.1		
1304+346	B 340	82	2/10/78	0.65	0.37	13	16	16.7		
1305+069	3C 281	69	4/04/78	0.34	0.34	5	29	16.5		
1308+326	B2	83	5/11/78	14.80	0.40	130	1			0.9M
			5/12/78	13.82	0.22	130	1	15.0		UT=4:43
			5/12/78	14.29	0.23	130	1	15.0		UT=9:04
			5/20/78	15.05	1.29	88	2			0.9M
			5/21/78	11.18	0.89	103	2			0.9M
			5/26/78	9.64	0.56	77	2			0.9M
			5/27/78	5.74	0.25	63	1			0.9M
			5/28/78	2.62	0.13	47	1	14.8		UT=5:30
			5/28/78	2.24	0.13	52	2	14.9		UT=7:28
			5/28/78	1.44	0.37	66	7		R-J	UT=7:50
			5/29/78	5.66	0.40	66	2		R-J	UT=4:00
			5/29/78	5.75	0.20	59	1	14.8		UT=4:20
			5/29/78	6.38	0.46	51	2		B-B	UT=4:33
			5/29/78	6.08	0.19	69	1	15.4		UT=8:57
			5/30/78	8.81	0.21	90	1	14.9		UT=3:55
			5/30/78	9.11	0.48	89	1		B-B	UT=4:23
			5/30/78	7.87	0.47	90	2		R-J	UT=4:44
			5/30/78	8.36	0.26	89	1	15.4		UT=8:05
			6/02/78	7.86	0.19	97	1			1.5M
			6/03/78	1.93	0.33	160	5			1.5M
			6/08/78	3.28	0.18	84	1	14.9		
			6/09/78	7.90	0.13	79	1	15.0		
			7/11/78	10.23	0.62	58	2	17.2		
			4/02/79	13.11	0.50	69	1	17.0		
			4/30/79	13.49	0.63	84	1	17.0		
			5/21/79	9.20	0.36	90	1	16.7		
			5/22/79	12.49	0.32	90	1	16.5		
			4/11/80	15.39	0.49	131	1	16.9		
			4/11/80	-0.08	0.17					CIRC(D)
			12/01/80	16.92	0.54	101	1	17.5		
1309-056	OS	57	6/09/78	2.33	0.57	179	7	17.1		
			1/14/80	1.50	0.69	167	13	17.5		
1317+277	TON 153	84	3/04/78	0.15	0.20	94	38	15.5		
1317+520	4C 52.27	65	7/01/78	0.52	0.35	15	19	16.7		
1318+290	TON 155	83	4/05/78	0.51	0.39	17	22	16.8		
1318+290	TON 156	83	4/05/78	0.61	0.28	51	13	16.6		
1321+294	TON 157	83	4/05/78	1.20	0.27	111	6	16.3		
			4/01/79	0.21	0.34	32	48	16.6		
			4/30/79	0.90	0.38	80	12	16.7		
			5/21/79	0.23	0.38	146	48	16.8		

Table 2.--Continued

OBJECT	NAME	b^{II}	DATE	P	σ_P	θ	σ_θ	m	FIL	COMMENTS
1328+254	3CR 287	81	4/02/79	0.61	0.66	119	31	17.6		
1328+307	3CR 286	81	5/12/78	1.29	0.49	47	11	17.0		
1331+170	MC 3	76	6/09/78	0.37	0.32	90	24	16.4		
1332+552	4C 55.27	61	7/01/78	0.33	0.89	109	77	17.9		
1333+280	RS 23	80	1/17/80	0.26	0.49	14	54			4M
1340+289	B2	79	4/05/78	0.81	0.35	45	12	16.6		
1346-036	OS	56	6/09/78	0.17	0.48	37	78	17.0		
1351+640	PG	52	2/10/78	0.66	0.10	11	4	14.4		
			5/28/78	0.63	0.16	3	7	14.5		
			5/28/78	0.89	0.24	17	8		B-A	
			5/28/78	0.61	0.16	4	7		R-E	
			1/14/80	0.70	0.11	14	4	14.6		
			3/17/80	0.69	0.13	3	5	14.9		
1354+195	PKS	73	6/08/78	0.34	0.27	167	23	16.2		
1356+581	4C 58.29	57	4/04/78	0.40	0.29	116	20	16.3		
1358+043	PG	62	6/08/78	0.47	0.27	170	16	16.2		
1415+172	OQ 125	68	7/01/78	0.85	0.52	85	17	17.2		
			5/21/79	0.44	0.65	161	42	17.5		
1416+159	MC 3	67	5/21/79	1.06	0.85	95	23	17.9		
1416+067	3CR 298	61	6/09/78	0.77	0.39	123	14	16.7		
1421+330	MKN 679	69	4/05/78	0.32	0.32	80	29	15.9		
1421+122	OQ 135	64	6/08/78	0.42	0.91	111	62	17.8		
1422+202	4C 20.33	67	5/12/78	0.40	0.56	166	40	17.2		
1423+242	4C 24.31	69	5/12/78	0.17	0.56	40	90	17.2		
1425+267	TON 202	69	6/08/78	1.42	0.23	74	5	16.0		
			1/23/79	2.20	0.27	83	3	16.2		
			4/01/79	2.10	0.28	71	4	16.3		
			4/01/79	1.41	0.35	68	7		B-B	
			4/01/79	2.68	0.57	70	6		R-G	
			1/14/80	1.74	0.24	73	4	16.5		
1453-109	MSH14-121	41	8/07/78	1.08	0.99	47	26	17.8		
			4/02/79	1.64	0.54	59	9	17.4		
			5/21/79	1.89	0.90	48	13	17.7		
1458+718	3CR 309.1	42	6/09/78	0.65	0.47	164	20	16.9		
1508-055	PKS	43	7/01/78	1.51	0.46	67	9	16.9		
			3/15/80	2.02	0.82	71	12	17.9		
1510-089	PKS	40	4/04/78	1.90	0.40	79	6	16.7		
			4/02/79	1.32	0.36	26	8	16.5		
			3/15/80	7.84	0.50	63	2	17.3		
			3/17/80	2.18	0.24	112	3	16.5		
			4/11/80	1.60	0.59	101	11	16.9		
			4/12/80	2.06	0.42	119	6	16.8		
			4/13/80	2.54	0.31	104	3	17.1		
			4/14/80	1.23	0.39	119	9	16.9		
			6/20/80	1.73	0.67	139	11	16.8		
1511+103	MC 2	53	6/09/78	0.58	0.50	71	25	17.2		
			5/22/79	0.46	0.60	79	38	17.6		
1512+370	4C 37.43	58	6/08/78	1.10	0.23	109	6	16.0		
			5/05/78	1.51	0.48					1.5M(C)
			4/30/79	1.17	0.24	77	6	16.0		
1517+176	MC 3	54	5/22/79	2.25	1.15	169	15	18.5		
			9/09/80	2.52	2.50	176	28	19.1		
1517+239	LB 9612	57	6/08/78	0.24	0.55	60	66	17.2		
1522+155	MC 3	53	6/21/79	12.55	1.23	8	3	18.2		
			8/29/79	3.42	1.22	103	10	18.2		
			6/20/80	7.90	1.46	32	5	18.6		
			9/09/80	3.60	1.84	154	15	18.9		

Table 2. --Continued

OBJECT	NAME	b^{II}	DATE	P	σ_P	θ	σ_θ	m	FIL	COMMENTS
1523+214	LB 9707	55	7/01/78	0.24	0.77	23	90	17.7		
1525+227	LB 9743	54	9/12/77	0.63	0.32	139	15	16.6		
			4/12/80	0.81	0.44	104	16	16.7		
1542+373	4C 37.45	52	4/02/79	1.43	1.02	154	20	18.1		
1545+210	3CR 323.1	49	9/11/77	1.65	0.24	16	4	16.1		
			5/05/78	2.37	1.25					1.5M(C)
			4/02/79	1.51	0.30	19	6	15.8		
			5/22/79	1.03	0.20	4	5	15.6		
			5/22/79	0.82	0.24	172	8		B-B	
			5/22/79	0.61	0.26	176	12		R-G	
			3/15/80	1.45	0.30	6	6	16.3		
1546+027	PKS	41	4/11/80	3.37	0.45	123	4	17.5		
			4/13/80	4.10	0.62	140	4	17.7		
1548+114	MC 2	45	9/12/77	0.87	1.31	170	43			(B)
1556+335	GC	49	9/11/77	0.16	0.56	67	90	17.5		
1611+343	DA 406	46	5/12/78	1.66	0.67	134	11	18.0		
			5/29/78	1.37	1.22	94	25	18.2		
1612+266	NAB	45	9/09/77	1.24	0.56	81	13	17.5		
1612+261	TON 256	45	4/04/78	0.07	0.13	151	52	15.2		
			4/12/80	0.36	0.28	109	22	15.9		
1618+177	3CR 334	41	9/08/77	0.81	0.42	95	15	17.1		
1622+238	3CR 336	42	5/12/78	4.00	2.01	68	14	18.5		
			5/30/78	4.17	1.37	32	9	18.9		
			6/02/78	4.28	1.97	149	13			1.5M
			6/08/78	2.99	1.37	51	13	18.3		
			4/30/79	1.02	0.71	57	20	18.2		
1623+269	4C 26.48	43	5/30/78	3.32	1.45	109	12	18.6		
			7/01/78	1.72	0.99	33	16	18.5		
1628+363	4C 36.28	43	8/07/78	0.59	0.68	127	33	17.9		
			4/30/79	0.88	0.78	112	25	17.8		
1633+382	4C 38.41	42	6/20/80	2.55	0.95	97	11	18.2		
			9/06/80	1.35	1.12	171	24	18.1		
1634+269	4C 26.49	40	5/12/78	1.19	0.66	108	16	17.6		
			8/07/78	2.10	0.78	123	11	17.7		
1635+119	MC 2	35	9/08/77	0.82	0.38	175	13	16.9		
			9/08/80	0.39	0.63	77	46	17.4		
1641+399	3CR 345	41	9/08/77	3.57	0.19	173	1	15.6		
			5/05/78	8.78	1.71					1.5M(C)
			5/28/78	13.81	0.26	62	1	15.5		
			5/28/78	14.09	0.28	62	1		R-E	
			5/29/78	15.39	2.00	70	1		B-A	(E)
			5/29/78	16.48	0.26	68	1		R-E	
			5/29/78	15.57	0.25	68	1	15.8		
			5/30/78	11.72	0.81	71	1		B-A	
			7/07/78	4.49	0.34	32	2			UT=6:00
			7/07/78	3.31	0.49	23	4		B-A	1.5M
			7/07/78	5.14	0.37	31	2		R-E	1.5M
			7/07/78	4.32	0.58	31	4			UT=8:07
			7/11/78	6.16	0.21	32	1	16.5		
			8/28/79	9.32	0.38	50	1	16.2		
			4/12/80	7.22	0.50	44	2	16.5		
			4/12/80	-0.05	0.23					CIRC(D)
			8/09/80	12.27	0.47	166	1	16.3		
1704+608	3CR 351	36	9/08/77	0.31	0.17	96	16	15.5		
			7/11/78	0.34	0.20	87	17	15.7		
1720+246	V396 HER	30	9/09/77	0.70	0.48	64	19			(B)

Table 2.--Continued

OBJECT	NAME	b^{II}	DATE	P	σ_P	θ	σ_θ	m	FIL	COMMENTS
1721+343	4C 34.47	32	9/09/77	1.14	0.25	145	7	16.2		
			5/30/78	0.58	0.39	148	19		B-A	
			5/30/78	0.23	0.30	27	38		R-E	
			5/22/79	0.74	0.16	143	6	15.3		
1741+279	4C 27.38	26	5/12/78	0.84	0.61	72	21	17.5		
1745+163	MC 3	21	9/08/80	0.86	0.96	117	32	18.0		
1828+487	3CR 380	24	9/08/77	0.44	0.38	171	25	16.8		
1830+285	4C 28.45	16	9/11/77	1.28	0.56	166	12	17.5		
			4/30/79	0.73	0.57	72	22	17.4		
1954+513	OV 591	12	9/07/80	1.51	0.53	164	10	18.2		
2044-168	PKS	-33	6/21/79	1.01	0.67	22	19	17.3		
2044-027	3C 422	-27	9/08/80	3.18	1.58	100	14	19.6		
2120+168	3CR 432	-23	6/09/78	1.06	0.63	109	17	17.5		
			8/07/78	2.03	0.95	137	13	18.3		
2126-158	PKS	-42	8/09/80	0.87	0.55	118	18	17.4		
2128-123	PKS	-41	10/08/78	0.26	0.20	23	22	15.4		
			7/07/78	0.72	0.27	34	11			1.5M
			10/27/78	0.56	0.19	10	10	15.4		
2134+004	PHL 61	-36	6/09/78	0.42	0.37	84	25	16.7		
			6/03/78	1.28	0.83	119	19			1.5M
			8/28/79	0.50	0.54	146	31	17.3		
2135-147	PHL 1657	-43	7/01/78	0.34	0.34	80	29	16.0		
			7/07/78	0.62	0.48	75	22			1.5M
			10/08/78	0.54	0.39	173	21	16.0		
2141+175	PKS	-26	9/08/77	0.22	0.18	72	24	15.6		
2142+110	MC 2	-31	6/21/79	0.91	0.66	147	22	18.0		
2145+067	PKS	-34	9/08/77	0.61	0.23	138	11	16.1		
			12/07/77	0.47	0.43	65	26		B-A	
			12/07/77	0.32	0.46	152	41		R-H	
2156+297	4C 29.64	-20	10/08/78	2.10	2.95	133	40	19.3		
2201+315	4C 31.63	-19	9/08/77	0.23	0.14	80	18	15.1		
2201+171	MC 3	-30	6/22/80	2.72	1.28	11	13	18.6		
2208-137	PKS	-50	8/28/79	5.14	0.36	98	2	16.6		
			8/29/79	8.71	0.38	119	1	16.5		
			8/29/79	6.65	0.67	117	3		B-B	
			8/29/79	8.68	0.77	120	2		R-G	
			10/23/79	1.08	0.46	133	12	16.8		
			11/24/79	1.56	0.66	171	12	16.9		
2209+080	4C 08.64	-38	8/09/80	2.93	1.90	116	18	20.0		
			9/06/80	2.31	2.14	151	26	19.8		
2214+350	GC	-18	9/09/80	1.13	0.58	87	15	18.3		
2216-038	PKS	-47	9/08/77	1.09	0.44	139	11	17.2		
2223-052	3C 446	-49	9/12/77	13.58	0.36	153	1	16.8		UT=5:46
			9/12/77	13.48	0.61	147	1		B-A	UT=6:40
			9/12/77	12.26	0.55	142	1		R-F	UT=7:26
			9/12/77	11.90	0.31	142	1	16.7		UT=7:36
			9/12/77	12.24	0.38	145	1	17.0		UT=9:12
			7/11/78	7.32	0.15	81	1	14.6		UT=8:42
			7/11/78	7.85	0.35	84	1		B-A	UT=9:02
			7/11/78	7.16	0.22	81	1		R-F	UT=9:15
			7/11/78	7.10	0.22	83	1	14.7		UT=9:35
			7/11/78	7.16	0.21	83	1	14.6		UT=11:05
			8/01/78	8.10	0.26	89	1	15.3		
			10/08/78	14.45	0.33	147	1	15.5		
			10/27/78	10.64	0.29	104	1	15.2		
			10/28/78	8.05	0.28	111	1	15.3		

Table 2. --Continued

OBJECT	NAME	b^{II}	DATE	P	σ_P	θ	σ_θ	m	FIL	COMMENTS
2225-055	PHL 5200	-50	9/11/77	4.09	0.79	166	6	17.9		
			10/05/77	3.86	1.20	155	9	18.5		
			10/28/78	4.40	0.65	167	4	17.5		
			11/05/78	3.42	0.47	162	4		R-G	4M
2230+114	CTA 102	-39	7/01/78	7.32	0.32	118	1	16.5		
			7/11/78	1.46	0.48	114	9	16.6		
			8/01/78	0.92	0.94	102	29	17.2		
			10/08/78	10.92	0.36	162	1	16.3		
			10/27/78	7.28	0.33	166	1	16.3		
			10/27/78	5.34	0.63	169	3		B-A	
			10/27/78	9.41	0.52	163	2		R-E	
			10/28/78	5.70	0.36	168	2	16.4		
			10/28/78	5.20	0.56	167	3		B-D	
			10/28/78	7.69	0.45	167	2		R-E	
2234+282	B2	-26	8/09/80	3.58	1.82	11	15	19.9		
			9/06/80	4.54	1.10	18	7	19.1		
			9/08/80	2.66	0.84	133	9	19.2		
			12/01/80	12.28	2.69	134	7	19.6		
2247+140	4C 14.82	-39	9/09/77	1.39	0.38	75	8	16.9		
			8/28/79	0.44	0.39	83	25	16.9		
2251+156	3CR 454.3	-38	9/11/77	0.36	0.38	137	30	16.9		
			6/08/78	2.94	0.32	144	3	16.4		
			7/11/78	0.92	0.38	162	12	16.3		
			8/01/78	1.47	0.56	32	11	16.9		
			10/08/78	0.56	0.35	46	18	16.4		
			10/27/78	0.06	0.43	149	90	16.3		
			11/27/78	0.21	0.33	127	45	16.3		
			8/28/79	1.02	0.48	53	13	16.7		
			10/23/79	3.52	0.58	24	5	17.1		
2251+113	PKS	-42	9/06/77	0.89	0.22	50	7	16.0		
			11/04/78	1.27	0.17	39	4			4M
			11/04/78	1.34	0.16	45	3		B-B	4M
			11/04/78	1.00	0.15	49	4		R-G	4M
2251+244	4C 24.61	-31	8/01/78	5.08	1.64	112	10	16.8		
			11/27/78	1.34	0.67	113	14	17.9		
			6/22/80	0.62	1.14	70	52	18.3		
2305+187	4C 18.69	-37	9/07/77	0.38	0.45	21	33	17.1		
2308+098	4C 09.72	-46	9/11/77	1.08	0.24	121	6	16.0		
			10/08/78	0.70	0.25	130	10	15.5		
			10/28/78	1.73	0.33	99	5	15.7		
			10/28/78	1.21	0.32	109	8		B-A	
			10/28/78	0.62	0.33	134	15		R-E	
			6/23/80	1.14	0.16	105	4	16.0		
2325+269	4C 27.52	-32	10/08/78	0.85	0.65	70	22	17.5		
2325+293	4C 29.68	-30	8/07/78	0.86	0.61	101	20	17.8		
			10/08/78	0.45	0.65	117	41	17.5		
2328+107	MC 2	-47	6/23/80	1.72	1.78	46	29	19.0		
			9/09/80	0.19	0.52	139	77	17.6		
2340-036	PKS	-61	9/11/77	0.87	0.25	130	8	16.2		
2344+092	PKS	-50	9/11/77	0.35	0.21	92	17	15.9		
			12/07/77	0.90	0.34	49	11		R-H	
2345-167	PKS	-72	11/27/78	4.93	1.45	70	8	18.3		
			8/28/79	3.10	0.76	156	7	18.1		
			11/24/79	18.54	1.67	161	3	19.2		
2349-010	PG	-60	7/01/78	0.91	0.21	143	7	15.7		
2351-154	OZ-187	-72	8/28/79	3.73	1.56	13	12	18.5		
2353+283	4C 28.59	-33	10/27/78	1.43	0.54	76	11	17.2		

Table 2--Continued

Footnotes: (A) Filter R-E used to improve statistics; considered broadband observation.

(B) Broadband magnitude not reliable.

(C) Position angle not calibrated.

(D) Circular polarization measurement (V/I).

(E) σ_p is large due to uncertain modulation efficiency; σ_θ is correct.

Filter Codes: (Effective wavelength and bandpass in microns.)

B-A $CuSO_4$ (λ_{eff}=0.45, $\Delta\lambda$ = 0.27)

B-B Hoya B-390 + $CuSO_4$ (λ_{eff}=0.41, $\Delta\lambda$ = 0.15)

B-C Hoya B-390 (λ_{eff} = 0.41, $\Delta\lambda$ = 0.15)

B-D Hoya L-42 + $CuSO_4$ (λ_{eff} = 0.51, $\Delta\lambda$ = 0.14)

R-E Corning 2-63 (λ_{eff} = 0.73, $\Delta\lambda$ = 0.26)

R-F Corning 2-64 (λ_{eff} = 0.77, $\Delta\lambda$ = 0.19)

R-G Schott RG 715 (λ_{eff} = 0.79, $\Delta\lambda$ = 0.12)

R-H Hoya O-56 (λ_{eff} = 0.71, $\Delta\lambda$ = 0.30)

R-I Hoya R-64 (λ_{eff} = 0.74, $\Delta\lambda$ = 0.20)

R-J Schott RG 780 (λ_{eff} = 0.82, $\Delta\lambda$ = 0.08)

B. General Distribution of QSO Polarization

The initial objective of this discussion is to determine the general distribution of polarization for radio-loud and radio-quiet QSOs. In order to determine this distribution, we restrict our attention to the initial measurements of the bright QSO survey. This survey is large (142 QSOs) and is least susceptible to selection effects; in addition, the measurements of these brighter QSOs are, in general, more accurate and therefore more suitable to defining the distribution. The bright QSO sample contains 96 radio-selected and 46 optically-selected QSOs.

The probability distributions of polarization for the initial measurements of the bright QSO sample, derived by the Lucy algorithm (§ II.B.1), are shown in Figure 4. The top panel (4a) is the distribution for the entire sample, while the lower panels illustrate the distributions for the subsets of radio-selected (4b) and optically-selected (4c) QSOs. Each distribution has a comparison interstellar polarization distribution, as discussed in § II.B.2. In all cases, the distribution of QSO polarization is clearly weighted towards higher polarizations than the comparison distribution, implying that each sample exhibits significant intrinsic polarization.

The most outstanding feature of these distributions is that the great majority of QSOs have very low optical polarization. Of 142 initial measurements of the QSOs in this sample, only five exhibit polarizations $P \geqslant 4\%$ (and would lie to the right of the figures).

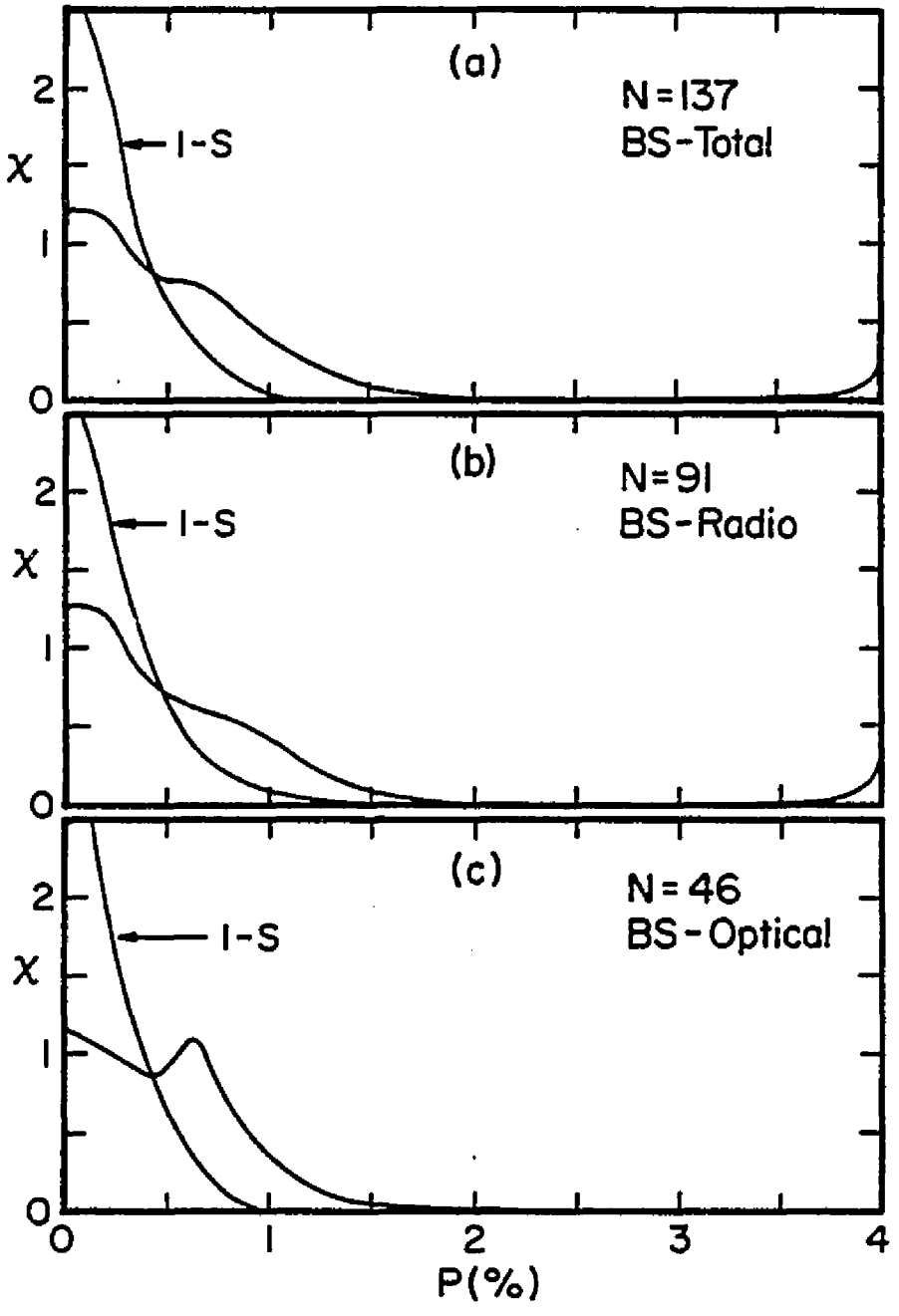

Figure 4. The probability distributions of polarization for the initial measurements of (a) the entire bright QSO sample, (b) the radio-selected bright QSOs, and (c) the optically-selected bright QSOs.

remainder of the QSOs exhibit distinctly lower polarizations ($P < 2\%$). The distributions are continuous for $P \lesssim 2\%$; the typical polarization is only $\sim 0.6\%$.

There is little difference between the distributions of polarization for radio- and optically-selected QSOs, as shown in (b) and (c) of Figure 4. There is a stronger peak in the distribution for optically-selected QSOs at $P \sim 0.65\%$; this peak is caused by several accurate measurements near this value and it is not clear if this is, in fact, a preferred value. To the limits of this survey, we would conclude that there do not appear to be any significant differences in the distribution of polarization (at low polarizations) between radio-loud and radio-quiet QSOs.

For completeness, we show in Figure 5 the polarization probability distributions for the initial measurements of the entire general QSO survey. Excluding the initial measurements which showed high polarization, there are 162 radio-selected QSOs (panel b) and 49 optically-selected QSOs (c) for a total of 211 QSOs (a). The characteristics of the three distributions are similar to those for the bright survey (Figure 4).

The discontinuity in the distribution of polarization between low polarization QSOs ($P < 2\%$) and highly polarized QSOs is an important result of the survey. In all our observations, very few QSOs exhibit intermediate polarizations in the range $2\% < P < 4\%$; the few measurements in this range often have large errors which act to increase the measured polarization. This break in the distribution is

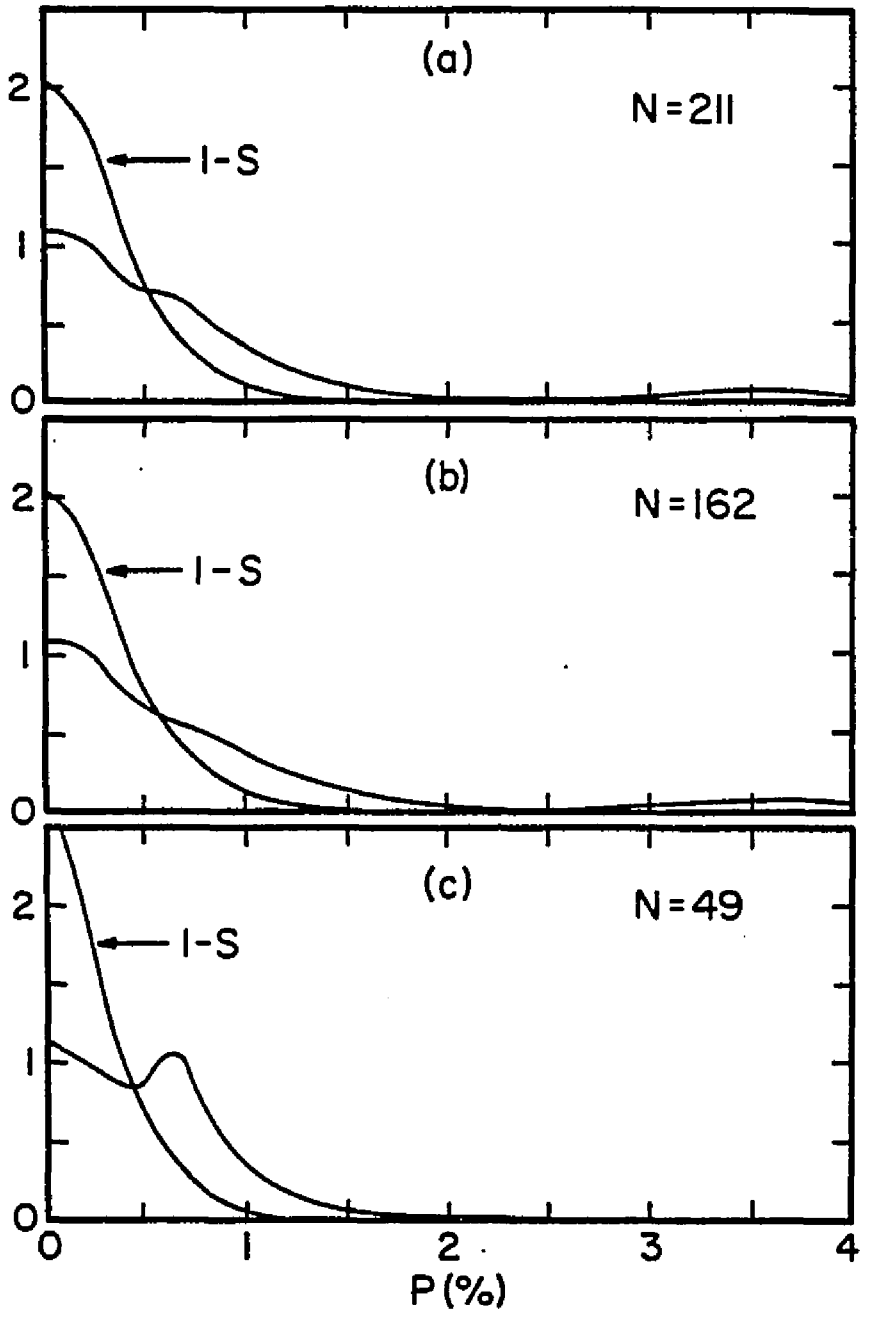

Figure 5. The probability distributions of polarization for the initial measurements of (a) the entire QSO survey, (b) all radio-selected QSOs, and (c) all optically-selected QSOs.

evidence for two distinct classes of QSOs--the "normal" low plarization QSOs and the rare highly polarized QSOs. The precise value of polarization used to distinguish the two classes is somewhat arbitrary. We have adopted $P \geqslant 3\%$ to denote a "highly" polarized QSO (HPQ). The additional criterion which must be imposed is that the significance of the measurement be $P \geqslant 3\ \sigma_p$.

Five of the 142 QSOs in the bright survey show high polarization on the initial measurement. In determining the fraction of QSOs which are highly polarized, it is necessary to note two further results. First, some HPQs exhibit phases of low polarization and therefore any survey will reveal only some of the HPQs in the sample; this behavior does blur the distinction between normal QSOs and HPQs. For example, repeated measurements of the bright QSO sample show three additional QSOs to be highly polarized, for a total of eight known HPQs in the sample. Second, the eight HPQs in this sample are all radio-loud QSOs. In fact, of 27 definite and possible HPQs now known, only one (PHL 5200) is radio-quiet. This correlation, that the HPQs are (nearly all) radio-loud, is the one polarimetric distinction which can be made between radio-loud and radio-quiet QSOs (and will be discussed further in § IV.B). Thus, the results of the bright survey show that (at least) 8 of 96 radio-loud QSOs are HPQs, while none of the 46 optically-selected QSOs surveyed exhibit high polarization.

C. Polarization Characteristics

In this section, we discuss the characteristics of the polarization of QSOs. The above analysis of the distribution of polarization suggests that there is a fundamental distinction between low and high polarization QSOs. Therefore, the properties of polarization are discussed separately for the two classes.

1. Highly Polarized QSOs

The degree of polarization of the HPQs ranges from 0 - 20%. The typical polarization appears to be different for various HPQs. For example, PKS 0403-132, 0736+017, and 1510-089 usually have relatively low polarization ($P \sim 1 - 5\%$), while PKS 0420-014 and 3C 446 (2223-052) have always been observed to be high ($P > 10\%$). Many of the HPQs are observed to have low polarization phases; this aspect of the polarization was not known from previous observations of HPQs (e.g., Visvanathan 1973). This behavior implies that some QSOs in the general survey which have only been observed to have low polarization may actually be "latent" HPQs. Based on the frequency that known HPQs show polarization $P < 3\%$, we estimate the completeness of HPQs from the survey to be $\gtrsim 70\%$.

The observations of the HPQs show that strong rapid polarimetric variability is a common property of nearly all HPQs. Strong month to month variations (the most common baseline of monitoring) are frequently observed. In eleven of twelve cases (excluding B2 1308+326) when observations of definite HPQs were made over baselines of one or two

nights, there was statistically significant variability. The most rapid variability was observed in 3C 446 on 12 September 1977, when there was a 10° position angle rotation in two hours. Strong hourly variability appears to be rare, however, as it was not observed in 3C 446 on 11 July 1978 (during a bright flare), in 3C 345 (1641+399), or in B2 1308+326; also, the nightly variations often have moderate amplitude. Characteristic time scales for large amplitude variability are probably on the order of a few days. A detailed discussion of the variability of B2 1308+326 is presented in § VI.A; this intensive monitoring program supports the conclusions that the characteristic time scale of variability is $\tau \sim 1$ day and strong hourly variability is not present.

At least two HPQs are distinct in their lack of polarimetric variability. OI 287 (0752+258) has been observed nine times over three years and has shown virtually constant polarization, position angle, and brightness. This behavior marks OI 287 as an atypical HPQ. PHL 5200 (2225-055) has shown no variability in three measurements over one year. This radio-quiet HPQ is clearly unusual in most aspects from other HPQs and will be discussed further in § IV. Another radio-loud HPQ, 3CR 68.1 (0229+341), has been measured twice over a period of nine months and did not exhibit variability; additional monitoring is required to determine if it is also a non-variable HPQ.

An interesting question is whether there is a consistent pattern between the variability of the brightness and the degree of polarization (e.g., Kinman 1977). One might expect the polarization to increase with

brightness if there is an underlying constant unpolarized component. Using the crude broadband magnitudes, we find no consistent pattern. Two HPQs, 4C 29.45 (1156+295) and 3C 446 (2223-052) brightened by $\sim$2 mag between successive observations and had lower polarizations. The opposite pattern is seen in our observations of 3C 279 (1253-055) and 3CR 345 (1641+399), which had higher polarizations when brighter. Other HPQs, such as PKS 0403-132, 0736+017, 1522+155, and 2208-137 have shown marked polarimetric variability during relatively stable phases of brightness. In summary, the polarization can be high and variable during both bright and faint phases, and there is not a simple correlation for all HPQs between polarization and brightness. The observations of HPQs by Visvanathan (1973) are consistent with this conclusion. Simultaneous polarimetric and (more accurate) photometric monitoring are required to examine the details of any correlation.

While most HPQs exhibit a wide range of position angles, there are suggestions of a preferred position angle in PKS 0403-132, 0420-014, and 0906+015 (as well as the apparently constant HPQs OI 287, PHL 5200, and 3CR 68.1). Further monitoring is required to establish this behavior.

Circular polarization measurements of three HPQs are included in Table 2. These observations were made when the objects, 4C 29.45 (1156+295), B2 1308+326, and 3CR 345 (1641+399), had high linear polarization ($P > 7\%$). Null results were obtained in each case, with upper limits of $|V/I| < 0.5\%$. These results support the conclusion of

Landstreet and Angel (1972) and others that QSOs do not have significant circular polarization in the optical regime.

We have made fifteen pairs of filtered observations of eleven HPQs in order to determine the wavelength dependence of polarization. Observations of an object are normally made within an hour in order to avoid the effects of variability. Although dilution of the continuum polarization by (presumably) unpolarized emission lines (Visvanathan 1973) may occur, the equivalent widths of any emission lines are <10% of the bandpass. It is assumed here that the measurements are representative of the continuum.

Generally, there is not strong wavelength dependence of either the strength or position angle of polarization in the HPQs. In Figure 6, all the pairs of wavelength dependence measurements (blue and red bandpasses) are plotted. A distinction is made in the figure between filter pairs which have wide and adjacent bandpasses or narrow and separated bandpasses; if wavelength dependence is present, the narrow pairs should demonstrate the dependence more clearly. There are examples of moderate but statistically significant wavelength dependence in the strength of polarization (Figure 6 (a)); the best examples are PKS 0736+017, 3CR 345 (1641+399), B2 1308+326, and CTA 102 (2230+114). In all these cases of statistically significant differences between blue and red polarization, the polarization is higher in the red. Given the limited number of observations, it is premature to state that this tendency is a general characteristic of HPQs. Variability of the wavelength dependence is observed in several HPQs.

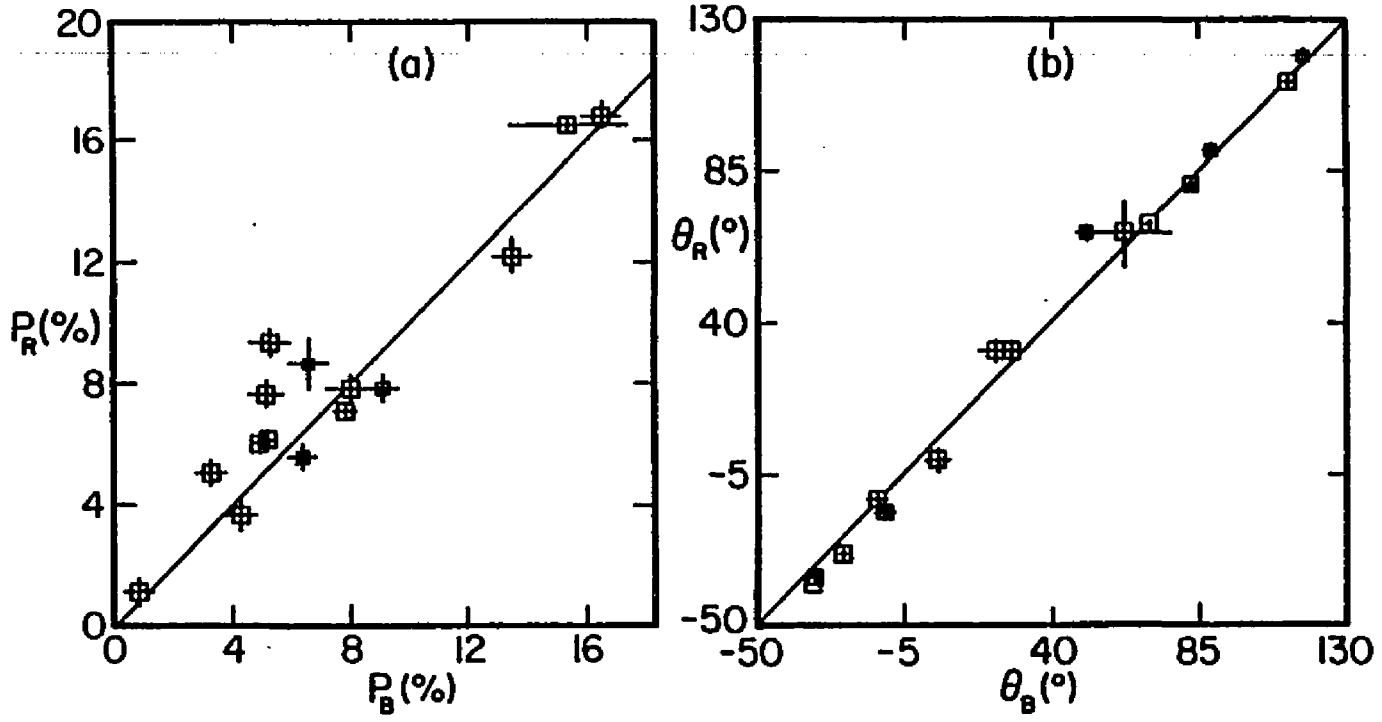

Figure 6. The wavelength dependence of polarization for highly polarized QSOs.

(a) The degree of polarization in the blue ($\lambda \sim 0.43$ μm) versus red ($\lambda \sim 0.75$ μm) bandpasses. Wide filter pairs are denoted by □, while narrow pairs are denoted by ▫.

(b) The position angle of polarization in the blue versus red bandpasses.

There is very little differential rotation of position angle observed (Figure 6 (b)). The largest rotation is $\sim$ 15° from 0.4 μm to 0.8 μm in B2 1308+326 on 29 May 1978. Even in this object, there was no differential rotation the following night. The only other statistically significant rotation observed was $\sim$5° in PKS 0420-014.

2. Low Polarization QSOs

We have already examined the distribution of polarization for the low polarization QSOs. The typical polarization is $\sim$ 0.6%. and essentially all normal QSOs have polarization < 2%. The two properties to be discussed here are the variability and wavelength dependence of the polarizaiton.

The low polarization QSOs appear markedly different from the HPQs in that their polarization does not vary significantly. In order to analyze the polarimetric variability, it is necessary to examine the variability of Q and U rather than P and θ because the errors in Q and U are normally-distributed. We restrict the analysis to variability measurements of bright survey QSOs since these generally have smaller errors and constitute the majority of variability measurements. For each bright survey QSO which has been measured more than once, we have calculated the following quantity for the change in Q (and U) between each successive broadband observation:

$$V_Q = \frac{(Q_1 - Q_2)}{(\sigma_{Q_1}^2 + \sigma_{Q_2}^2)^{\frac{1}{2}}} \quad . \tag{10}$$

The quantity V_Q (and V_U) is a measure of the significance of the variability between the two observations, and the distribution of V_Q (and V_U) would be Gaussian with a standard deviation of one if there were no variability. A histogram of the combined distribution of $|V_Q|$ and $|V_U|$ is shown in Figure 7 for the 76 repeated measurements of bright survey low polarization QSOs (152 values of V_Q and V_U). A normal curve fit to this distribution (standard deviation of 1.25) is also shown. The normal curve is a reasonable fit to the histogram distribution; the standard deviation is slightly higher than would be expected if there were no variability.

While this result suggests that there is slight variability in the low polarization QSOs, it is not strong evidence. The tabulated errors are derived from photon statistics alone and therefore are only lower limits to the true uncertainty of the observations. If the true uncertainty were 25% higher than that derived from photon statistics, this would completely account for the distribution of V_Q and V_U. This underestimate of the true uncertainty is feasible, particularly with the slow sky-chopping. On the other hand, we cannot rule out the possibility of moderate variability in normal QSOs. It is true that for many low polarization QSOs, the measured degree of polarization is comparable to the uncertainty of the measurement; moderate variability could be masked by the (relatively) large uncertainty.

There is additional evidence that the polarization of normal QSOs is not variable. We have observed at least twice nearly all QSOs which exhibit low and definite ($P>3\sigma_P$) polarization on the initial

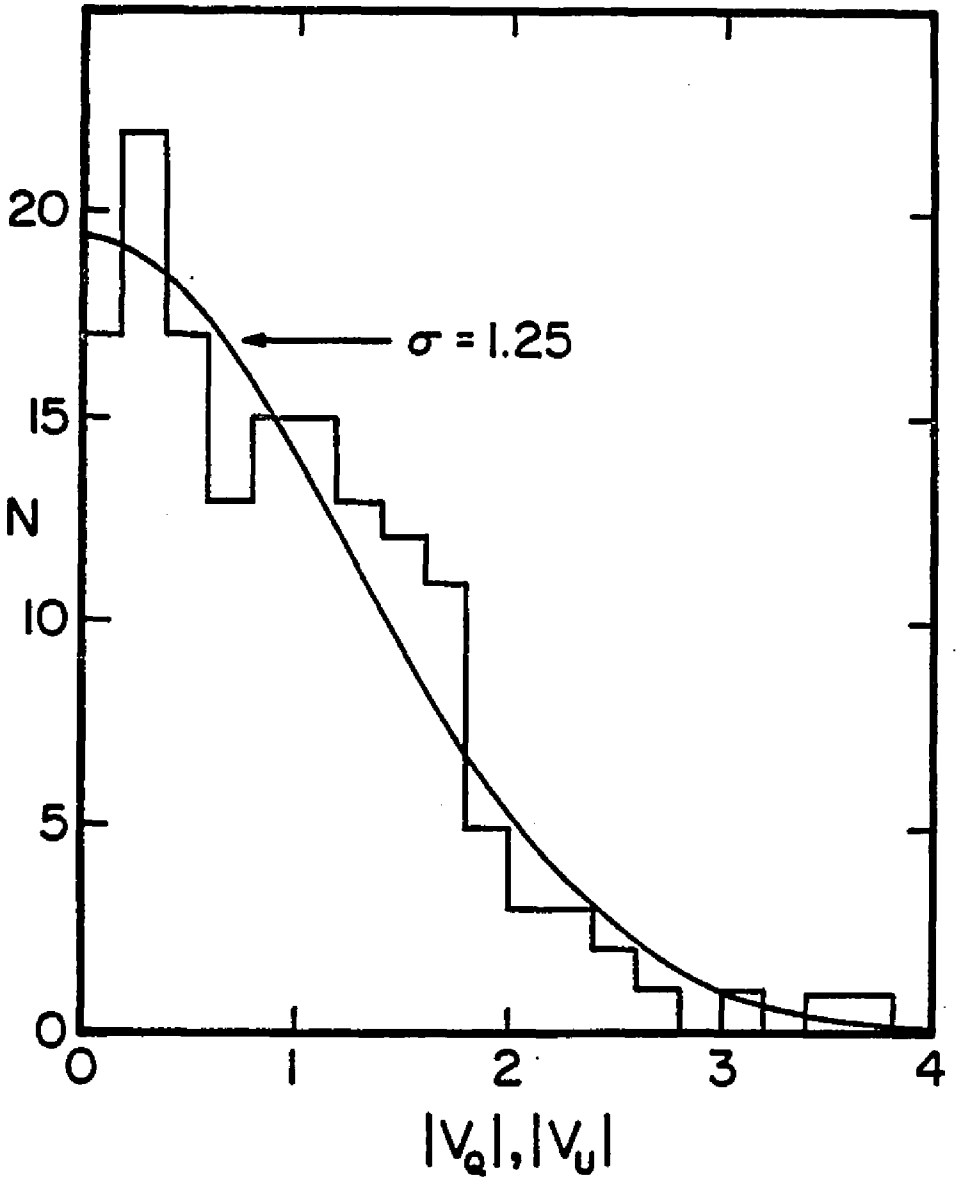

Figure 7. The polarimetric variability of low polarization QSOs.

Histogram of the Stokes parameter variability indices $|V_Q|$ and $|V_U|$ for repeated measurements of bright survey low polarization QSOs. Overlying the histogram is a normal curve with a standard deviation of 1.25.

survey measurement. The position angles of polarization for these measurements are meaningful and well-determined ($\sigma_\theta < 10°$) and can be used to examine the variability. Our observations of this group of QSOs show that the position angles are virtually constant within the errors over time scales $\tau \gtrsim$ year. Position angle variability is important because, if the low polarizations of most QSOs are due to dilution by unpolarized emission of highly polarized emission (as in the HPQs), the position angle behavior should still be similar to that observed in HPQs. This result not only illustrates the lack of variability in normal QSOs, but also establishes that the low polarization is not simply diluted HPQ-type emission.

Wavelength dependence measurements have been made for most normal QSOs with $P/\sigma_P \gtrsim 4$. The results of these measurements are shown in Figure 8. While most of the individual measurements could be statistically consistent with wavelength independent polarization, nearly all of the observations show a slightly higher degree of polarization in the blue; this tendency is clearly visible in (a) of Figure 8. A regression analysis of all available data suggests that the typical polarization at ~ 0.45 μm is $\sim 50\%$ higher than at ~ 0.75 μm for low polarization QSOs. This result cannot be regarded as conclusive, however, until more measurements of higher accuracy are available.

As in the HPQs, there does not appear to be significant differential rotation of position angle. There are no statistically significant examples of differential rotation among the low

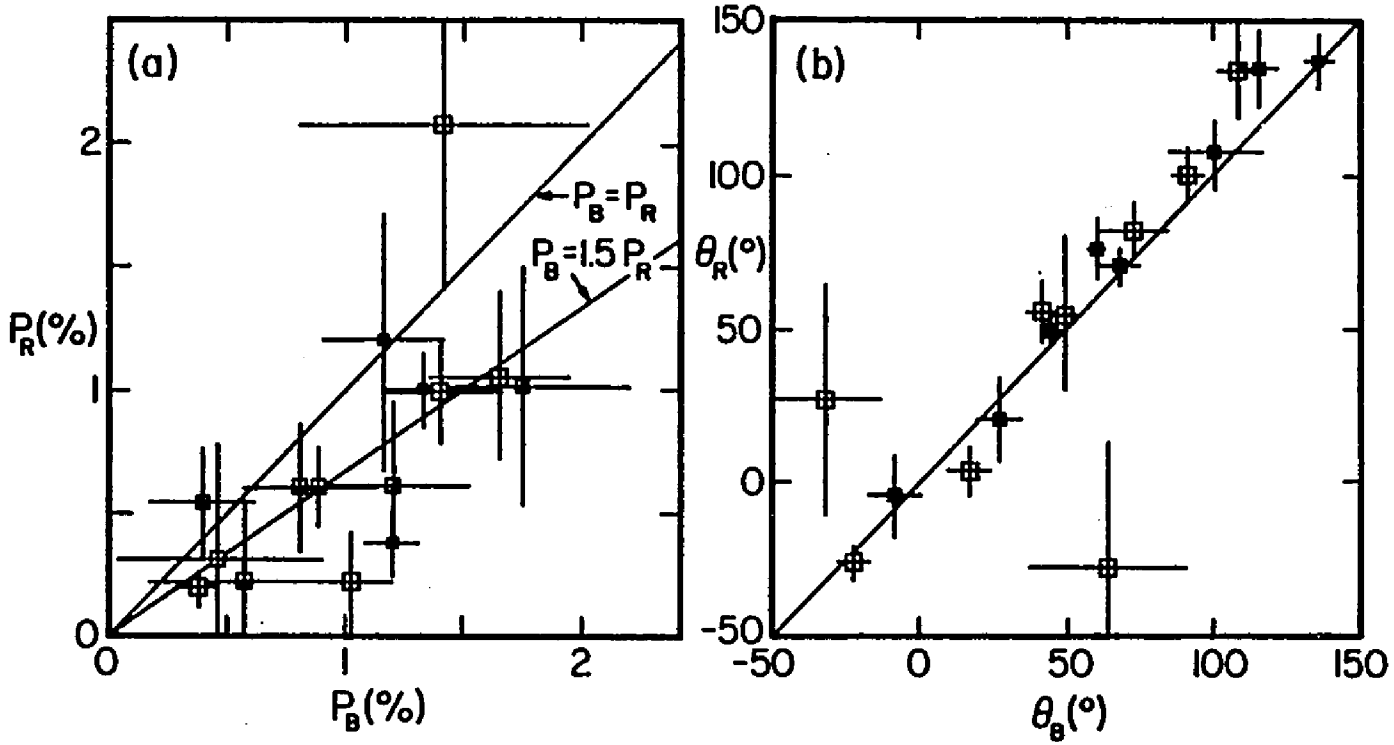

Figure 8. The wavelength dependence of polarization for low polarization QSOs.

(a) The degree of polarization in the blue versus red bandpasses (see Fig. 6 for symbols). Two measurements lie off the graph: 1246-057 (P_B = 3.77 ± 0.64, P_R = 1.46 ± 0.44) and 1425±267 (P_B = 1.41 ± 0.35, P_R = 2.68 ± 0.57).

(b) The position angle of polarization in the blue versus red bandpasses. The two measurements with large error bars are not significant ($P \lesssim \sigma_P$).

polarization QSOs, as can be seen from (b) in Figure 8. Of course, since the polarizations are lower, the typical uncertainties of the position angles are higher and rotations of $\lesssim 10°$ would be difficult to detect.

3. Summary

The concept of a physical distinction between high and low polarization QSOs originally arises from the discontinuity in the distribution of polarization. To some extent, the polarization can be regarded simply as high or low, without regard to the specific value. Once this distinction is made, we have shown that both the variability and wavelength dependence of polarization have different morphologies for the two groups. Thus, there is strong evidence that there are two distinct classes of QSOs, which can be distinguished on the basis of polarization.

The majority of radio-loud QSOs and essentially all radio-quiet QSOs exhibit a small degree of intrinsic optical polarization ($P < 2\%$, $\bar{P} \sim 0.6\%$). At low polarizations, we find no polarimetric differences between radio-loud and radio-quiet QSOs. These normal QSOs do not exhibit strong variability, at least over the time scales of our monitoring ($\tau >$ year). Within the accuracy of the measurements, it is doubtful whether we have observed any variability of low polarization QSOs. It is clear that the polarization of normal QSOs is not simply HPQ-type polarization which is diluted by unpolarized emission. The strength of polarization statistically appears to be

higher at shorter wavelengths; however, additional more accurate measurements are required before this can be regarded as conclusive. The position angle of polarization is wavelength independent, to the accuracy of our measurements.

The known HPQs are, with one exception, all radio-loud QSOs. Approximately 10-15% of radio-loud QSOs are highly polarized (this is discussed further in §IV.B). The range of polarization observed among HPQs is 0-20%. The fact that some HPQs have phases of low polarization is one factor which blurs the polarimetric distinction between HPQs and normal QSOs. The HPQs exhibit strong, rapid variability; characteristic time scales of polarimetric variability are on the order of a few days. Two HPQs (OI 287 and PHL 5200) are atypical in their lack of variability. No general relationship between the degree of polarization and brightness is observed. The degree of polarization is generally wavelength independent; in the few cases where wavelength dependence is observed, the polarization is slightly higher at longer wavelengths. The position angle is also normally wavelength independent; occasional slight differential rotations are observed.

CHAPTER IV

CORRELATIONS OF POLARIZATION AND OTHER QSO PARAMETERS

There are two basic objectives of this chapter. The first is to determine the properties, other than optical polarization, which are associated with the HPQs as compared to low polarization QSOs. The second purpose is to examine any correlations which might exist between polarization and other source parameters, if the HPQs are excluded. It is important to draw a larger picture of the properties of the HPQs in order to test current theories and motivate future work concerning this class of QSOs. The second objective provides a clue to whether those correlations which exist on a gross scale with polarization are extreme examples of continuous correlations among all QSOs.

A number of source parameters are discussed in this chapter. Generally, a specific number is assigned to a QSO to parametrize the source characteristic; these are the values listed in Table 1. The parameters to be discussed are radio luminosity (only in terms of objects being radio-loud or radio-quiet), redshift, optical luminosity, variability amplitude and time scale, optical spectral index, X-ray luminosity, and optical/X-ray spectral index. A distinct type of correlation is also discussed which deals with the position angle rather than degree of polarization; this is the correlation between the position angle of optical polarization and the position angle of extended radio structure.

A. Methods of Analysis

The method adopted for examining the correlations with other parameters for HPQs versus normal QSOs is generally a histogram technique. The distribution of some parameter x for a given sample of QSOs is plotted along with the distribution of that parameter for the HPQs in the sample. It should be noted that only one distinction between QSOs is made in these histograms--whether the polarization is "on" or "off". A comparison of the distribution of the parameter for the HPQs versus the entire sample allows one to evaluate whether the HPQs exhibit a distinct distribution (i.e., whether a correlation exists).

In addition to the plotted histograms, we have evaluated the statistical significance of the correlations using the nonparametric Kolmogornov-Smirnov statistic (e.g. Lindgren, McElrath, and Berry 1978). The hypothesis tested is that the values of the source parameter x for the HPQs are drawn from the same parent population as the values of the non-HPQs in the sample. This technique is chosen over more common parametric techniques because the number of HPQs in a given sample is often small, and the total distribution of the source parameter is, in general, not easily described by a standard distribution. In this test, the values of x are ranked for the HPQs (i=1) and non-HPQs (i=2), and the normalized integral distributions $F_i(x)$ are calculated. Then the maximum absolute deviation between the two integral distributions, $D = \max |F_1(1) - F_2(x)|$, is found. The probability that the two distributions are from the same parent

population can be found for a given value of D, taking into account the number of objects in the distributions. This statistic tests for any type of difference between the two distributions. We note that tables for the Kolomornov-Smirnov (hereafter, K-S) statistic only give probabilities (that our hypothesis is true) in the range of 1-20%.

There is a bias in our observations which could influence the correlations we seek to determine. In selecting a QSO for additional measurements after the initial survey measurement, there is a bias to re-observe "good" candidates for high polarization (e.g. extremely variable or steep spectrum QSOs). If all QSOs exhibited phases of high polarization, this bias alone could produce correlations reflecting our initial prejudices. Thus, for purposes of examining correlations with polarization, the first polarization measurement is consistently used. The HPQs which exhibited high polarization on the first measurement, whether they are definite or possible HPQs, form a distinct group for the correlation analyses; they are referred to as HPQs(1) in the text (and D-1 or P-1 in Table 1). In the histograms, HPQs(1) are plotted separately from HPQs which were highly polarized in follow-up measurements. For the K-S test, the HPQ distribution is determined from HPQs(1) only; all other objects are placed in the comparison sample.

The method adopted to determine whether correlations exist between polarization and the source parameters x (when the HPQs are excluded) is to compare the distributions of polarization (determined by the Lucy algorithm) for those QSO with $x \leqslant x_o$ and $x > x_o$: generally

x_o is chosen near the median of the distribution of x. This technique is used rather than a standard correlation coefficient because of the non-Gaussian errors in polarization. In this analysis, all HPQs (whether or not they showed high polarization on the first measurement) are excluded, since we are interested in examining correlations among normal QSOs. It should be noted that it is possible that "latent" HPQs remain in the sample of low polarization QSOs (i.e., those QSOs that have only been measured in phases of low polarization or for which the measurements were not accurate enough to know if the polarizations were high).

B. Radio Luminosity

In this section, we discuss in more detail the relationship between QSOs being highly polarized and radio-loud. The discussion is qualitative in that we only consider whether QSOs are radio-loud or radio-quiet. The radio luminosity is not quantified for several reasons. First, it is necessary to compare luminosities at a common rest frame frequency; many QSOs do not have adequate spectral coverage to interpolate the flux at $\nu_o/(1+z)$. Another difficulty is that most flux measurements are single dish observations which do not distinguish the flux from the central core and extended structure; these two components arise from different processes and it is misleading to compare the total flux.

It is useful to note at the outset the unusual nature of PHL 5200 (2225-055). It is the only radio-quiet HPQ known. The most

stringent current flux limit is f_ν(1.4 GHz) < 0.5 mJy (Gopal-Krishna and Sramek 1980). It does not appear to be variable in brightness or polarization; this lack of variability is atypical for HPQs. Its optical spectrum shows broad, deep absorption troughs blueward of resonance emission lines. High polarization is not observed among other absorption trough QSOs (Stockman, Angel, and Hier 1980). Spectropolarimetry of PHL 5200 establishes that the polarization is intrinsic to the continuum and is not due to scattering outside this region (Stockman, Angel, and Hier 1980). Regardless of the origin of the polarization, it is clear that PHL 5200 is an exceptional HPQ.

Excluding PHL 5200, the remaining 26 definite and possible HPQs are all radio-loud QSOs. In the general survey, 50 optically-selected and 181 radio-selected QSOs have been observed. Thus, the success rate for observing high polarization is markedly higher in radio-loud QSOs than in radio-quiet QSOs. Although this is a selection effect which could influence this result (to be discussed in §IV.F), its effect is probably minimal. It is our opinion that the typical HPQ properties (e.g. high variable polarization) are associated exclusively with radio-loud QSOs.

Among radio-loud QSOs, only a small percentage are highly polarized. Of 181 radio-selected QSOs observed, 26 (14.4%) are HPQs and 19 (10.5%) of these were highly polarized on the first measurement. Restricting the survey to the bright QSO sample, 96 radio-selected QSOs were observed; five (5.2%) are HPQs(1) and eight (8.3%) are HPQs. A large number of the radio-loud QSOs are from the 4C (178 MHz) or

Ohio (1420 MHz) surveys. Of 109 4C QSOs observed, 10 (9.2%) are HPQs(1) and 12 (11.0%) are HPQs; of 122 Ohio QSOs observed, 13 (10.7%) are HPQs(1) and 17 (13.9%) are HPQs. There is some incompleteness in these percentages since some "latent" HPQs may have been observed only in low polarization phases. Based on the frequency that known HPQs exhibit low polarization, the completeness of the initial survey is $\sim$70%. While our repeated observations of many QSOs partially compensate for this incompleteness, it is possible that the "latent" HPQs exhibit high polarization less frequently than the known HPQs. Another factor affecting the percentages of radio-loud QSOs which are HPQs is the frequency of the radio survey from which the QSOs are identified. As will be discussed in §IV.J, the HPQs generally have flat radio spectra. Thus, the fraction of QSOs which are HPQs will increase for higher frequency radio surveys. Most of the QSOs in our survey are identified from low frequency ($\nu \leq 1400$ MHz) surveys. We would conclude that 10-20% of QSOs from low frequency surveys are HPQs.

Recognizing the strong correlation between high polarization and radio emission, we will frequently restrict the correlation analyses below to only radio-loud QSOs.

C. Redshift

The existence of a correlation between polarization and redshift would indicate that highly polarized emission represents an evolutionary stage of QSOs. For example, if HPQs are preferentially at low redshifts, this suggests that high polarization is a late stage

of QSO evolution. Histograms of the distribution of redshift for three samples are shown in Figure 9. The distribution for all QSOs surveyed is shown in (a) of Figure 9, followed by the distribution for all radio-selected objects (b) of Figure 9, and all radio-selected objects in the bright QSO survey. These distributions are dominated by low redshift QSOs ($z \lesssim 1$) because our surveys are roughly magnitude-limited at a relatively bright magnitude. The distribution of redshift for the HPQs(1) (i.e., QSOs which showed high polarization on the first measurement) is shown by the shaded areas, while other HPQs are shown by crossed areas. (This convention is adopted in all further histograms.) Although nearly all HPQs have redshifts $\lesssim 1$, the distributions show that this is to be expected given the redshift distribution of the objects surveyed. The K-S statistic applied to the three samples shows that the probability that the two distributions are drawn from the same parent population is >20%. Thus, there is no evidence that high polarization is correlated with redshift.

The distributions of polarization for all low polarization radio-selected QSOs with $z \leqslant 0.7$ and $z > 0.7$ are shown in Figure 10, (a) and (b) respectively. The distribution for large redshift objects (10b) extends to higher polarization, but the interstellar simulations show that some of this may be accounted for by extrinsic polarization. There are no clear differences between the two distributions. Thus, we find no evidence for a correlation between polarization and redshift. It is important to note, however, that we have surveyed few high redshift QSOs. Since the density of QSOs rises rapidly with redshift (e.g. Lynds

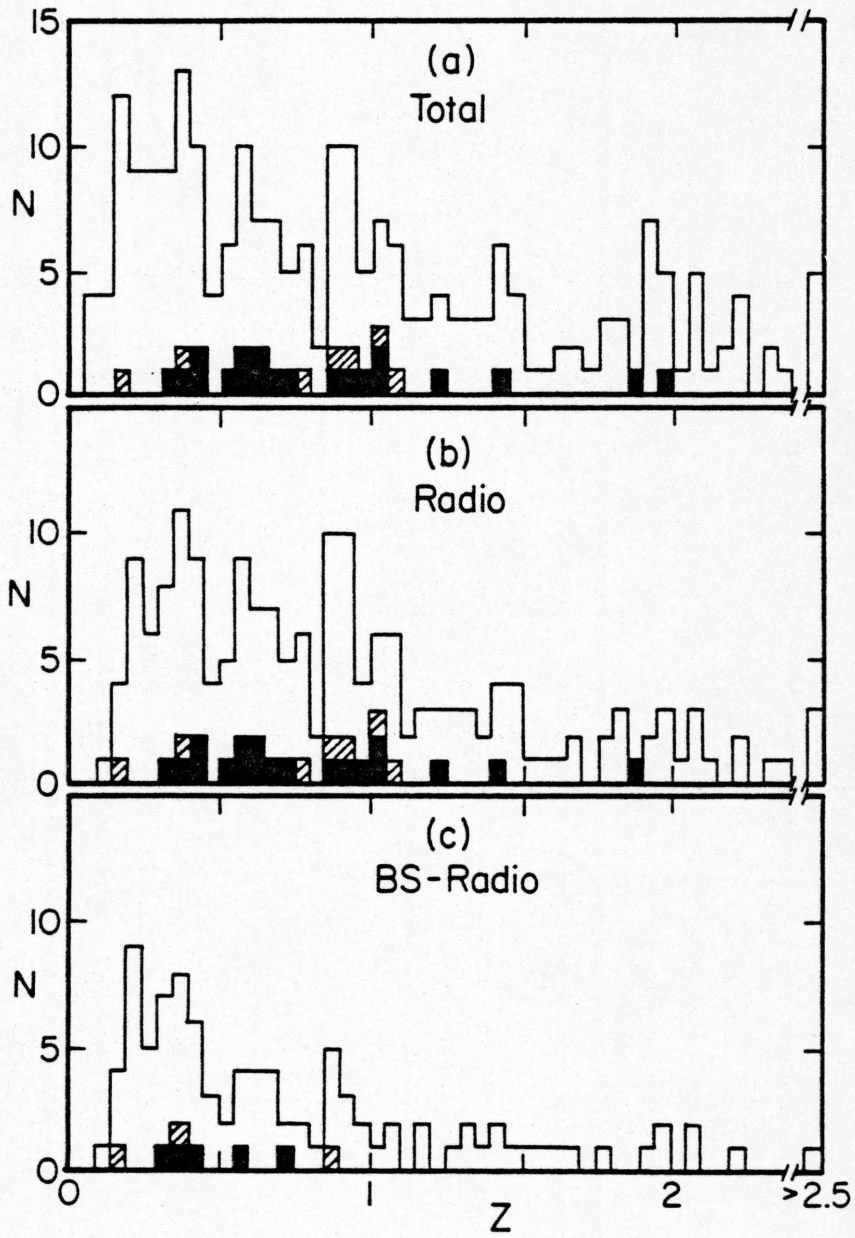

Figure 9. The distributions of redshift, z, for (a) all QSOs surveyed, (b) all radio-selected QSOs, and (c) all radio-selected bright QSOs.

HPQs (1) are shown by shaded areas; other HPQs are shown by crossed areas.

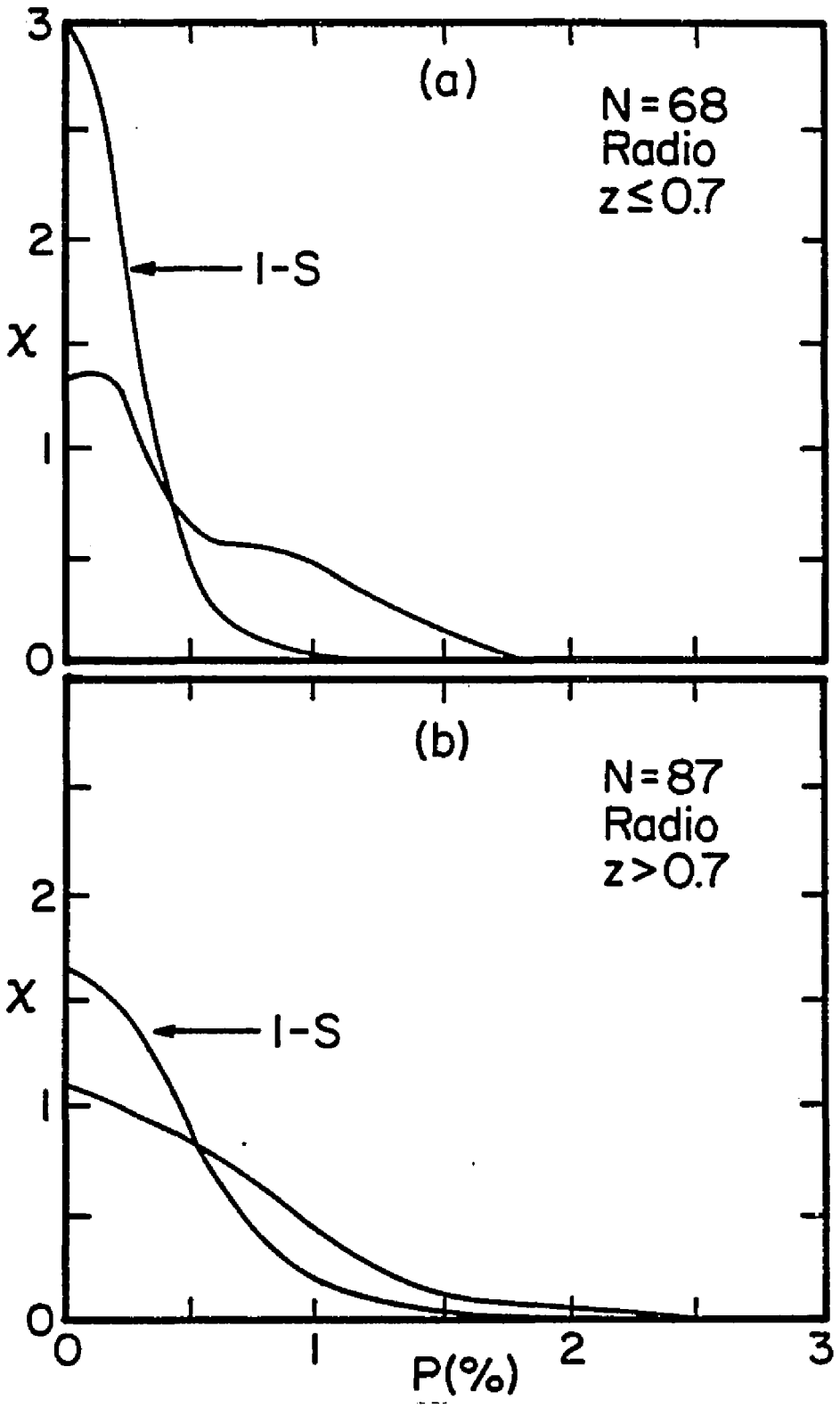

Figure 10. The distributions of polarization for all low polarization radio-selected QSOs with (a) $z \leq 0.7$, and (b) $z > 0.7$.

and Wills 1972, Schmidt 1976), there is a large population of QSOs which is poorly sampled for polarization. Only four HPQs are known at redshifts>1.1 (one of which is PHL 5200). Additional measurements of high redshift radio-selected QSOs would be valuable.

D. Optical Luminosity

The monochromatic luminosity at λ_{rest} = 2500 Å is included in Table 1 for all QSOs observed. This luminosity is calculated from the V magnitude in BCS, the spectral index, and the redshift (as explained in §II.C.2). Histograms of the optical luminosity are shown in Figure 11 for the same samples as were shown in Figure 9: all QSOs surveyed (11a), all radio-selected QSOs (11b), and bright survey radio-selected QSOs (11c). If a correlation exists between high polarization and luminosity, it is in the sense that the HPQs are less luminous than other QSOs. This impression from the histograms is confirmed by the K-S statistic. The probability that the QSOs which showed high polarization on the first measurement, HPQs(1), are drawn from the same population as the remainder of the QSOs in the samples is 6% for the entire sample (a), 4% for the radio-selected sample (b), and > 20% for the radio-selected bright survey QSOs (c). The high value for the final sample probability is due in part to the small number of HPQs(1) in that sample. These correlations are of moderate significance. A major source of uncertainty in this result is introduced by the photometric variability of QSOs, particularly HPQs (see §IV.E). If the maximum brightness of QSOs were used to characterize their luminosity, the HPQs would probably be somewhat

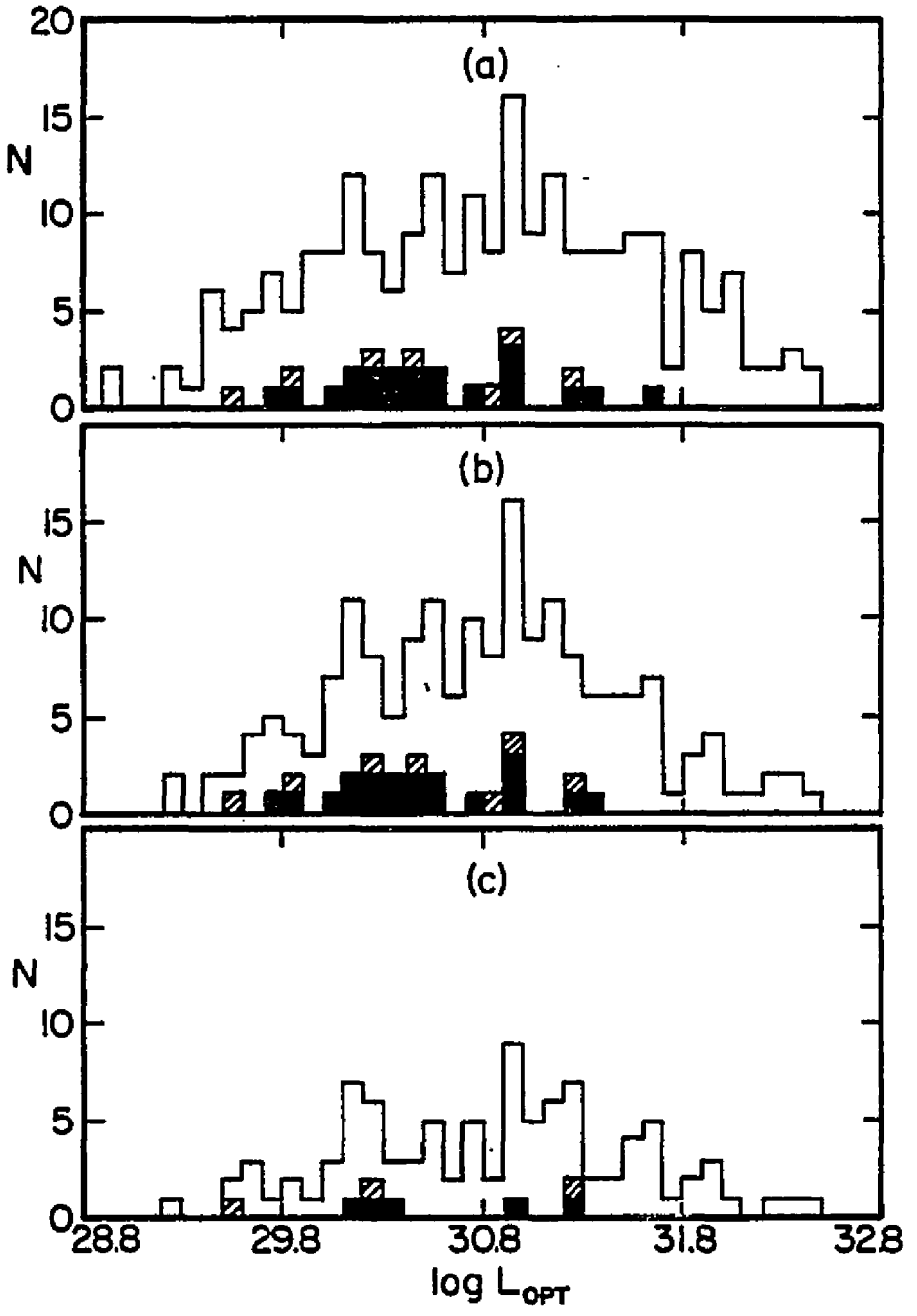

Figure 11. The distributions of optical luminosity, log L_{OPT}, for (a) all QSOs surveyed, (b) all radio-selected QSOs, and (c) all radio-selected bright QSOs.

overluminous. Given this uncertainty, we would not claim that a definite correlation exists in the sense that HPQs are less luminous that other QSOs. However, it is clear that the HPQs exhibit a wide range of luminosity and are not, at typical brightnesses, substantially more luminous than other QSOs.

In Figure 12, the polarization distributions are shown for all radio-selected low polarization QSOs with log $L_{OPT} \leqslant 30.8$ (12a) and > 30.8 (12b). These two distributions, compared to the interstellar simulations, do not appear significantly different. There does not appear to be any sign of a continuous correlation between optical luminosity and polarization.

E. Optical Photometric Variability

One of the most outstanding characteristics of the original four HPQs is their rapid large amplitude photometric variability. This correlation between high polarization and optically violent variable (OVV) photometric behavior must be established, however, by observing a large number of QSOs with a range of variablity. As discussed in §II.C.1, we have constructed and observed a sample of QSOs for which variability data is available. The photometric variability is parameterized by the maximum amplitude and minimum characteristic time scale of variability which has been observed.

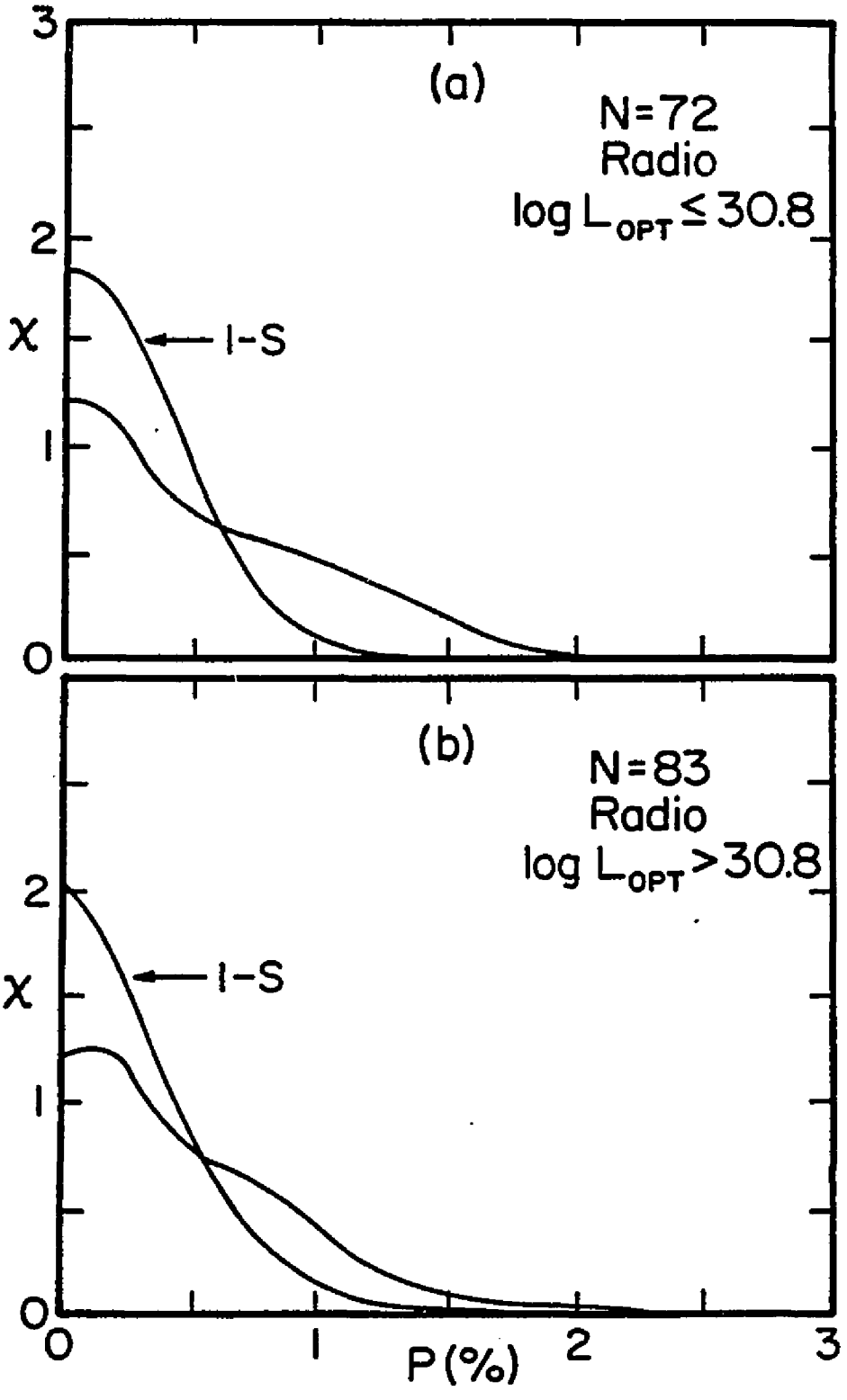

Figure 12. The distributions of polarization for all low polarization radio-selected QSOs with (a) log $L_{OPT} \leq 30.8$, and (b) log $L_{OPT} > 30.8$.

1. Amplitude of Variability

The strongest correlation we have found between high polarization and other source parameters is with the amplitude of variability. Histograms of the distribution of Δm are shown in Figure 13 for all QSOs (13a) and all radio-selected QSOs (13b) in the variability sample. The distribution of variability for the HPQs in the sample is clearly weighted towards large amplitude variability. The probability that the HPQs(1) are drawn from the same parent population is $< 1\%$ for both samples shown in Figure 13. The specific values used to characterize the variability are, of course, very uncertain since the monitoring programs from which these data are derived are very heterogenous. However, once this sample was compiled and values assigned to the QSOs, it is clear that large amplitude variables are much more likely to be highly polarized. The HPQs with moderate variability may well exhibit more dramatic photometric variability when monitored more extensively.

The polarization distribution of low polarization QSOs with $\Delta m \leqslant 0.7$ mag and $\Delta m > 0.7$ mag are shown in Figure 14, (a) and (b). The tail of the distribution for larger amplitude variables extends to slightly higher polarizations. This difference between the two polarization distributions is in the same sense as the correlation shown for the HPQs--that larger amplitude variables may be slightly more polarized. The figures are suggestive but not conclusive that a continuous correlation exists.

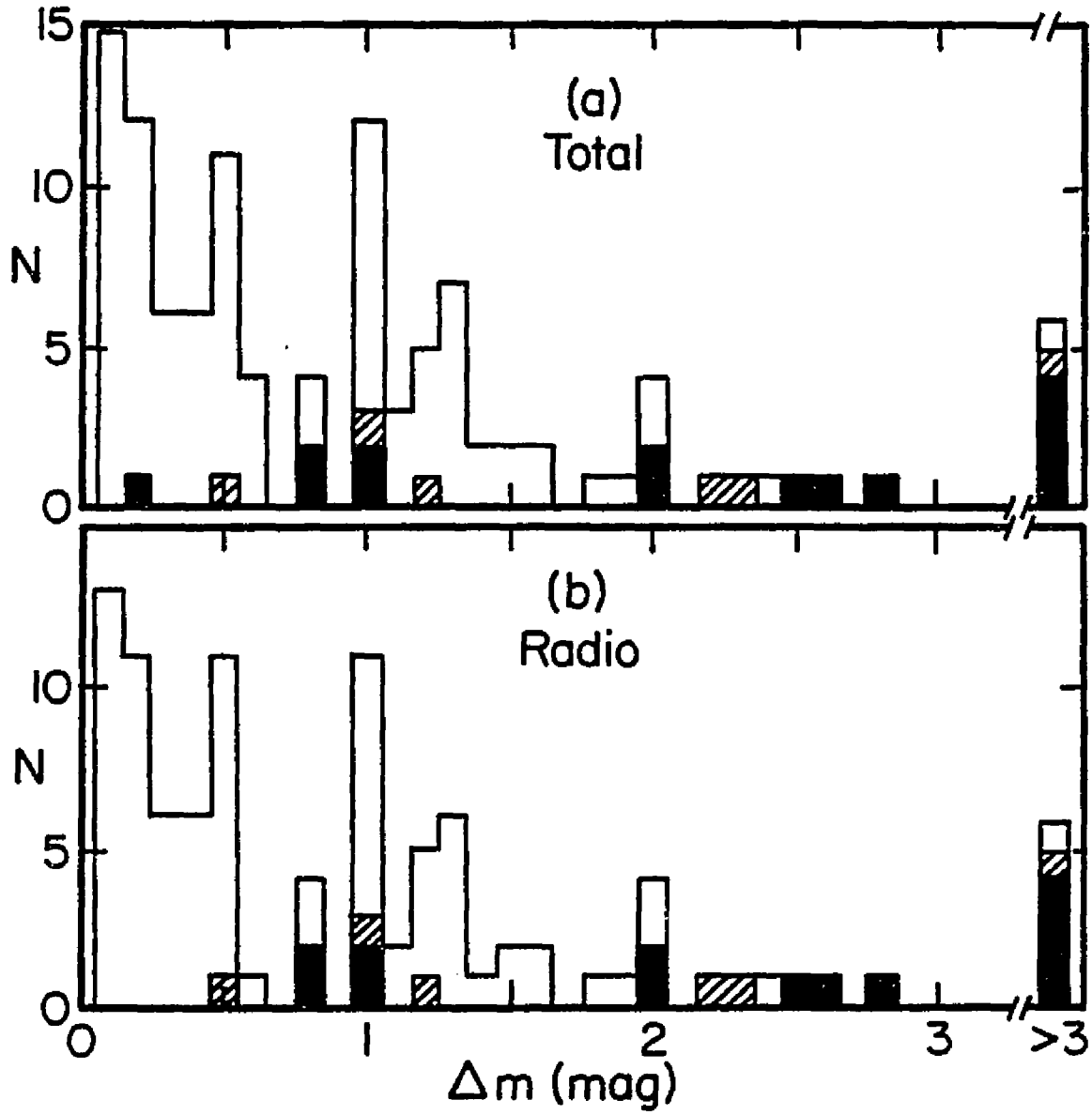

Figure 13. The distributions of the amplitude of photometric variability, Δm, for (a) all QSOs, and (b) all radio-selected QSOs in the variability sample.

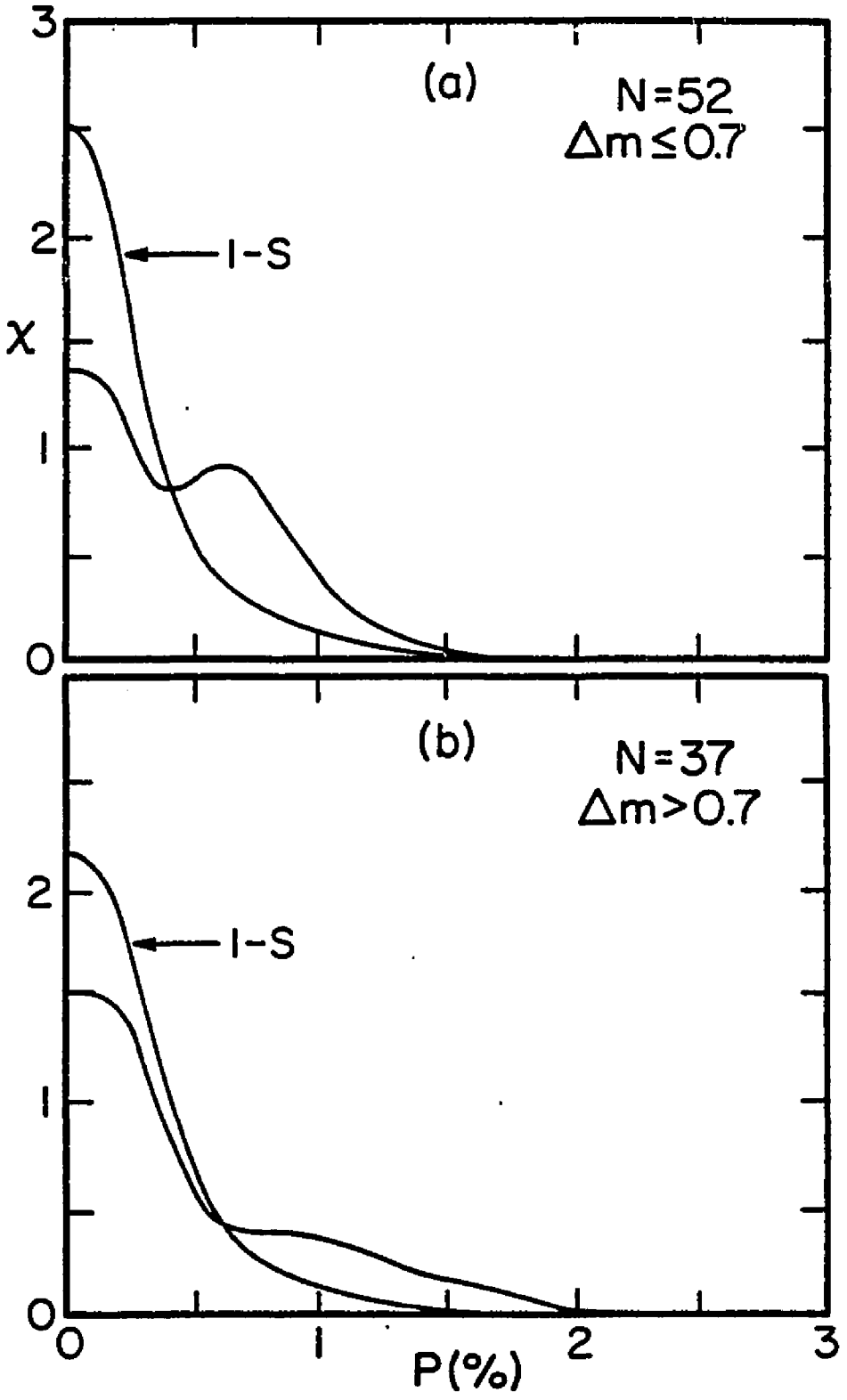

Figure 14. The distributions of polarization for all low polarization QSOs in the variability sample with (a) $\Delta m \leq 0.7$ and (b) $\Delta m > 0.7$.

2. Time Scale of Variability

For those QSOs with sufficient monitoring to estimate the time scale of photometric variability, we have assigned this time scale as another parameter to characterize the variability. The minimum time scale of variability is an important parameter as it is the only optical means of determining an upper limit to the size of the emitting region. Histograms of the time scale of variability are shown in Figure 15 for all QSOs (15a) and all radio-selected QSOs (15b) in the sample. There is a clear indication that the distribution of time scales for the HPQs is strongly biased towards short time scales. The statistical probability from the K-S test shows that the distribution of HPQs(1) is different from the remainder of the samples with a probability of 2.5%. We would note that the time scale of 4C 25.40 (1223+252), the low polarization QSO with $\tau \sim 1$ day, is uncertain and is based on only one set of observations (Jackisch 1971).

There is possible evidence of a continuous correlation between polarization and the time scale of variability. The distributions of polarization for low polarization QSOs with time scales $\tau < 1$ year and $\tau \gtrsim 1$ year are shown in Figure 16 (a) and (b). The numbers of QSOs used to derive these distributions are small (14 and 23 respectively), so both the distributions and the interstellar simulations are uncertain. However, if the interstellar simulations are reasonable, the polarization of the long time scale QSOs can almost entirely be accounted for by interstellar polarization, while shorter time scale QSOs exhibit a relatively large amount of intrinsic polarization.

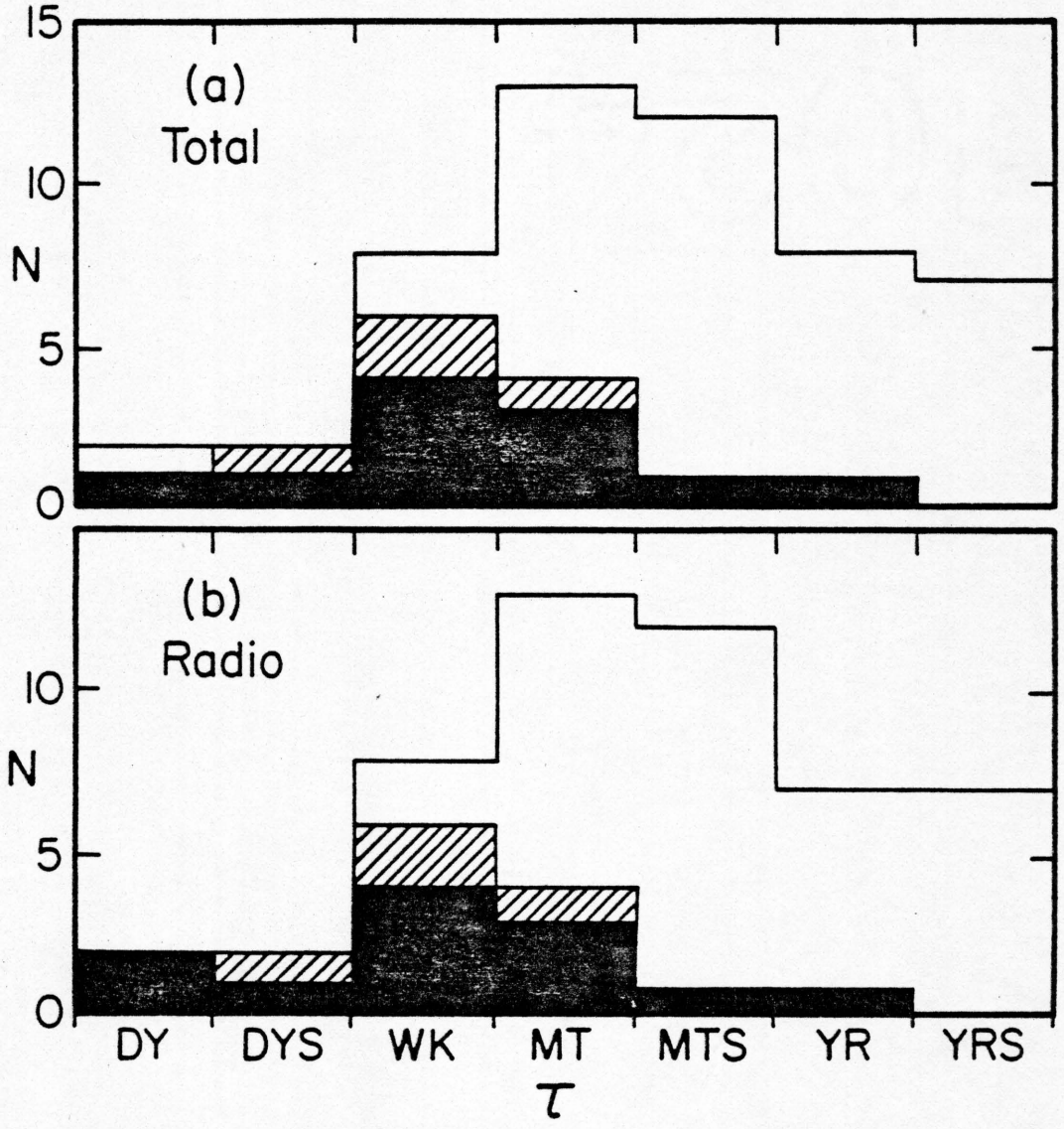

Figure 15. The distributions of the time scale of photometric variability, τ, for (a) all QSOs and (b) all radio-selected QSOs with a time scale classification.

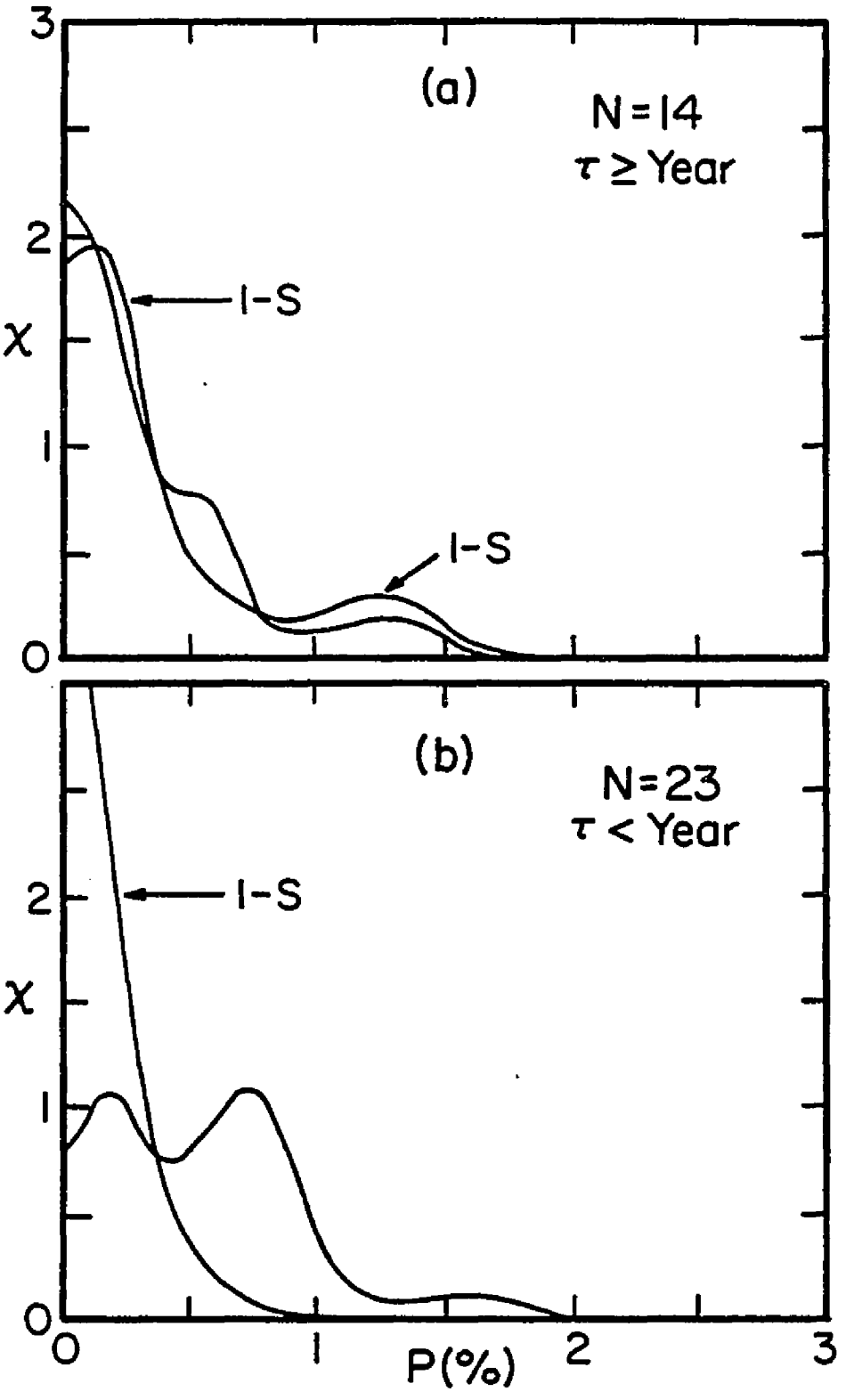

Figure 16. The distributions of polarization for all low polarization QSOs with (a) $\tau \geq 1$ year, and (b) $\tau < 1$ year.

Again, the distributions are suggestive but not conclusive of a continuous correlation.

One should be aware that only known photometric variability time scales are being used in this analysis. Some of the HPQs in the sample (e.g. PKS0403-132, 0420-014, 0736+017, and 4C 29.45) have polarimetric time scales substantially shorter than the photometric time scales assigned for this analysis.

The correlation between high polarization and dramatic variability illustrates the strong link between HPQs and OVV QSOs. There are, however, some reservations and exceptions to a one-to-one correspondence. Many of the new HPQs have not been extensively monitored; it is important to monitor these new HPQs photometrically to establish whether they are OVVs. At least two HPQs, OI 287 and PHL 5200 do not appear to be variable either photometrically or polarimetrically. There are some QSOs which have been described as OVVs but which have low polarizations. We have obtained upper limits of $P < 5\%$ for two definite OVVs, PKS 0440-003 (Pollock et al. 1979) and 3CR 138 (McGimsey et al. 1975). There are other low polarization QSOs, for example PHL 658 (Penston and Cannon 1970) and PHL 1657 (Lü 1972) which have been mentioned as OVVs (Visvanathan 1973) but have not been well-monitored photometrically. The low polarization OVVs may be exceptions to the correlation, may be misclassified as OVVs, or may simply have been observed in low polarization phases.

It is also of interest to note the behavior of 3CR 454.3, an HPQ which has been extensively monitored photometrically and

polarimetrically. In recent years it has had relatively low polarization and relatively stable brightness (Pollock et al. 1979), compared with high polarization and strong variability when observed by Visvanathan (1973). This behavior suggests that long-term phases of high polarization may be associated with periods of strong photometric variability.

F. Optical Spectral Index

The optical continua of the four original HPQs have long been noted as steeper than the continua of most QSOs (e.g. Oke, Neugebauer and Becklin 1970). As with the variability characteristics of the original HPQs, this apparent correlation is tested by observing a large sample of QSOs with a range of continuum spectral indices.

The histograms of the spectral index distribution are shown in Figure 17 (a) and (b) for the entire spectrophotometry sample and for all radio-selected QSOs in this sample. The HPQs in the sample lie preferentially at high values of the spectral index. The K-S statistic applied to the distribution of HPQs(1) versus the remainder of the sample yields a probability of <1% for both samples that the HPQs are drawn from the same parent population. The median spectral index of the samples is $\sim$ 0.7, while the median index for all the HPQs is 1.4. Only one HPQ, MC 1522+155, has a spectral index less than 0.9; in this case, the index was determined over a very narrow spectral range (Smith et al. 1977). It should be noted that not all steep spectra QSOs are HPQs.

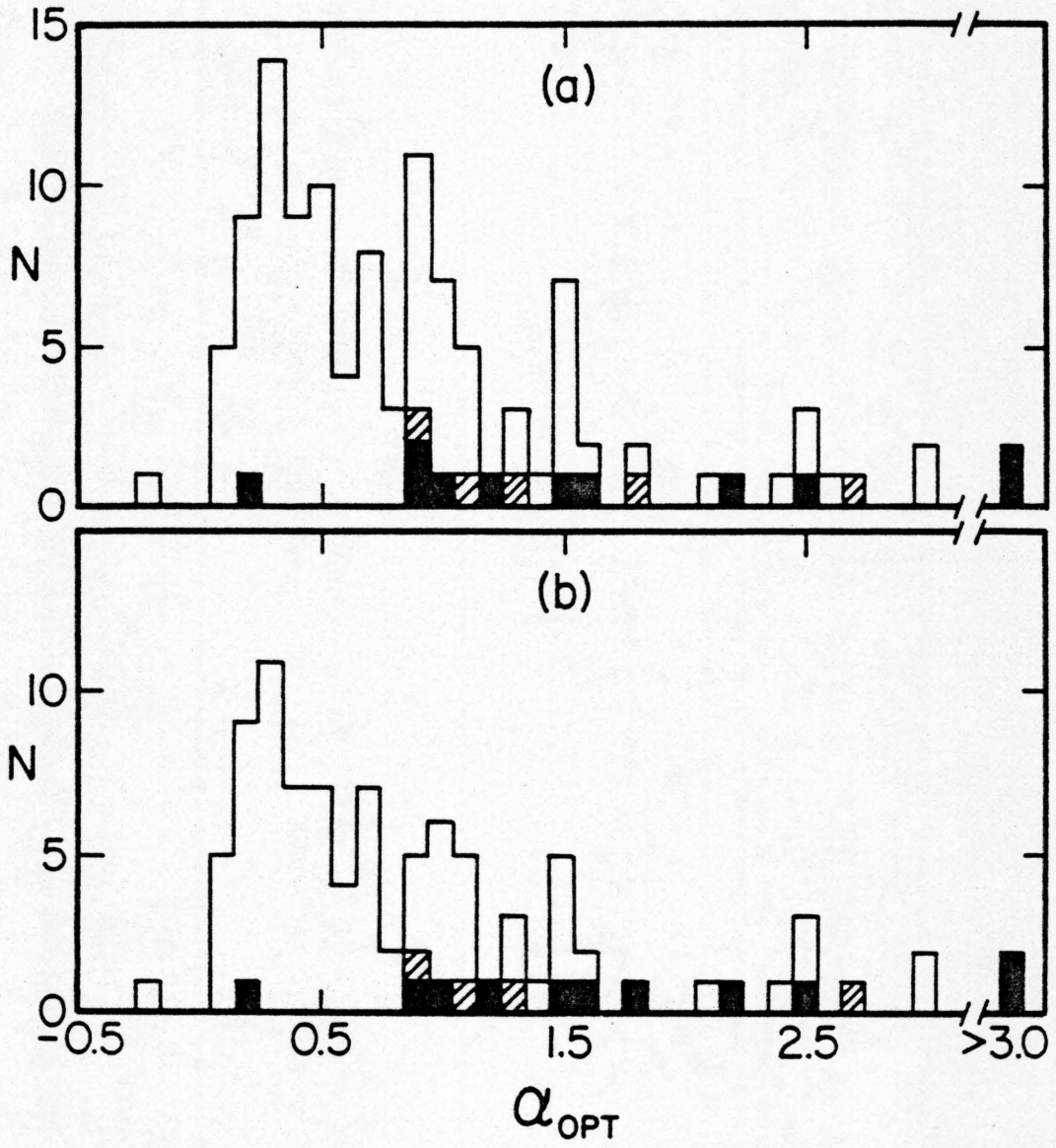

Figure 17. The distributions of the optical spectral index, α_{OPT}, for (a) all QSOs and (b) all radio-selected QSOs in the spectrophotometry sample.

The polarization distributions of low polarization QSOs with spectral indices $\alpha_{OPT} \leqslant 0.65$ and $\alpha_{OPT} > 0.65$ are shown in Figure 18 (a) and (b). Both distributions show significant intrinsic polarization, but there is a strong suggestion that the distribution is weighted towards higher polarization for the steeper index QSOs. This tendency is in the same sense as the large scale correlation shown above for the HPQs. Thus, a continuous correlation between polarization and spectral index may be present.

In §IV.B, a selection effect concerning the correlation between polarization and radio luminosity was mentioned; this effect is discussed here. Optically-selected QSOs are often selected on the basis of a UV excess. However, we have shown that the HPQs are redder than most QSOs. Thus there is a bias against optically selecting the redder HPQs. To evaluate the significance of this possible selection effect, we can compare the success rates for finding HPQs among steep spectra radio- and optically-selected QSOs. Of seven optically-selected QSOs with $\alpha_{OPT} \geqslant 0.9$ which have been surveyed, none are highly polarized. This compares with 14 of 38 radio-selected QSOs with $\alpha_{OPT} \geqslant 0.9$ which are HPQs. This result suggests that color bias is not responsible for the lack of radio-quiet HPQs.

Another correlation between high polarization and the optical continuum has been proposed by Rieke and Lebofsky (1979). They suggest that the HPQs have smoother continua which better approximate a power law energy distribution (from the optical through the infrared) than is typical of most QSOs. Normal QSOs have relatively complex

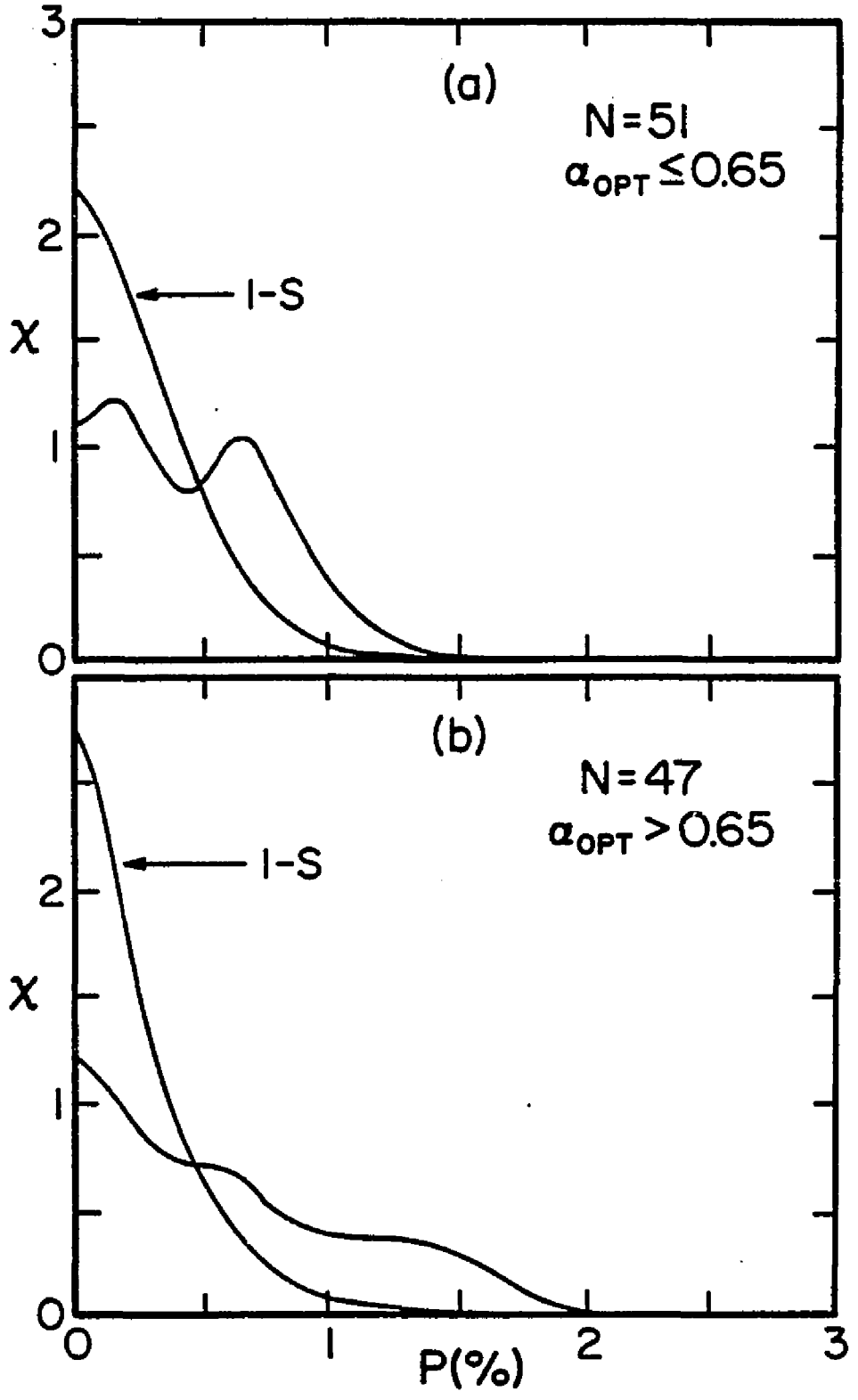

Figure 18. The distributions of polarization for all low polarization QSOs in the spectrophotometry sample with (a) $\alpha_{OPT} \leq 0.65$ and (b) $\alpha_{OPT} > 0.65$.

optical/infrared continua which show structure and are not well characterized by a (single) power law (e.g. Neugebauer et al. 1979). The original four HPQs do have smooth, straight power law continua (Rieke and Lebofsky 1979, Neugebauer et al. 1979). Not all HPQs exhibit such straight power law energy distributions. For example, the continuum flattens at higher frequencies in PKS 0736+017 (Baldwin 1975), PKS 1510-089 (Neugebauer et al. 1979), and CTA 102 (Oke 1966) while 3CR 68.1 steepens drastically into the ultraviolet (Rieke and Lebofsky 1979). However, published spectra support the suggestion that the HPQs exhibit smoother (roughly power law) optical/infrared continua than normal QSOs; curvature, if present, is generally on a large scale.

G. Emission Line Equivalent Width

It is already clear from the correlations discussed that the optical continua of HPQs are similar to BL Lac objects (high polarization, extreme variability, steep energy distribution). It is important, then, to examine the correlation between polarization and emission line strengths for QSOs; perhaps the HPQs exhibit line strengths intermediate between normal QSOs and BL Lac objects.

The sample of QSOs used to examine the relationship between polarization and emission line strength consists of all QSOs in the general survey for which the equivalent width of Mg II λ2798 is published. The distribution of equivalent width is shown in Figure 19 for all QSOs (a) and all radio-selected QSOs (b) in this sample. No correlation with high polarization is apparent; there are HPQs with

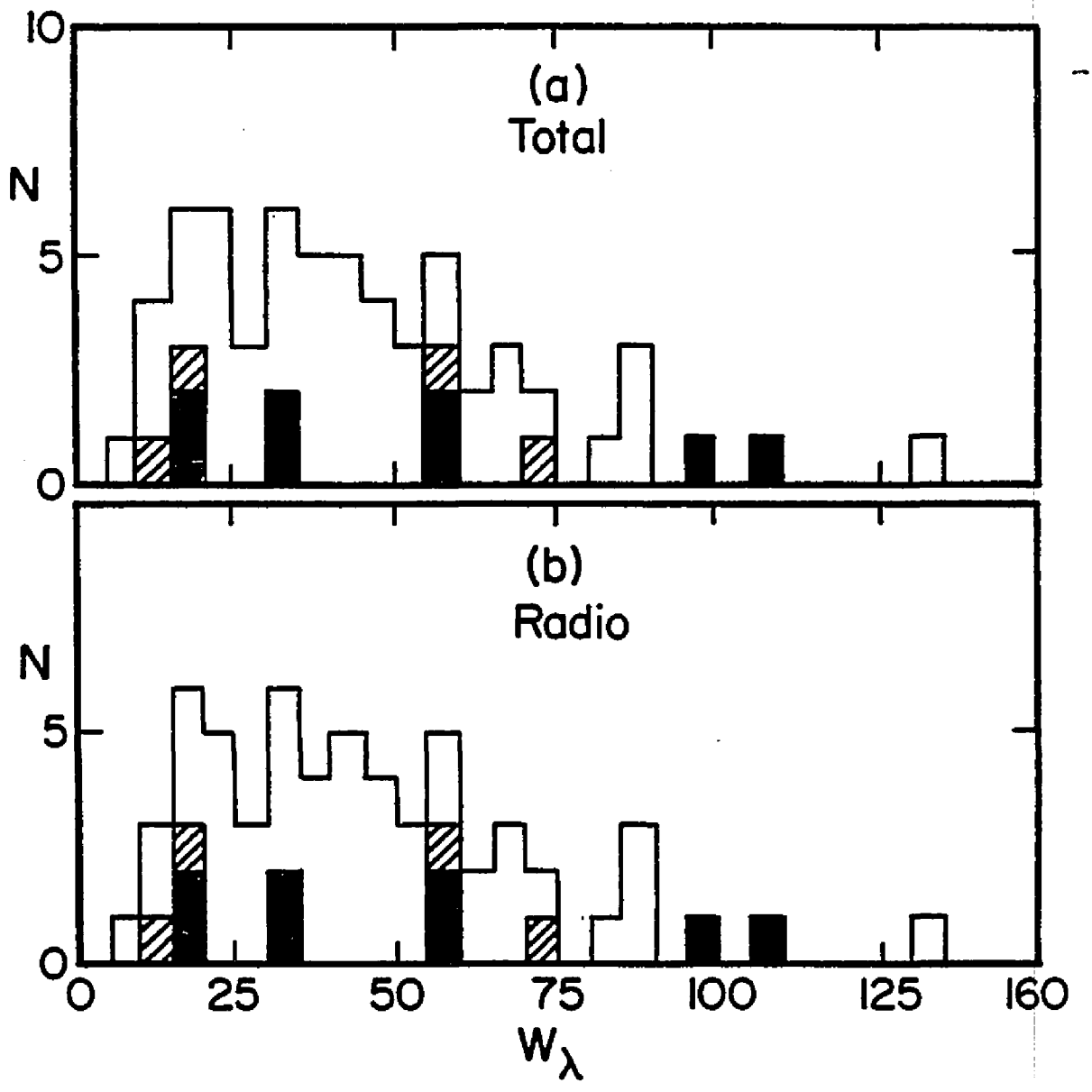

Figure 19. The distributions of equivalent width of Mg II, W_λ, for (a) all QSOs and (b) all radio-selected QSOs with this information available.

both low and high equivalent widths. The K-S probability that the distributions are taken from the same population is <20% for both samples. Thus, given the sample selection and available data (discussed in §II.C), there is no evidence that the HPQs have a different distribution of (Mg II) emission line strengths than normal QSOs.

The distributions of polarization for low polarization QSOs with W_λ(MgII) $\leq$ 40 Å and > 40 Å are shown in (a) and (b) of Figure 20. There is no apparent difference between the distribution for QSOs with weak and strong Mg II emission, and no evidence of a correlation among normal QSOs.

H. X-Ray Emission

A number of sensitive HEAO-B (Einstein) X-ray observations of QSOs are now available (Tananbaum et al. 1979, Ku and Helfand 1980, Zamorani et al. 1980). All HEAO-B measurements (including non-detection limits) of the QSOs in our general survey are listed in Table 1. For the correlation analysis below, only detected QSOs are used. We examine first the X-ray luminosity and then the optical/X-ray spectral index (a measure of the ratio of optical to X-ray luminosity).

1. X-ray Luminosity

Histograms of the distribution of X-ray luminosity for all detected QSOs and all detected radio-selected QSOs are shown in (a) and (b) of Figure 21. There is an indication that the HPQs may have slightly higher values of L_X than other QSOs in these samples. The probability that the HPQs(1) are drawn from the same parent population

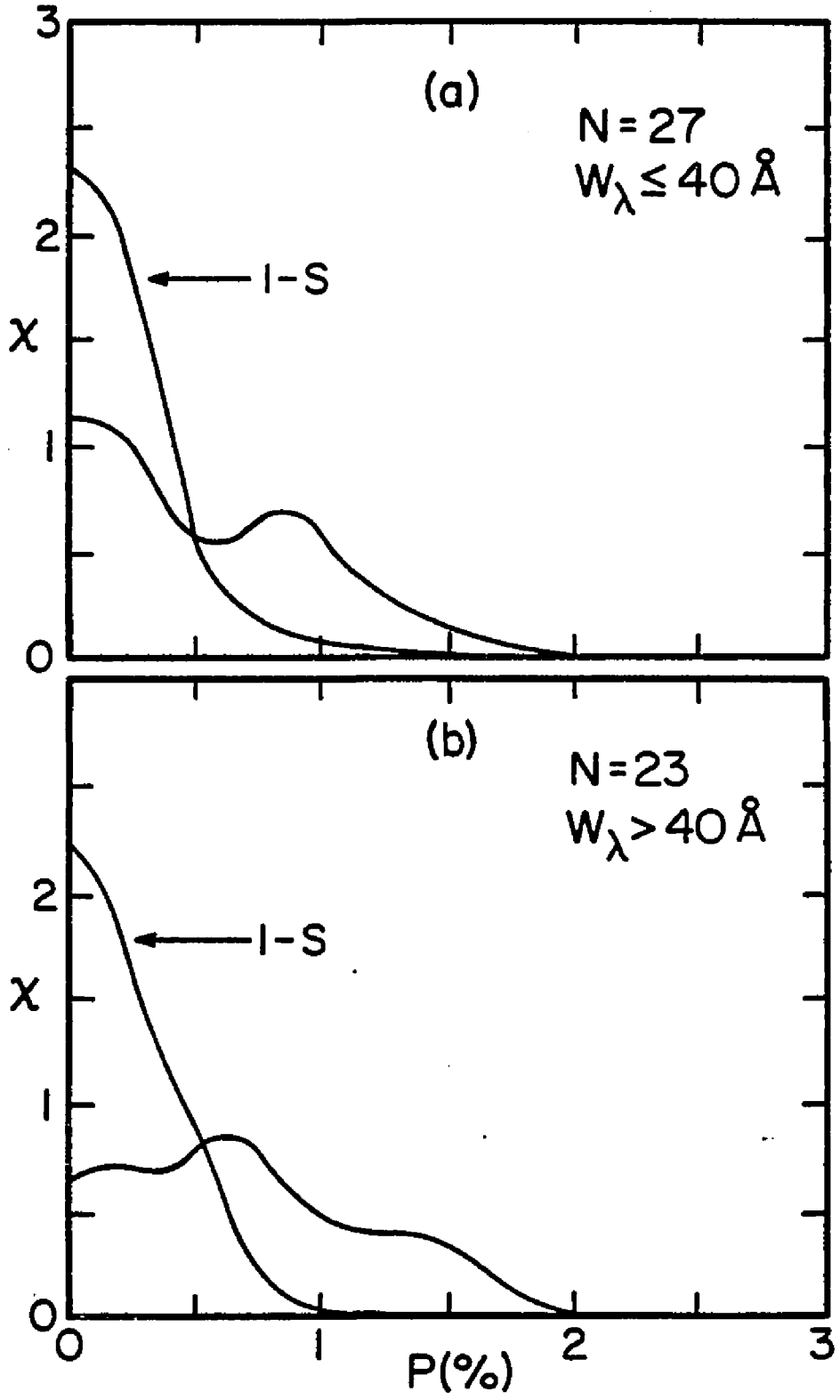

Figure 20. The distributions of polarization for all low polarization QSOs with (a) $W_\lambda \leq 40$ Å and (b) $W_\lambda > 40$ Å.

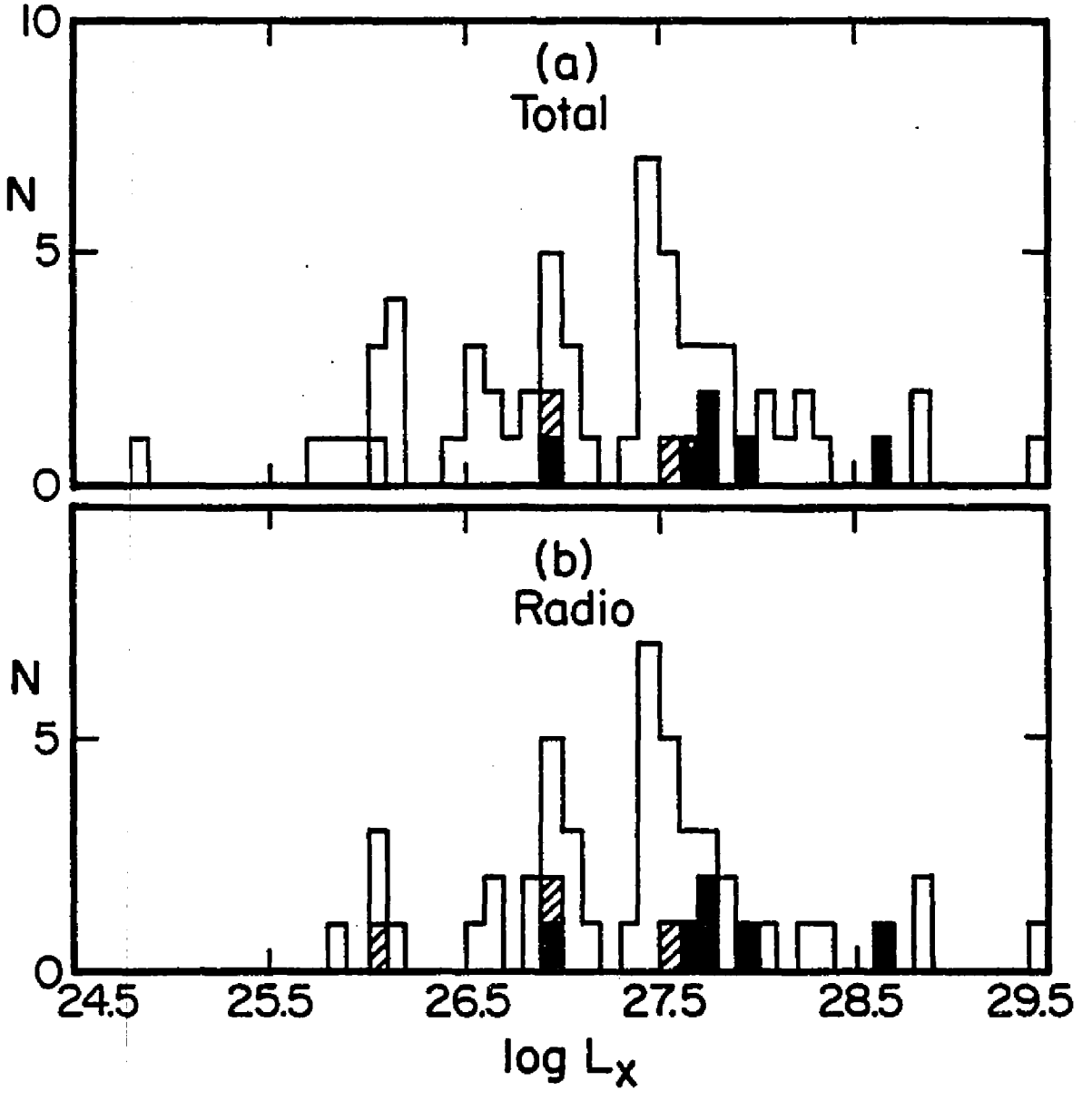

Figure 21. The distributions of the X-ray luminosity, log L_x, for (a) all QSOs surveyed and (b) all radio-selected QSOs surveyed which have been detected by HEAO-B.

as the remainder of the sample is ∿5% for both samples. This correlation is of moderate significance.

The distributions of polarization for detected normal QSOs are shown in Figure 22 for QSOs with log $L_X \leqslant 27.4$ (a) and < 27.4 (b). If the interstellar polarization distributions are good estimates, neither of these samples exhibits very much intrinsic polarization. There is not evidence for a continuous correlation between polarization and X-ray luminosity.

2. Optical/X-ray Spectral Index

The optical/X-ray spectral index, α_{ox}, is a convenient parameter to compare the ratio of optical to X-ray luminosity. Use of this parameter does not require nor imply that the spectrum between 2500 Å and 2 keV is a power law. Given the results obtained for the optical and X-ray luminosity correlations, it is not surprising that there is a strong correlation between high polarization and the spectral index. Histograms of α_{ox} are given in Figure 23 for all detected QSOs (a) and all radio-selected detected QSOs (b). All of the HPQs lie near lower values of α_{ox}. The K-S probability comparing the distribution of HPQs(1) with the remainder of the samples is 1%. We note that the significance is lower if all HPQs are included; the K-S probability is then 5%. This result suggests that the HPQs exhibit a higher ratio of X-ray to optical luminosity. There is one major reservation concerning this correlation, however. The optical and X-ray observations are not simultaneous, and we have shown that the HPQs are extreme variables. For example, if the optical brightness of an HPQ at

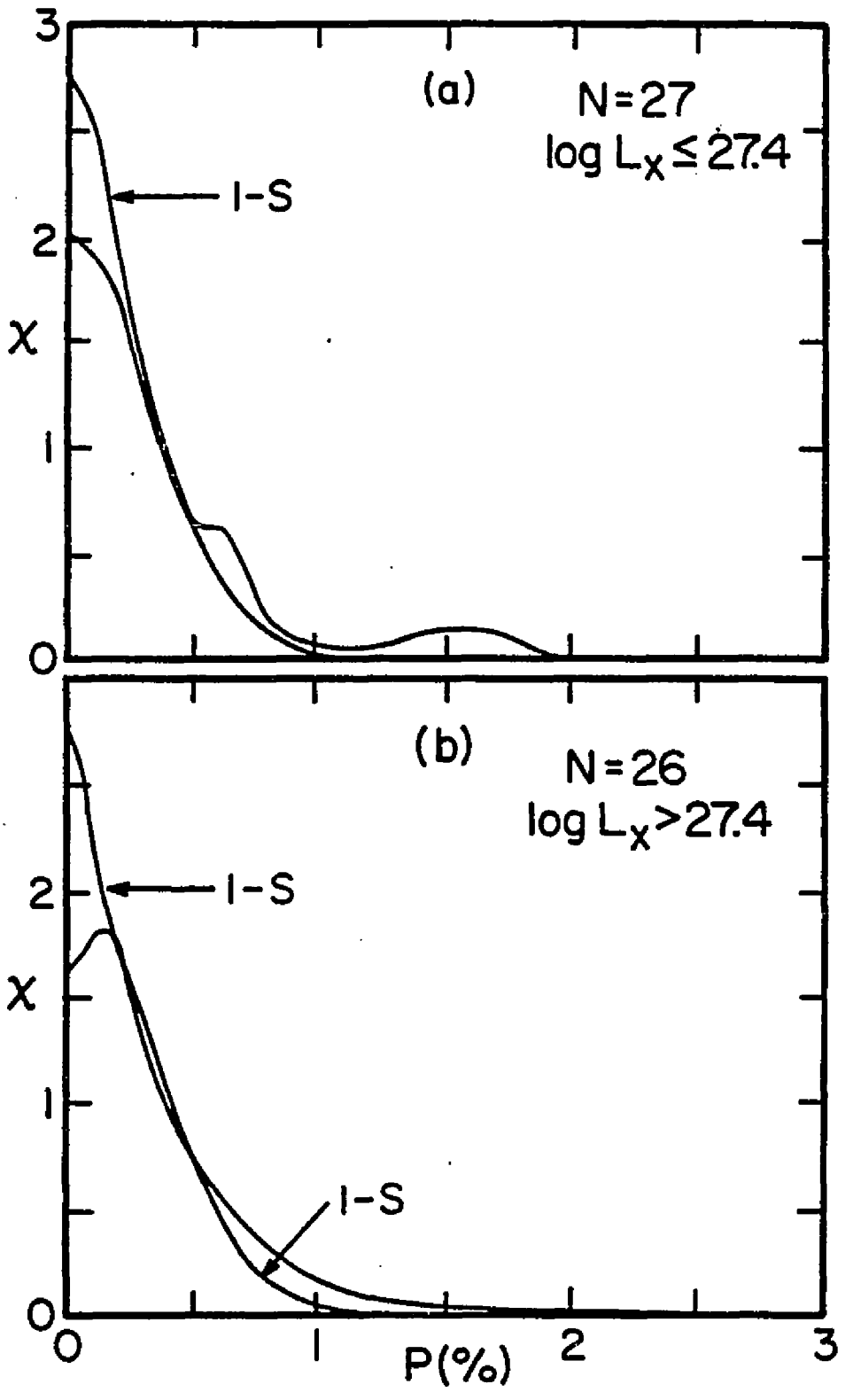

Figure 22. The distributions of polarization for all low polarization QSOs with (a) log $L_x \leq 27.4$ and (b) log $L_x > 27.4$.

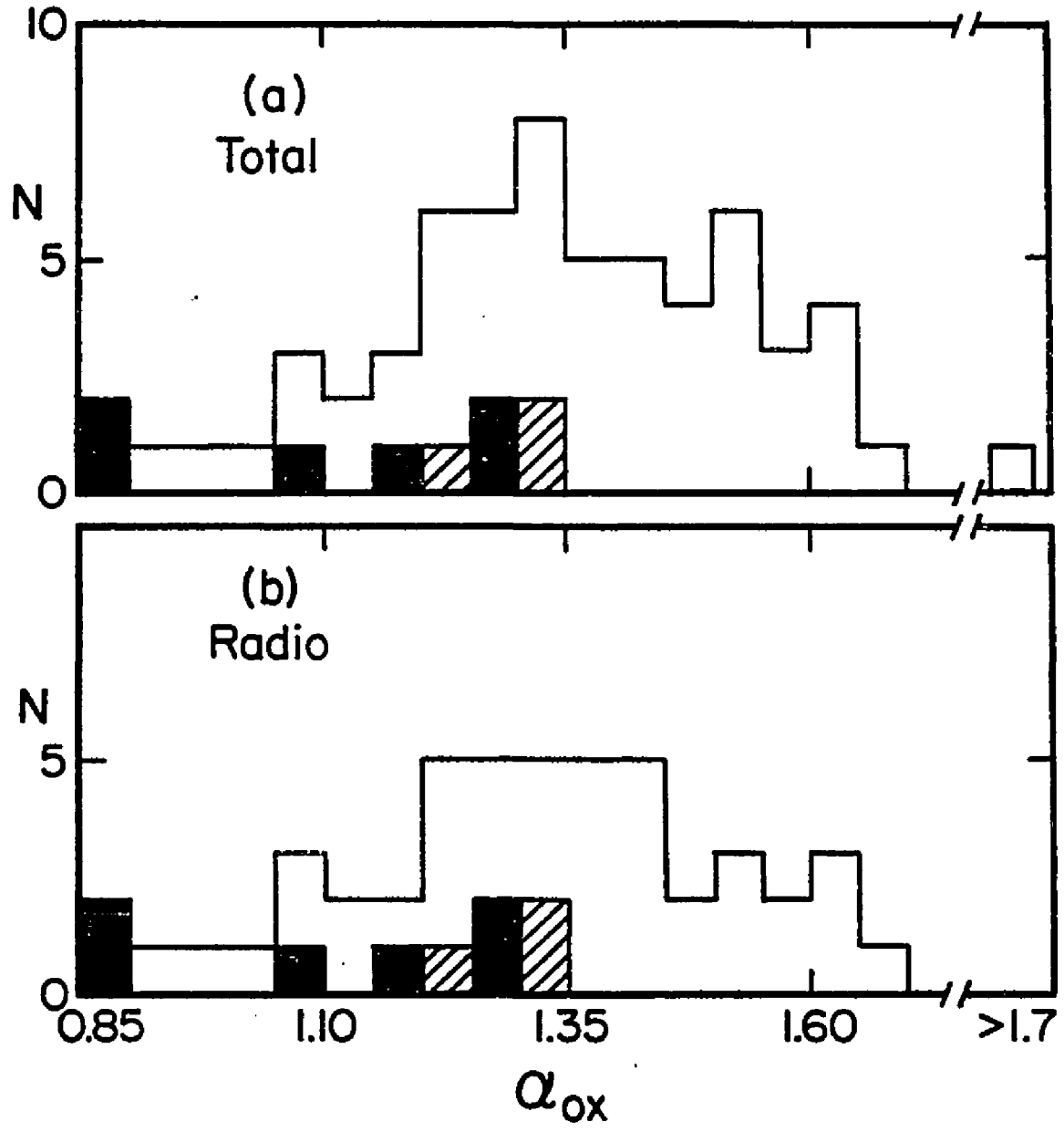

Figure 23. The distributions of the optical/X-ray spectral index, α_{ox}, for (a) all QSOs surveyed and (b) all radio-selected QSOs surveyed which have been detected by HEAO-B.

at the time of its X-ray observation were 2 magnitudes brighter than is listed in BCS, the true value of α_{ox} would be underestimated by 0.31. The magnitude of this uncertainty is large enough to strongly affect the distribution of α_{ox}. The consistently low values of α_{ox} exhibited by the HPQs do provide evidence that the correlation is real despite the uncertainty; it is difficult to imagine that all the HPQs would happen to be optically brighter than their catalog magnitude at the time of the X-ray observations.

The distributions of polarization for QSOs with $\alpha_{ox} \leqslant 1.35$ and > 1.35 are shown in Figure 24 (a) and (b). Most of the distributions can be accounted for by interstellar polarization. There is perhaps slightly more intrinsic polarization for the sample with low values of α_{ox}, however, the numbers of QSOs used to derive these distributions are fairly small. There is only weak evidence for a continuous correlation.

We note that PHL 5200 has not been detected by Einstein and has a spectral index $\alpha_{ox} > 1.35$. If its ratio of optical to X-ray luminosity were similar to other (radio-loud) HPQs, it would probably have been detected.

I. Radio Structure Position Angle

The correlation between optical polarization and the position angle of extended radio structure is of a different nature than other correlations discussed here; it involves the position angle rather than the degree of optical polarization. A preferential alignment between the position angle of optical polarization and the angle of extended

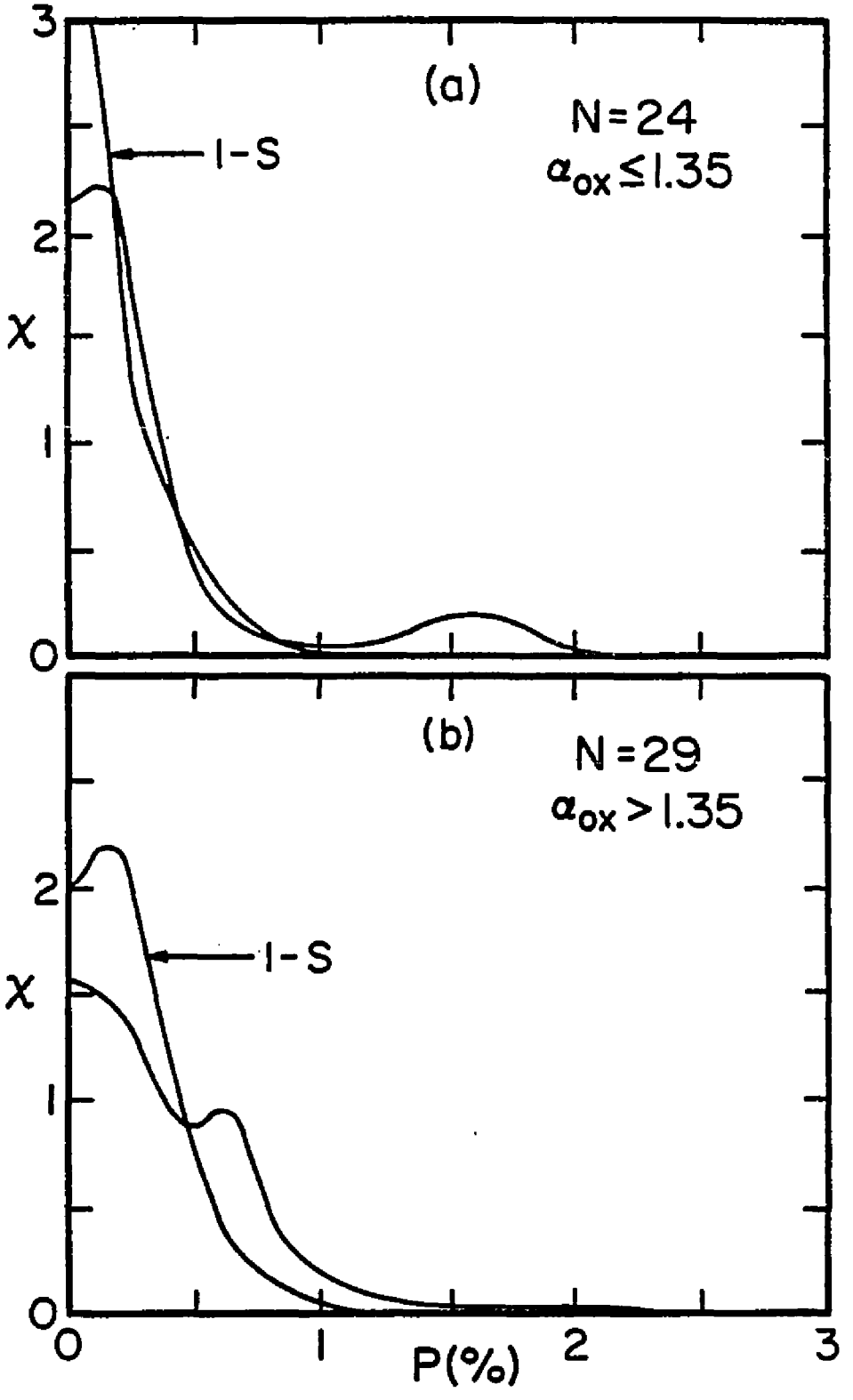

Figure 24. The distribution of polarization for all low polarization QSOs with $\alpha_{ox} \leq 1.35$ and (b) $\alpha_{ox} > 1.35$.

radio structure was first discovered by Stockman, Angel, and Miley (1978). The data presented here include all QSOs polarimetrically observed for which extended radio structure data are available. Since the low polarization QSOs are not significantly variable, we have combined all broadband polarization measurements to improve the accuracy of the polarization position angle.

In Figure 25, we show a histogram of $|\Delta\theta|$, the absolute difference between the position angles of optical polarization and radio structure, for all QSOs in the sample with $\sigma_{|\Delta\theta|} \leq 25°$ and $\sigma_{\theta_{OPT}} < 14°$. The latter limit on the uncertainty of the optical position angle is imposed to ensure that the measured polarization is significant (§ II.A). Relaxing this limit would include more of the QSOs in Table 1 with radio data but introduces some uncertainty; the results are not substantially different if these limits are slightly increased. The HPQs are marked as in previous histograms; the purpose, however, is only to distinguish the HPQs, not to examine the correlation of $|\Delta\theta|$ with high polarization as in previous histograms.

The distribution of $|\Delta\theta|$ is dominated by QSOs where the two position angles are aligned. If the HPQs are excluded, 25 of 31 low polarization QSOs are aligned within $\lesssim 40°$. Using the K-S statistic, the probability that the values of $|\Delta\theta|$ are random is <1%. There are several examples of "aligned" QSOs ($|\Delta\theta| < 40°$) where the two angles are statistically significantly different. This implies that the width of the distribution for aligned QSOs is intrinsic and is not due simply to measurement errors. There are also at least six low polarization QSOs which are clearly misaligned; the misaligned QSOs cluster near

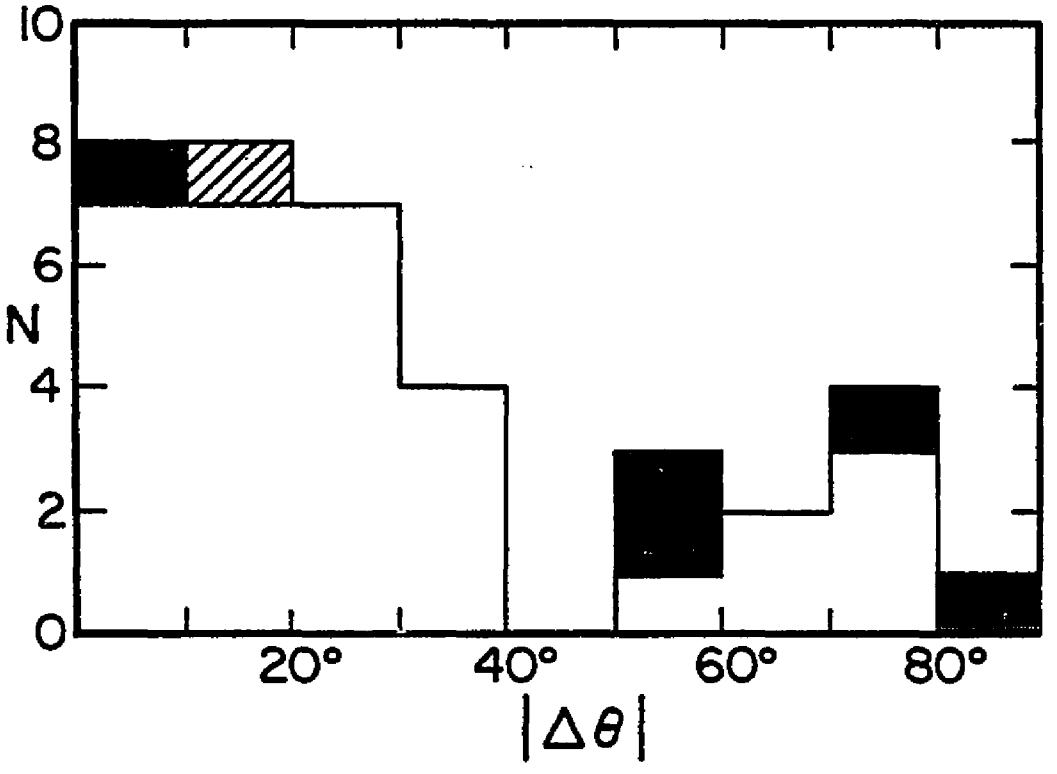

Figure 25. The distribution of the angle between the position angles of optical polarization and extended radio structure, $|\Delta\theta|$, for all QSOs with $\sigma_{|\Delta\theta|} \leq 25°$ and $\sigma_{\theta_{OPT}} \leq 14°$.

$|\Delta\theta| \sim 70°$ but the statistics are insufficient to determine if this peak is significant. Two or more polarization measurements of five of these misaligned QSOs have been made; the position angles of their polarization do not appear to be variable.

The HPQs which have extended radio structure exhibit a wide range of $|\Delta\theta|$. The average polarization position angle is not necessarily meaningful since our sampling of the variable polarization is not systematic. The two "aligned" HPQs in this sample are PKS 2345-167 and 3CR 336 (1622+238). PKS 2345-167 has only been observed three times and it is not clear whether it exhibits a preferred position angle. 3CR 336 is a possible HPQ; all five measurements of this object have large errors and it may be a low polarization QSO.

There is one radio-loud HPQ, OI 287, which has a constant position angle of optical polarization. Although these data are not included in Table 1, preliminary results from the VLA indicate that OI 287 has extended radio structure at a position angle of 140° (Moore, Wardle, and Angel 1981), almost exactly aligned with the position angle of optical polarization. Thus, it exhibits the position angle alignment characteristic of low polarization QSOs. OI 287 has already been noted for its lack of polarimetric and photometric variability (§ III.C.1). Except for the fact that its polarization is ∿8%, OI 287 is in many respects similar to normal low polarization QSOs.

J. Summary of Correlations

The relationships between the optical polarization and numerous other source parameters have been analyzed and discussed

in this chapter. Now that a large sample of HPQs is available, it is possible to present a more complete picture of the characteristics of the class of highly polarized QSOs. It is also possible to examine whether the correlations which exist on a large scale (i.e. the polarization being simply high or low) are also present among low polarization QSOs.

An important characteristic of the HPQs is that they are all radio-loud, with the exception of PHL 5200. The percentage of radio-loud QSOs in our survey which are highly polarized is 10-20%. This percentage would increase for a sample of QSOs from a high frequency radio survey. The percentage may also be an underestimate if many radio-loud QSOs exhibit only brief phases of high polarization. PHL 5200, the only radio-quiet HPQ, is an atypical HPQ in many respects. It does not appear to be polarimetrically or photometrically variable, and its spectrum shows broad, deep absorption troughs (Stockman, Angel, and Hier 1980) have observed additional absorption QSOs and found them all to have low polarization. Additional measurements of a larger sample of radio-quiet QSOs should be made to determine if PHL 5200 is unique or if it is indicative of a small percentage of radio-quiet QSOs which are HPQs. We would conclude that the typical characteristics of HPQs (high polarization and strong variability) are associated exclusively with radio-loud QSOs.

There is no evidence for a correlation between polarization and redshift, either for the HPQs or among low polarization QSOs. This result suggests that high polarization (and associated

characteristics) is not an evolutionary phase of QSO activity. Our survey is dominated by low redshift QSOs, so the occurrence of high polarization is less well known among high redshift QSOs.

There is a suggestion of a correlation between high polarization and optical (λ_{rest} = 2500 Å) luminosity, in the sense that the HPQs are typically less luminous than other QSOs in the sample. This correlation is of moderate significance (K-S probability of $\sim$5%) for both the entire survey and the entire radio-selected survey; it is subject to uncertainty due to the optical variability of the HPQs. It is important to note, however, that our results (using catalog magnitudes) show that the HPQs are not typically more luminous than other QSOs. There is no apparent correlation among low polarization QSOs.

The association between high polarization and strong photometric variability is confirmed by the photometric variability sample. Although the variability data are heterogenous, it is clear that the HPQs found in the survey preferentially have large amplitude and rapid photometric variability (as well as polarimetric variability as shown in § III). There is not a one-to-one correspondence between HPQs and OVV QSOs. PHL 5200 and OI 287 appear to be constant in both polarization and brightness; further polarimetric monitoring of known OVVs is also required. There is at least one example, 3CR 454.3, which suggests that long term phases of active variability may be associated with phases of high polarization. The analysis of low polarization QSOs is suggestive of a continuous correlation between polarization and both amplitude and time scale of photometric variability.

A similar correlation is seen between polarization and the optical spectral index. The HPQs have a markedly different distribution of α_{OPT} than the remainder of the spectrophotometry sample, and preferentially exhibit steeper (redder) spectra. The median index of the HPQs is 1.4, compared to 0.7 for the non-HPQs. Not all steep spectrum QSOs are highly polarized. A correlation in the same sense may be present among low polarization QSOs. The HPQs also appear to exhibit smoother optical continua which more closely resemble a power law than normal QSOs.

There does not appear to be a correlation between polarization and the equivalent width of the Mg II emission line. As with the optical luminosity, these data are uncertain due to the variability of the HPQs. However, no systematic differences are present between the HPQs and other QSOs. Neither is there any indication of a correlation between polarization and emission line strength among normal QSOs.

There is a weak correlation between high polarization and the X-ray luminosity in the sense that HPQs have slightly higher luminosity than normal QSOs. This correlation has a significance of $\sim$5%. There is no evidence of a continuous correlation among low polarization QSOs.

Since the HPQs appear slightly underluminous at 2500 Å and overluminous at 2 keV, it is not surprising that we find a strong correlation between high polarization and the optical/X-ray spectral index. The HPQs preferentially have a higher ratio of X-ray to optical luminosity. The correlation has a probability of 1% for HPQs(1); using all HPQs, the probability that the distributions are from the

same population is 5%. Again, the variability of HPQs introduces uncertainty in this correlation since the optical and X-ray measurements were not simultaneous. However, the variabilty should not systematically bias the ratios in one direction; therefore, while individual estimates of the spectral index may be in error, the systematic preference for low spectral indices among HPQs is evidence that the correlation is real. There is also possible evidence that the correlation is present among normal QSOs.

Using the most complete set of data available, we have verified the preferred alignment between the optical polarization position angle and the angle of extended radio structure among low polarization QSOs. This alignment is not only evidence that the low polarizations observed are intrinsic but also establishes a physical relationship between the compact optical emission region and the giant radio lobes. This will be discussed further in §VII. Among the few variable HPQs with extended radio structure, there is no preferred alignment. However, OI 287 (an atypical HPQ with constant polarization) does have extended radio emission which is aligned with the polarization position angle.

It is curious that, for those parameters (Δm, τ, α_{OPT}, α_{ox}) where a strong correlation is found with high polarization (using the histogram and K-S analyses), the analysis of the low polarization QSOs is always suggestive of a correlation in the same sense. It is important to recall that the distribution of polarization is not continuous; there is a clear break between low and high polarization QSOs. However, among normal QSOs, our analyses suggest that there may be a slight

increase in the typical intrinsic polarization for QSOs which are more like HPQs in other parametrized characteristics. There are major reservations concerning this conclusion. First, the distributions of polarization (and interstellar simulations) are often derived for relatively few QSOs. The source parameters are also frequently uncertain and/or heterogenous. Finally, since some HPQs exhibit occasional low polarization, latent HPQs (perhaps with intermediate polarization) may be present in the samples used to derive the low polarization distribution. Thus, without additional, more accurate polarization measurements and better defined source parameters, we cannot conclude that these analyses prove that continuous correlations exist.

The radio properties of the HPQs are an important aspect of their physical nature. Moore and Stockman (1981) have discussed these properties in detail and a summary of their results is presented here. The HPQs generally have relatively flat radio spectra from 1-90 GHz, which is characteristic of compact optically thick emission regions. Many of the HPQs also have a steep low-frequency component, characteristic of extended optically thin emission, although some exhibit a low-frequency turnover. Radio flux variability is common at high frequencies for the HPQs. Low-frequency variability has also been observed in five of seven definite HPQs which have been monitored. For comparison, Condon et al. (1979) have found that $\sim$25% of flat spectrum sources exhibit low-frequency variability. Although the number of HPQs monitored is small, this suggests that HPQs are more likely to be low-frequency variables. It is also interesting to note that two of the four known superluminally expanding radio sources

(e.g. Cohen et al. 1977) are HPQs (3C 279 and 3CR 345). The other two superluminal sources, 3C 273 and 3C 120, both have low polarizations (this paper, Maza 1979). Finally, most of the HPQs have the majority of flux from a compact central source. Two HPQs, 3CR 345 and 3CR 454.3, are asymmetric D2 sources (Davis, Stannard and Conway 1977). Two definite HPQs, 3CR 68.1 and PKS 2345-167, are reported to be double-lobed radio sources. The map of 3CR 68.1 (Mackay 1969) shows possible, but not conclusive, structure on a scale of 1 arcmin. PKS 2345-167 is barely resolved with the Westerbork telescope (Miley and Hartsuijker 1978). There are three possible HPQs, 3CR 212, 4C 49.22, and 3CR 336, which are double-lobed sources (Mackay 1969, Miley and Hartsuijker 1978); further polarization measurements are required to determine whether these QSOs are indeed HPQs.

We can summarize the typical properties of the HPQs now known. The general emission properties are that the HPQs exhibit strong, rapid photometric (and polarimetric) variability, they have steep, relatively smooth optical continua, and they probably have a high ratio of X-ray to optical luminosity. They are compact flat spectrum radio sources, and frequently exhibit extreme properties such as superluminal expansion or low-frequency variability. Exceptions to these general properties have been noted in the discussion above. Relative to other QSOs in our samples, the HPQs are not markedly different in terms of their redshift, optical or X-ray luminosity, or emission line strength.

CHAPTER V

BL LACERTAE OBJECTS AND THEIR RELATIONSHIP TO HIGHLY POLARIZED QSOS

In this chapter we present the characteristics of BL Lacertae objects and demonstrate their relevance to highly polarized QSOs. Several reviews of the properties of BL Lac objects have been published which more extensively describe their properties (e.g. Stein, O'Dell, and Strittmatter 1976, Stein 1978, Condon 1978, Angel and Stockman 1980). We first describe the polarimetric properties of BL Lac objects and then discuss other emission properties of these objects. As we will show, the characteristics of BL Lac objects are strikingly similar to the properties of HPQs which we have established in §III and IV. Since the HPQs share properties of both BL Lac objects and normal low polarization QSOs, they represent a key link between these two extragalactic phenomena.

A. Polarimetric Characteristics of BL Lac Objects

One of the defining characteristics of BL Lac objects is high, variable optical polarization (Stein, O'Dell and Strittmatter, 1976). A complete reference list of all polarization measurements of BL Lac objects, compiled by the author, appears in the recent review by Angel and Stockman (1980). Without discussing individual objects, we present here a general description of the polarimetric behavior of BL Lac objects.

The degree of polarization measured in BL Lac objects ranges from 0% up to 35%. Most objects typically have polarization in the range 5-15%. As with some HPQs, some BL Lac objects do exhibit phases of low polarization ($P < 3\%$) during their variability. A comparison of the maximum degrees of polarization exhibited by BL Lac objects and the HPQs suggests that BL Lac objects may have somewhat higher polarization than HPQs (Angel and Stockman 1980). However, the BL Lac objects have generally been observed more extensively than HPQs.

Rapid variability of the polarization is common to essentially all BL Lac objects. The best study of general polarimetric variability is provided by the monitoring of 12 BL Lac objects by Angel et al. (1978). There is no simple characterization of the morphology of the variability. Changes in the degree of polarization are often observed without changes in the position angle, and vice-versa. Some BL Lac objects appear to always be variable (e.g. BL Lac itself); others may have brief periods of variability. The time scales of variability range from about one day to one month.

Two important morphological characteristics of the polarimetric variability do emerge from the monitoring by Angel et al. (1978). The first is that the shortest time scale of variability observed in any BL Lac object is about one day. Nightly variations are often of large amplitude but hourly variations are minimal. This minimum time scale of one day is also observed among the HPQs (§ III) and is confirmed by our intensive monitoring of B2 1308+326 and BL Lac (to be discussed in § VI).

The second significant property of the variability is that 5 of the 12 objects monitored by Angel et al. appear to have a preferred position angle of polarization. While the degree of polarization may vary dramatically, the position angle varies only slightly ($\sim \pm 20°$) about the preferred value. Observations over the last two years by the author of these preferred angle BL Lac objects consistently confirm the preferred angles over a long time baseline (Moore 1981). We note that there are suggestions of a preferred position angle in some HPQs (§ III), but additional monitoring of these objects is required.

The optical/infrared polarization of BL Lac objects is normally, but not always, wavelength independent. Wavelength dependence measurements have been reported by Visvanathan (1973), Kikuchi et al. (1976), Nordsieck (1976), Knacke, Capps, and Johns (1976, 1979), Rieke et al. (1977), and Puschell and Stein (1980). Generally, the polarization degree and position angle are constant, but some significant position angle rotations or changes in the degree of polarization are observed. This type of variable wavelength dependence is similar to that observed in HPQs.

B. Properties of BL Lac Objects

In this section we describe the general emission characteristics of BL Lac objects. Some of these characteristics are definitive properties of BL Lac objects (Stein, O'Dell, and Strittmatter 1976). As additional objects and better data are reported, it is clear that precisely defining what constitutes a BL Lac object is becoming more

difficult (e.g. the discussion at the Pittsburgh Conference on BL Lac objects, Wolfe 1978). However, the basic characteristics discussed here have been repeatedly confirmed for members of this class.

All known BL Lac objects are radio sources. Since most identifications of BL Lac objects have been made from radio surveys, there is a strong selection effect. However, all objects originally discovered from optical or X-ray surveys have been found to be radio sources (Angel and Stockman 1980). Further optical searches for BL Lac objects (e.g. field variability or polarization surveys) are necessary to search for radio-quiet BL Lac objects.

The radio spectra of BL Lac objects are generally flat or inverted (Condon 1978, Wardle 1978). Flux and polarization variability is common among BL Lac objects (Altschuler and Wardle 1976, Wardle 1978, and references in Angel and Stockman 1980). Nearly all BL Lac objects are compact radio sources. Wardle (1978) has found that some objects have assymetric extended emission on scales of a few arcseconds. At least one BL Lac object exhibits large scale double-lobed radio structure (Angel and Stockman 1980).

Most of the BL Lac objects with known redshifts are at low redshifts relative to QSOs (Angel and Stockman 1980). Since BL Lac objects, by definition, do not show (strong) emission lines, redshifts are derived from the redshifts of an associated galaxy, absorption lines, or very weak emission lines. Some high redshift ($z > 1$) BL Lac objects are known (Jauncey et al. 1978, Gaskell 1978). Certainly, the local space density of BL Lac objects appears to be higher than that for

radio-loud QSOs. Beyond this statement, it is difficult to discuss the redshift distribution of BL Lac objects. Similarly, since so few redshifts are known, it is difficult to characterize the typical luminosities of BL Lac objects.

Rapid large amplitude photometric variability is a common property of nearly all BL Lac objects. Numerous variability references are given by Stein, O'Dell, and Strittmatter (1976), Stein (1978), and Angel and Stockman (1980). Nearly all BL Lac objects in the compilation of Angel and Stockman (1980) have $\Delta m > 2$ mag. Monitoring programs indicate that the minimum time scales of variability are probably about one day for active BL Lac objects. More rapid variations have been reported (e.g. Bertaud et al. 1969, Weistrop 1973a) but are difficult to confirm (see also § VI).

Another characteristic of BL Lac objects is their steep optical continua. The median spectral index of BL Lac objects listed by Angel and Stockman (1980) is 1.8; the flattest spectrum has an index of 0.9. Thus, the optical energy distribution of BL Lac objects is similar to that of the HPQs.

The characteristic which distinguishes BL Lac objects and QSOs is the lack of emission lines in BL Lac objects. Many BL Lac objects, even with high signal-to-noise observations, show no emission lines. However, weak emission lines have been discovered in some BL Lac objects (e.g. Baldwin et al. 1977, Miller, French, and Hawley 1978). This discovery clouds the distinction between BL Lac objects and QSOs. The weak emission lines which have been discovered are of low contrast

and have lower luminosity than QSO emission lines (Angel and Stockman 1980). The emission lines properties are a crucial element of this discussion and will be discussed further below.

C. Comparison of BL Lac Objects and Highly Polarized QSOs

It is clear from the discussion above that BL Lac objects and HPQs share many of the same characteristics. Both HPQs and BL Lac objects exhibit high optical polarization which is strongly variable on short time scales. Photometrically, both classes of objects exhibit large amplitude rapid variability. They have relatively steep optical continua. Nearly all the objects are compact flat spectrum radio sources. There are suggestions that HPQs may be intermediate in their properties between low polarization QSOs and BL Lac objects. For example, the maximum polarization, maximum variability, or typical spectral index may be systematically lower for HPQs than for BL Lac objects (see Angel and Stockman 1980); however, this could be due to the extent of monitoring and the few objects involved. In terms of the characteristics of their continuum emission, it is difficult to distinguish HPQs and BL Lac objects.

The only apparent observational distinction betwen HPQs and BL Lac objects is the presence of strong emission lines in HPQs. It is important to recognize that the HPQs do generally have strong emission line both in terms of luminosity and equivalent width (Oke 1966, Visvanathan 1973, Baldwin 1975, Neugebauer et al. 1979, Smith and Spinrad 1980). Our analysis in § IV.G reveals no significant difference

between the equivalent width of Mg II for HPQs and other normal QSOs. BL Lac objects have either no or very weak emission lines.

There are several points which must be made when discussing our classification of objects as BL Lac objects, HPQs, or normal QSOs. First, we have proceeded rather naively in originally selecting objects for the QSO polarization survey by simply taking objects from the catalog of QSOs by BCS. A few objects not in BCS, such as W1 0846+513 and B2 1308+326, have been included as QSOs; another object in BCS, MC 1400+162, was excluded as a BL Lac object. However, despite this naive approach in classifying objects as QSOs or BL Lac objects, we have shown that the HPQs in our survey appear to be similar to the low polarization QSOs in terms of their redshift and luminosity distribution. This is evidence that the HPQs are related to normal QSOs and that they are not an entirely different population.

The second point is related to the crucial question of emission line strengths. The conclusion (§ IV.G) that the HPQs do not have significantly different emission line strengths from normal QSOs is influenced by the initial distinction (on the basis of strong emission lines) between HPQs and BL Lac objects. If BL Lac objects were included in our analysis, the highly polarized objects certainly would have systematically weaker emission lines. Thus, a crucial question is whether the emission line strengths of HPQs and BL Lac objects represent a continuous or a bimodal distribution (i.e., is it reasonable to distinguish the two classes?). It is our impression from published spectra that the distribution is bimodal and a reasonable distinction

can be made between HPQs and BL Lac objects. However, a systematic spectrophotometric analysis of emission line strengths (or upper limits) in HPQs and BL Lac objects, observed over a range of brightness, is required to accurately determine the character of the distribution.

Although the distribution of emission line strengths is an important question, the semantics of classification should not obscure the more fundamental result which we have established. The HPQs, whether they are classified as highly polarized QSOs or strong-lined BL Lac objects, share properties of both normal QSOs and BL Lac objects and are a crucial link between these two phenomena. The redshift and luminosity distribution of the HPQs in our survey are similar to those of normal QSOs. This result indirectly justifies our naive classification of HPQs as QSOs and establishes that HPQs are related to normal QSOs. On the other hand, in terms of continuum characteristics, it is clear that the HPQs are intimately related to BL Lac objects.

CHAPTER VI

INTENSIVE MONITORING OF HIGHLY POLARIZED OBJECTS

We have chosen two highly polarized objects for intensive polarimetric and photometric monitoring in order to gain a more accurate picture of their short term variability. The primary objective of this monitoring is to determine accurately the minimum characteristic time scale of variability, as this sets an upper limit to the size of the emitting region (if there is no relativistic enhancement). In addition, we can examine the correlation of brightness and polarization, the morphology of the variations, and the wavelength dependence of the polarization.

The first object to be discussed is the QSO B2 1308+326, which was monitored during a very bright flare in 1978. This object, at maximum brightness during the flare ($L(0.3\text{-}10\ \mu m) \sim 10^{48}$ erg s^{-1}), was one of the most luminous objects known. Since the combination of high luminosity and rapid variability is a fundamental problem associated with HPQs and BL Lac objects, the high luminosity phase of 1308+326 can provide an extreme test of theoretical models.

The second object, BL Lac, was selected for an unprecedented worldwide monitoring effort because prior measurements had shown it to be consistently variable and it is bright enough to be well monitored with small telescopes. This program is designed to overcome a persistent

restriction is monitoring the variability of objects with a characteristic time scale of ∿1 day; this restriction is that the variability can only be sampled from one location about 8 hours per day. In this program, observers monitored BL Lac at ten telescopes located in Israel, Europe, and North America; with ideal conditions, it was possible to obtain coverage 20 hours per day, thus filling in the large monitoring gaps.

A. Monitoring of B2 1308+326

This object has been extensively observed at radio, infrared, and optical wavelengths by O'Dell, Puschell and Stein (1977), Owen et al. (1978), O'Dell et al. (1978), Puschell et al. (1979), and Jones et al. (1980). The observations discussed here were made during a bright flare in the spring of 1978, during which Puschell et al. (1979) also monitored the object. The results of this program have been published by Moore et al. (1980).

The optical polarization measurements are included in Table 2 (§ III.A) with other observations of B2 1308+326. In addition to these measurements, infrared polarimetry, infrared photometry, and optical photometry (B band) was carried out by other observers as part of the monitoring program. These observations are listed in Table 3.

The unfiltered optical polarization observations are shown in Figure 26. It is apparent from this figure that both the degree and position angle of polarization vary dramatically. The degree of polarization is generally quite high, ranging from 2 to 15%; the position angle varies from 45° to 160°. Although changes in the polarization

Table 3. Supplemental Observations of B2 1308+326.

Infrared Polarimetry (2.2 μm)

Date	UT	P(%)	θ(°)
5/20/78	7:00	17.0 ± 2.0	90 ± 3
5/28/78	6:30	<4.0 (2σ)	-
5/30/78	6:00	9.3 ± 1.2	89 ± 4

Infrared Photometry

Date	λ(μm)	f_ν (mJy)
5/28/78	1.25	8.9 ± 0.9
	1.6	10.7 ± 0.6
	2.2	15.8 ± 0.8
5/29/78	10.6	139.0 ± 23.0
5/30/78	2.2	12.5 ± 1.0

Optical Photometry (1978)

Date	B	Date	B	Date	B
3/18	16.38	5/17	15.83	6/30	15.95
4/10	16.16	5/28	15.65	7/1	16.02
4/16	15.59	5/29	15.69	7/2	16.06
4/18	15.73	6/7	15.91	7/3	16.23
5/9	15.89	6/8	15.95	7/3	16.21
5/12	15.90	6/9	15.83	7/4	16.35
5/13	15.91	6/10	15.66	7/5	16.35
5/13	15.89	6/15	16.10	7/6	16.31
5/14	15.90	6/26	16.03	7/7	16.37
5/16	15.93	6/27	15.87		

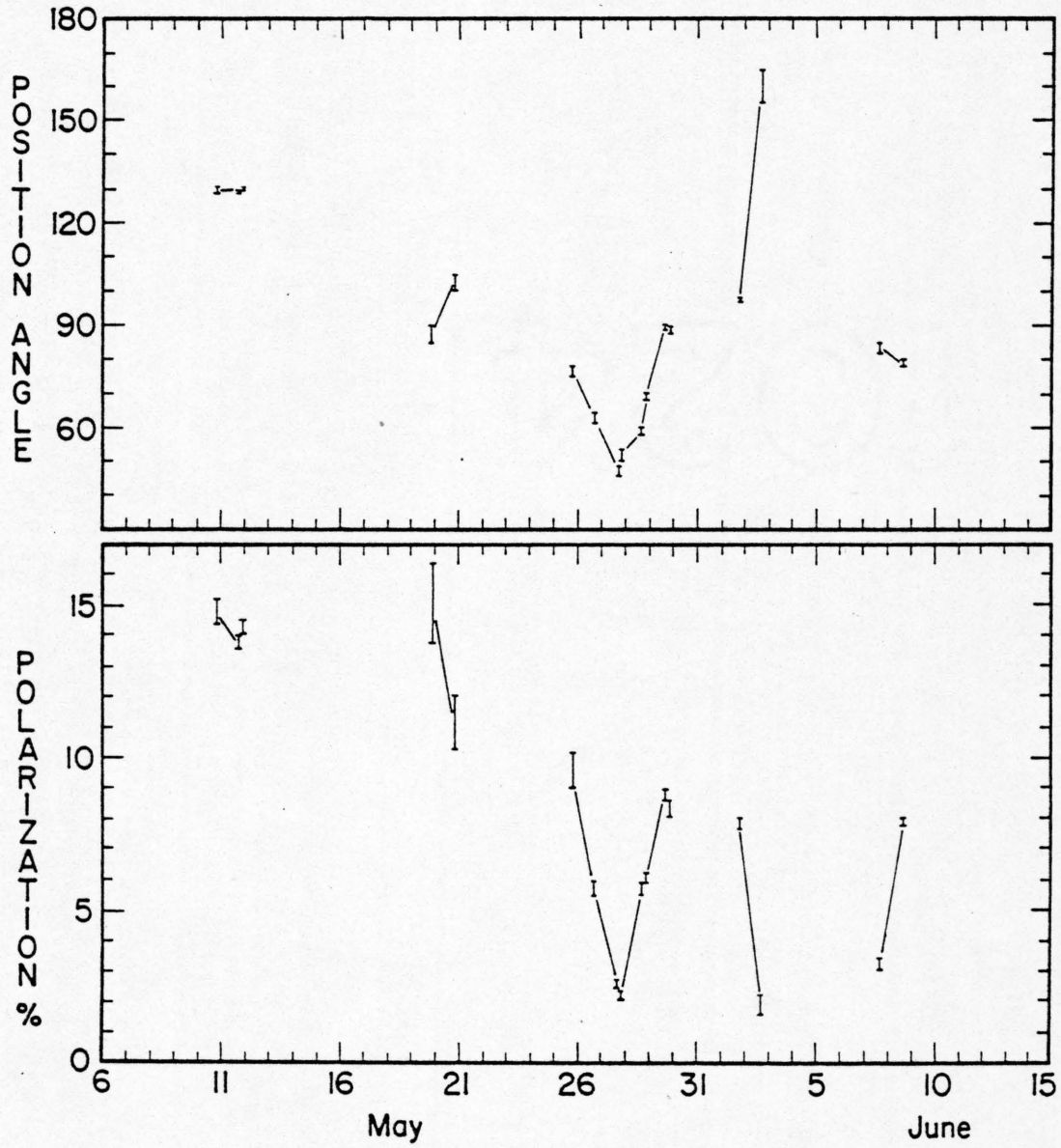

Figure 26. The broadband optical polarimetric variability of B2 1308+326 during the 1978 outburst.

occur on the same time scale as changes in the position angle, there is no apparent correlation characterizing their relationship.

The polarimetric data, in particular the well-monitored period of May 26-30, indicate that the characteristic observed time scale of variability is $\tau_{obs} \sim 2$ days (the rest-frame time scale is thus $\tau \sim \tau_{obs}/(1+z) \sim 1$ day). While large-amplitude nightly variations are frequently observed, there is no evidence for large-scale intranightly variability. Accurate measurements on four nights with the 2.3 m telescope over baselines of 2-5 hours reveal only small variations which are consistent with the nightly trends. Continuous observations over a period of 1-2 hours, obtained on four nights with the 0.9 m telescope, have been listed in Table 2 as a single measurement in order to improve accuracy. However, the residuals formed by subtracting these individual measurements from the nightly means show no significant deviation from the expected statistical distribution. The errors of these individual measurements are too large ($\sigma_p \sim$ 1-2%) to permit the detection of small variations; however, large-amplitude variability can be ruled out.

Puschell et al. (1979), who monitored 1308+326 during the same period, claimed that they observed dramatic changes in the optical polarization on a time scale of ~15 minutes. Although we did not observe the object on the same nights that they claim to have observed these rapid variations, their result is surprising in light of the consistent lack of such variability in our observations. However, a reanalysis by Puschell (private communication) of his data shows that the variations are not, in fact, statistically significant. Thus, the

variability is probably not as rapid as Puschell et al. report and we conclude our estimate of $\tau_{obs} \sim 2$ days is accurate.

The infrared polarimetry, obtained on three nights simultaneously with optical polarimetry, suggests that the polarization stays very nearly the same through both wavelength regions during the most rapid variations. On the two nights a definite infrared polarization was measured, both the strength and the position angle are essentially identical to that in the optical. Although the infrared measurement on May 28 is an upper limit, it is consistent with the optical polarization and is stringent enough to prove that the infrared polarization must have increased dramatically from May 28-30 (as did the optical polarization). The fact that the infrared polarization varies with the optical polarization establishes a direct association between the optical and infrared emission. This association is important because most of the luminosity of the source emerges in the infrared. Thus, arguments based on the optical emission apply to the dominant luminosity source of this type of object.

The degree of polarization appears to be independent of wavelength from the optical through the infrared regime. The polarization is slightly lower at 0.82 μm than that at 0.4 μm on May 29 and 30, but the difference is only marginally significant; the polarization at 2.2 μm is identical, within the errors, to that in the optical. A comparison of our polarimetry with that of Puschell et al. (1979) suggests a strong wavelength dependence on June 3 when we found an optical polarization of $1.9 \pm 0.3\%$ at $160° \pm 5°$, while they report a

polarization at 2.3 μm of 16 ± 5% at 100° ± 9°. However, Puschell (private communication) informs us that their published June 3 measurement is instead a four-day average from June 2-5. Their actual June 3 measurement was 8.4 ± 6.8% at 110° ± 28°; this value is entirely consistent with our optical measurement.

The position angle of polarization is a variable function of wavelength. The differential rotation between 0.4 μm and 0.82 μm is 15°.6 ± 2°.8 on May 29 and 1.°3 ± 2.°3 on May 30. A blue measurement was not made May 28, but the position angle at 0.82 μm was 14.°6 ± 7.°7 higher than the broadband position angle. On the two nights when the position angle was measured at 2.2 μm, there was little, if any, differential rotation. Variable differential rotation has been previously observed in a BL Lac object, OI 090.4, by Tapia et al. (1977). We also note that from previous observations of OI 090.4, PKS 0735+178 (Rieke et al. 1977) and BL Lac (Rieke, private communication), it appears that when differential rotation occurs in the optical regime, it continues to at least 2.2 μm.

The variability of the differential rotation implies that it is intrinsic to the source. There are several possible causes of the measured differential rotation: very rapid variations (this is unlikely in view of the lack of hourly variability in the broadband polarization), superposition of emission components with different energy distributions and polarizations, or Faraday rotation. If it were due to Faraday rotation, any model for the emitting region must have a high magnetic field and/or a high column density of thermal

electrons. The convergence of position angle with wavelength could be caused by a change in the magnetic field configuration so that the integrated line-of-sight component decreases. If one assumes that the intrinsic polarization is uniform across the source and that the observed rotation of 15° is due to Faraday rotation, then $\langle N_e B_{||} \rangle \ell \sim 10^{25}$ G cm^{-2}. Internal Faraday rotation would depolarize the radiation at lower frequencies; for the above parameters, the fractional decrease is $\sim$0.95 in the near-infrared bandpass (not detectable in our observations on May 29) and $\sim$0.5 at the K band. Measurements extending into the infrared are therefore feasible to test for the presence of Faraday rotation, both by determining the wavelength dependence of the rotation and by searching for depolarization effects.

Optical photoelectric photometry of B2 1308+326 was also obtained by several observers during the same period. Standard B filters of the UBV system were used, with integration times sufficient to yield statistical errors of $\lesssim$0.02 mag. On those nights when observations were made with more than one instrument, the magnitudes are consistent within the errors, implying that systematic differences between the photometers are minimal. The nightly mean magnitudes are included in Table 3 and are plotted in Figure 27. We include in the figure data from Puschell et al. (1979); the errors of their measurements are $\sim$0.06 mag, except for July 1 (σ_B = 0.13 mag).

As in the polarimetric monitoring, the brightness also shows rapid fluctuations on a time scale of days. The most dramatic example is April 8-10, during which the brightness decreased by more than

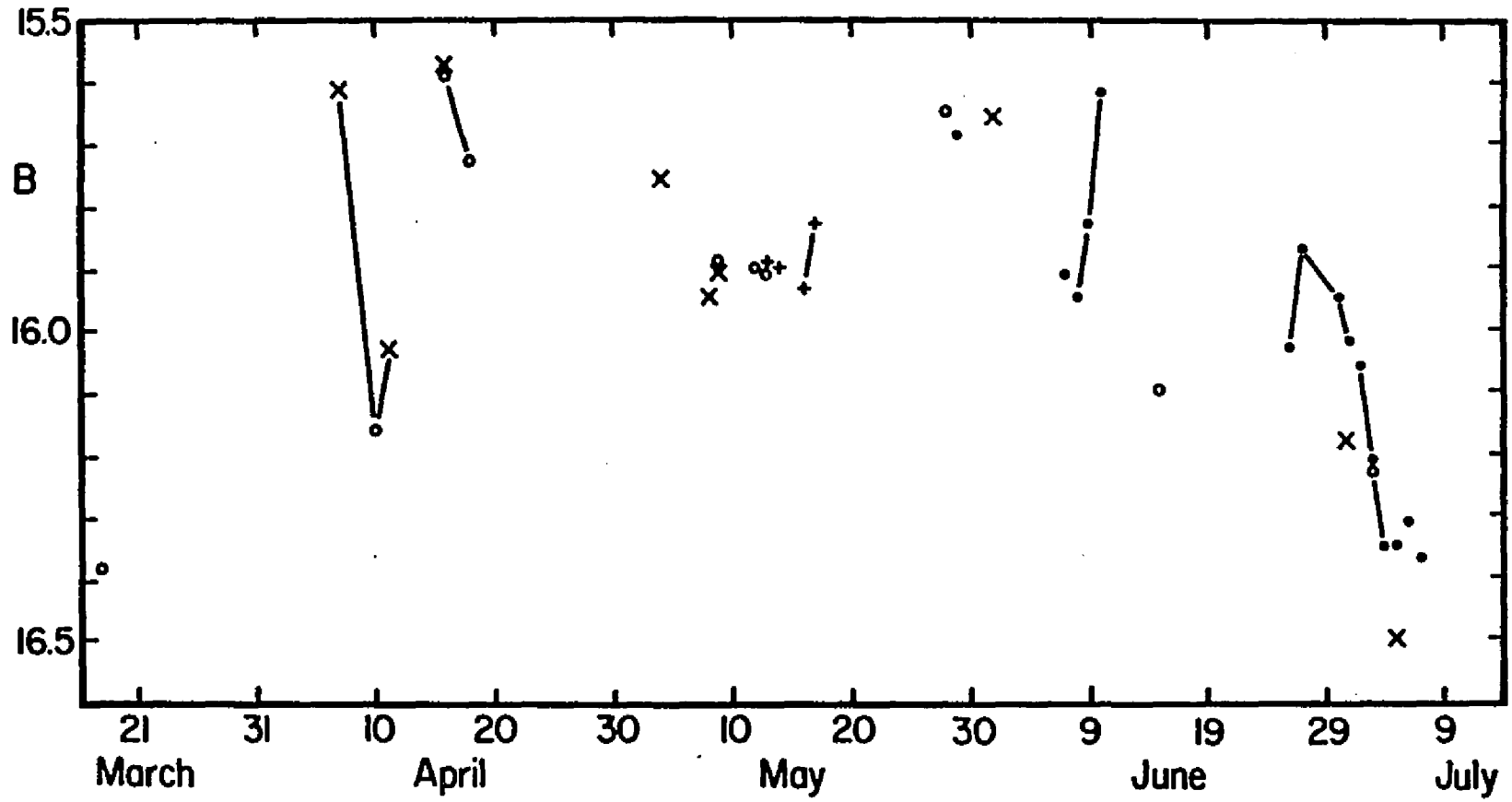

Figure 27. The photometric variability of B2 1308+326 during the 1978 outburst.

Symbols denote the various photometers used: • (USNO 1.0 m), o (UAO 1.5 m and 1.0 m), + (KPNO 0.9m). Data from Puschell et al. (1978) are included and denoted by x.

0.5 mag. Daily variations of 0.1 mag are observed frequently. There is a relatively stable phase from May 8-17 and a fairly long-term monotonic decrease in brightness from June 27-July 5. However, it is clear that daily brightness variations of 10-30% are quite common. The photometric variations are consistent with the polarimetric time scale of $\sim$2 days.

It is significant that both the polarimetric and photometric monitoring indicate a similar time scale of variability. There has been some question concerning the use of polarimetric monitoring for defining characteristic time scales of variability, since extremely polarized components constituting a small fraction of the total emission can significantly affect the net polarization. While this reservation is valid, we have shown that in this case, sizable flux variations occur on the same time scale as is found for large-scale polarimetric variability.

Infrared photometry is also included in Table 3. These measurements better define the energy distribution than do those of Puschell et al. (1979), since we have measured the spectrum through 10 μm. Our observations can be fitted with a power law of index $\alpha = 1.4 \pm 0.2$. The data of Puschell et al. are much more numerous and provide the best information on the infrared variability. In particular, they find a flattening of the spectrum with increasing wavelength early in the outburst, with evolution to a power law toward the end of the outburst. This behavior is similar to the spectral evolution found earlier for the BL Lac object, AO 0235+164 (Rieke et al. 1976).

The monitoring program of B2 1308+326 establishes several important characteristics of this object and supports the results concerning the variability of other (less well-observed) highly polarized objects. The most important characteristic established is that strong variability occurs on a characteristic time scale of days (and not on shorter time scales). We note that rapid variability is also observed when the object is much fainter (see Table 2). We have also established a close association between the optical and infrared emission since the polarizations in these two regimes track each other through rapid variations. The degree of polarization is generally wavelength independent, while there is variable differential rotation of position angle. Finally, we have shown that the optical brightness is also rapidly variable with a similar time scale as shown by the polarimetric variability.

B. Worldwide Monitoring of BL Lac

BL Lac is the prototype of BL Lacertae objects and has been extensively observed at radio, infrared, and optical wavelengths (see Stein, O'Dell, and Strittmatter 1976). The object lies in the nucleus of a giant elliptical galaxy which has a redshift of $z = 0.069$ and apparent magnitude of $V \sim 17.3$ in a 20" aperture (e.g. Miller, French, and Hawley 1978). BL Lac is noted for its very rapid variability both in the optical/infrared and at high radio frequencies (e.g. Aller and Ledden 1978).

Polarimetric monitoring of BL Lac has shown it to be consistently variable (Angel et al. 1978, Angel and Moore 1980, see

Angel and Stockman 1980 for further references). For this reason, and because it is bright enough to be monitored with small telescopes, BL Lac was chosen for a large-scale worldwide monitoring effort. This unprecedented effort was made in order to accurately describe both the nature and the time scale of the rapid variability. Polarimetric and photometric observers at ten telescopes located between Israel and California monitored BL Lac for more than one week in September 1979. With ideal conditions, it was possible to observe BL Lac for 20 hours per day, thus filling in the large monitoring gaps normally present with one-telescope programs. The time resolution of the observations is typically $\sim$15 minutes. There is also considerable overlap between various observers, allowing both a check on systematic differences between instruments and an evaluation of the reliability of individual measurements. The latter check is crucial, since previous monitoring programs occasionally reported dramatic variations which could not be verified (e.g. Bertaud et al. 1969, Racine 1970, Weistrop 1973a, Weistrop and Goldsmith 1973).

Information concerning the observations of all participants in the monitoring program is given in Table 4. For each telescope, the location (longitude), the type of observations (polarimetry and/or photometry), the identifying symbol for figures, and the observers are listed in the table. More than 600 polarization and 200 photometric measurements were made during the monitoring. The typical internal errors of these measurements are $\sigma_p \sim 0.2\text{-}0.5\%$ and $\sigma_V \sim 0.01\text{-}0.03$ mag. The tabulated data will be published by Moore et al. 1981.

Table 4. Instruments and Observers Monitoring BL Lac.

Telescope	Long.	Polar.[a]	Photom.[a]	Observers
Wise 1.0 m	-35	(✲)		R. Moore
Teneriffe 1.5 m	+16	(◇)	(◇)	D. Axon
				J. Bailey
				J. Hough
W. Ontario 1.2 m	+82	(□, ○)		I. Thompson
McDonald 2.1 m	+104	(X)		M. Breger
UAO 1.54 m	+111	(✖)		M. Lebofsky
				G. Rieke
UAO 1.5 m	+111		(□)	W. Wisniewski
UAO 2.3 m	+112	(✲)		H. Stockman
UAO 0.9 m	+112	(+)		G. Clayton
				R. Duerr
KPNO 0.9 m	+112		(+)	J. McGraw
Lick 3.0 m	+122	($\bar{X}$)		G. Schmidt
				J. Miller

a. The symbol used for plotting data from each instrument is given (Figures 28-32).

Common polarization standard stars were used by all polarimetric observers in order to minimize systematic differences between instruments. Most of the optical polarization measurements were made with unfiltered GaAs (RCA 31034A) photomultiplier tubes ($\lambda_{eff} \sim 0.6$ μm, $\Delta\lambda \sim 0.5$ μm); unfiltered, extended S20 PMTS (EMI 9659A) with comparable response were used at Teneriffe. A comparison of the reduced broadband polarization measurements reveals no significant systematic differences between any of the instruments, and no correction has been applied.

The brightness of BL Lac was monitored by differential photometry in the V band using the nearby star "C" from the comparison sequence of Bertaud et al. (1969). The measurements were reduced independently by each observer and then compiled. Systematic differences between observers are present in the photometric data and are probably due to slight aperture and response differences. In order to correct these errors, the mean magnitude for each observer for each night was determined and compared to other observers. The systematic differences for each night were then averaged to obtain a single correction to be applied to all data from that observer. The KPNO 0.9 m measurements are adopted as the reference; the corrections applied to the V measurements are - 0.038 mag for the UAO 1.5 m and + 0.084 mag for the Teneriffe 1.5 m. The presence of these systematic errors remains apparent in the corrected data and must be kept in mind when comparing the data from different observers.

The V magnitude, degree of broadband optical polarization, and position angle of polarization are plotted versus Julian Day (-2443400)

in Figure 28. There is clear variability in all measured quantities during the monitoring program. The brightness increases dramatically ($\Delta V \sim 0.4$ mag) from days 736-739, and then decreases slowly from days 739-743. There may be some shorter term flickering during each day, but it is difficult to determine the reality of small variations since systematic errors are present.

There are two discrepant points in the photometry which may be bad measurements or may indicate very rapid fluctuations. These points are at days 740.4 ($\Delta V = 0.25$ mag) and 742.8 ($\Delta V = 0.15$ mag). These discrepant measurements are both bracketed within less than an hour by measurements at the normal brightness for the respective nights. It is our opinion that these are simply inaccurate points and do not indicate rapid variability.

The degree of polarization is quite low ($P \lesssim 4\%$) during the first few days of the monitoring program, and then rapidly increases to $\sim 8\%$ from days 737-739. The strong increase in polarization does coincide somewhat with the brightening during this same period. This behavior cannot be due simply to a change in the relative contribution of the unpolarized galaxy component; the nuclear source was bright and clearly dominated the galaxy. For the remainder of the program, the polarization remains generally high although there is significant variability during each day and from day to day.

The position angle of polarization also shows strong variability throughout the program. The position angle variations are most dramatic on days 736 and 737 when the angle varies by 45° in 11

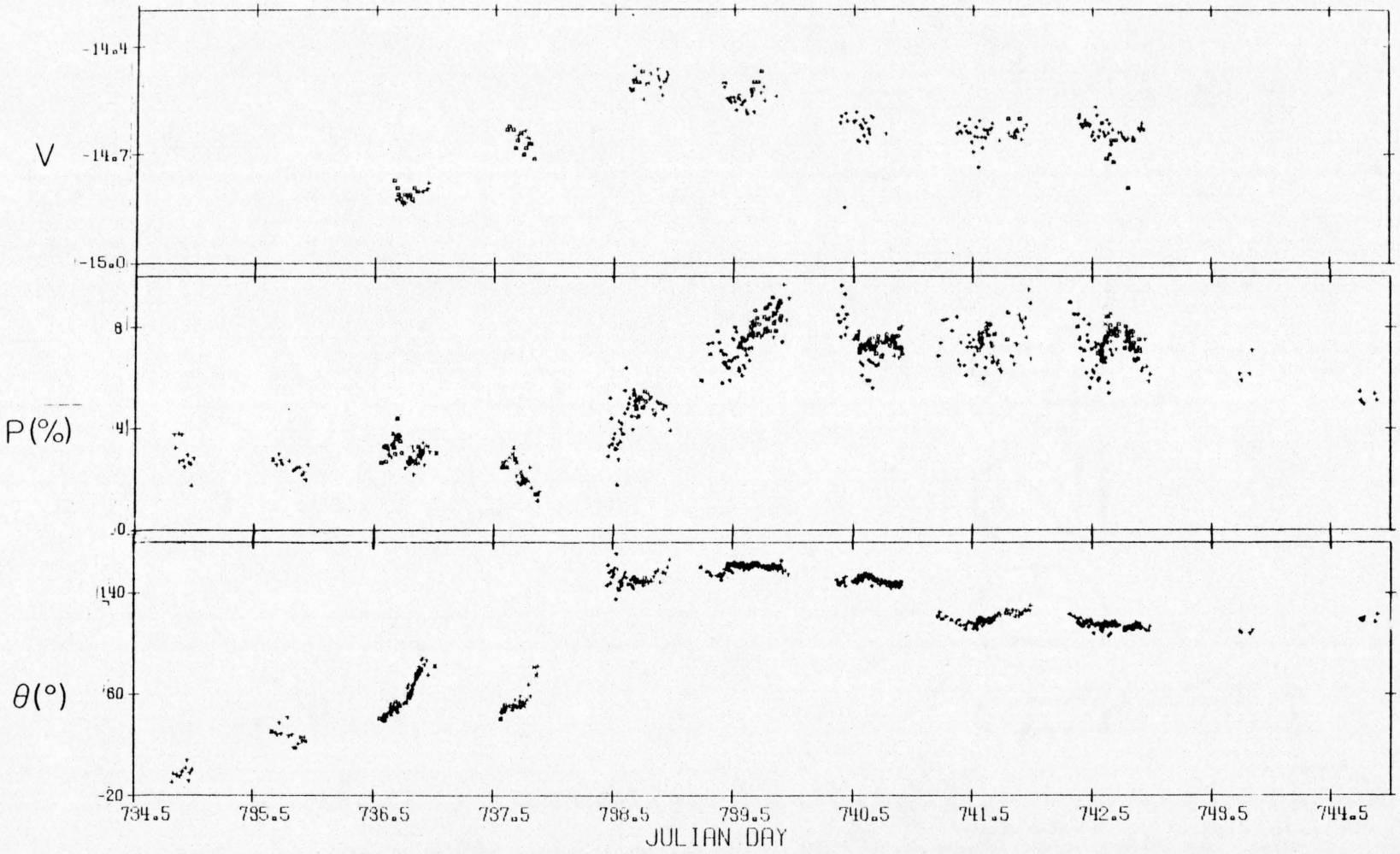

Figure 28. The variability of BL Lac during the 1979 monitoring program.

(a) The V magnitude, (b) the degree of broadband optical polarization, (c) the position angle of broadband optical polarization.

hours and 40° in 7 hours respectively. In the 14 hour monitoring gap between days 737 and 738, the position angle must have changed by 75°. Starting with day 738, the position angle variations are less dramatic, remaining within the range 100°-160° for the next seven days.

It is apparent from Figure 28 that the most rapid position angle rotations occur during the initial period of lower polarization. This characteristic implies that the very rapid rotations observed do not represent that large a change in the (Q,U) plane. For this reason, further figures of the polarimetric variability are given in terms of Q and U. The polarization measurements for the entire monitoring program, expressed in Q and U, are shown in Figure 29. One can see that the character of the variability is similar throughout the monitoring program. For both Q and U, there is a large amplitude (± 6%) long period wave with more rapid variations superimposed. Examination of the variations during each day (and connecting across gaps) repeatedly requires that short term ($\tau \sim 1$ day) variations of lesser amplitude be present. More rapid variations do not appear to be present. While a few measurements may be deviant, there is quite a bit of overlap between observers and none of the possible very rapid variations are confirmed. The time scale of the large amplitude wave is not well determined since it appears to have a time scale comparable to the length of the monitoring program ($\sim$ 10 days). This morphology of the variability in (Q,U) space, short term variations ($\tau \sim 1$ day) superimposed on a large amplitude wave ($\tau \sim 10$ days), is supported by previous observations of BL Lac (Angel et al. 1978, Angel and Moore

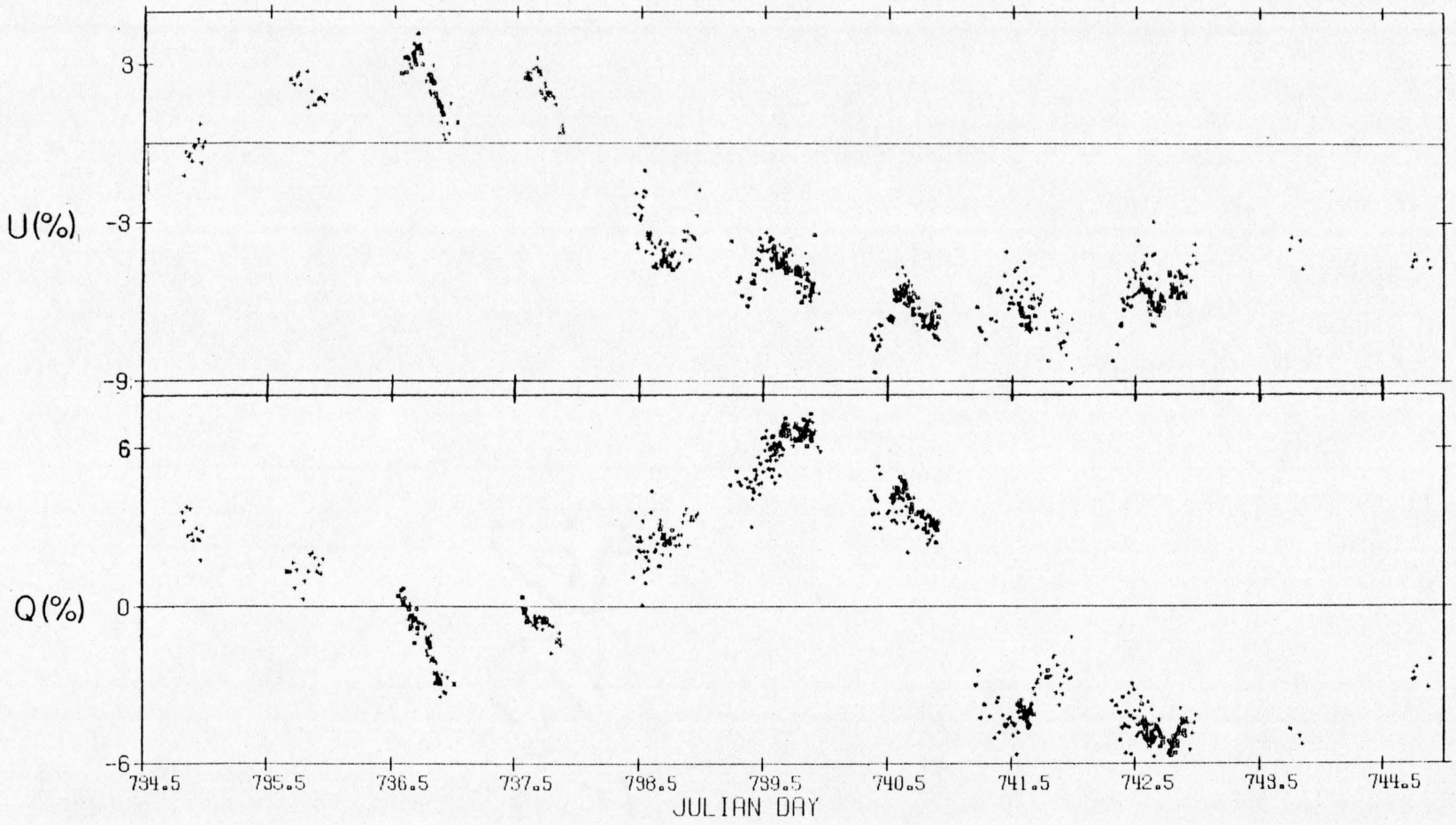

Figure 29. The polarimetric variability of the broadband Stokes parameters Q and U during the BL Lac monitoring program.

1980) during several months in both 1977 and 1978. Thus, we are confident that this morphology is typical of BL Lac and is not limited to the ten day period in September 1979.

To illustrate in more detail the short term behavior of the polarization and to discuss the wavelength dependence of the polarization, we plot in Figures 30 to 32 the data for days 736, 739 and 741 respectively. On day 736 (Figure 30), the polarization is relatively low ($P \sim 3\%$) and the position angle is rapidly variable. The variations in Q are roughly monotonic, while there is a definite inflection in U during this period at epoch 736.73. Infrared (2.2 μm) polarimetry measurements are noted in the figure. The agreement of infrared and optical data in Q is very good. There is a suggestion that the inflection point in U is slightly later (epoch 736.83) in the infrared, although the errors of the measurements are too large to be certain of this time delay. The measurements do illustrate that the infrared polarization tracks the optical through rapid variations.

Wavelength dependence measurements are also available on days 739 and 741, with filters centered at 0.45 μm and 0.85 μm. The data for these days are shown in Figures 31 and 32, with the filtered observations noted. In both figures, it can be seen that the blue and red measurements track each other during variations. Definite wavelength dependence is observed on both days. The magnitude of both Q and U is larger in the blue on day 739. The percentage polarization is about 35% larger in the blue bandpass than in the red; there is essentially no differential rotation on this night. Two days later (Figure 32),

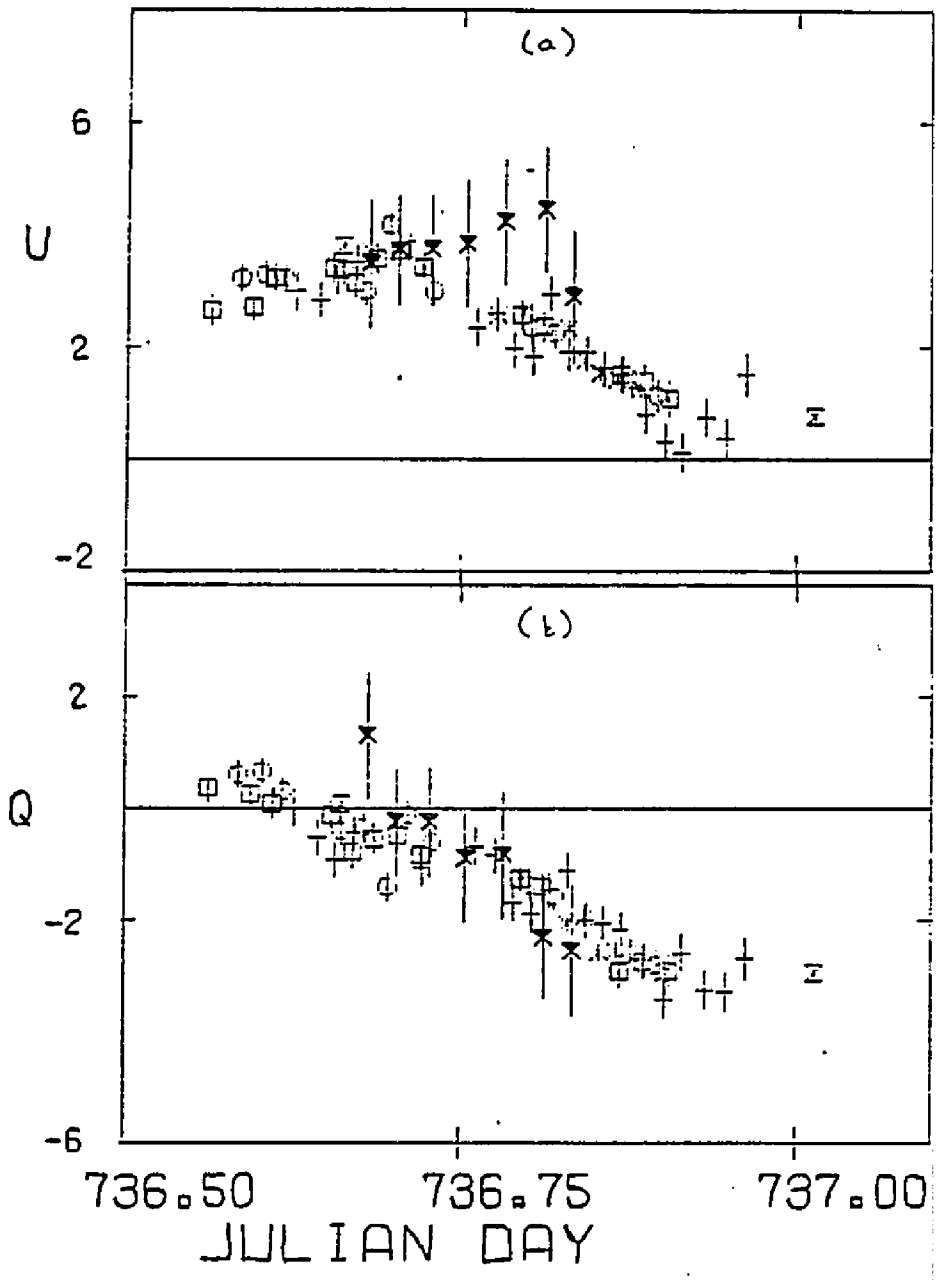

Figure 30. The variability and wavelength dependence of Q and U on day 736 of the BL Lac monitoring program.

Infrared (2.2 μm) polarization measurements are denoted by "X". All other symbols represent broadband optical measurements and are identified in Table 4.

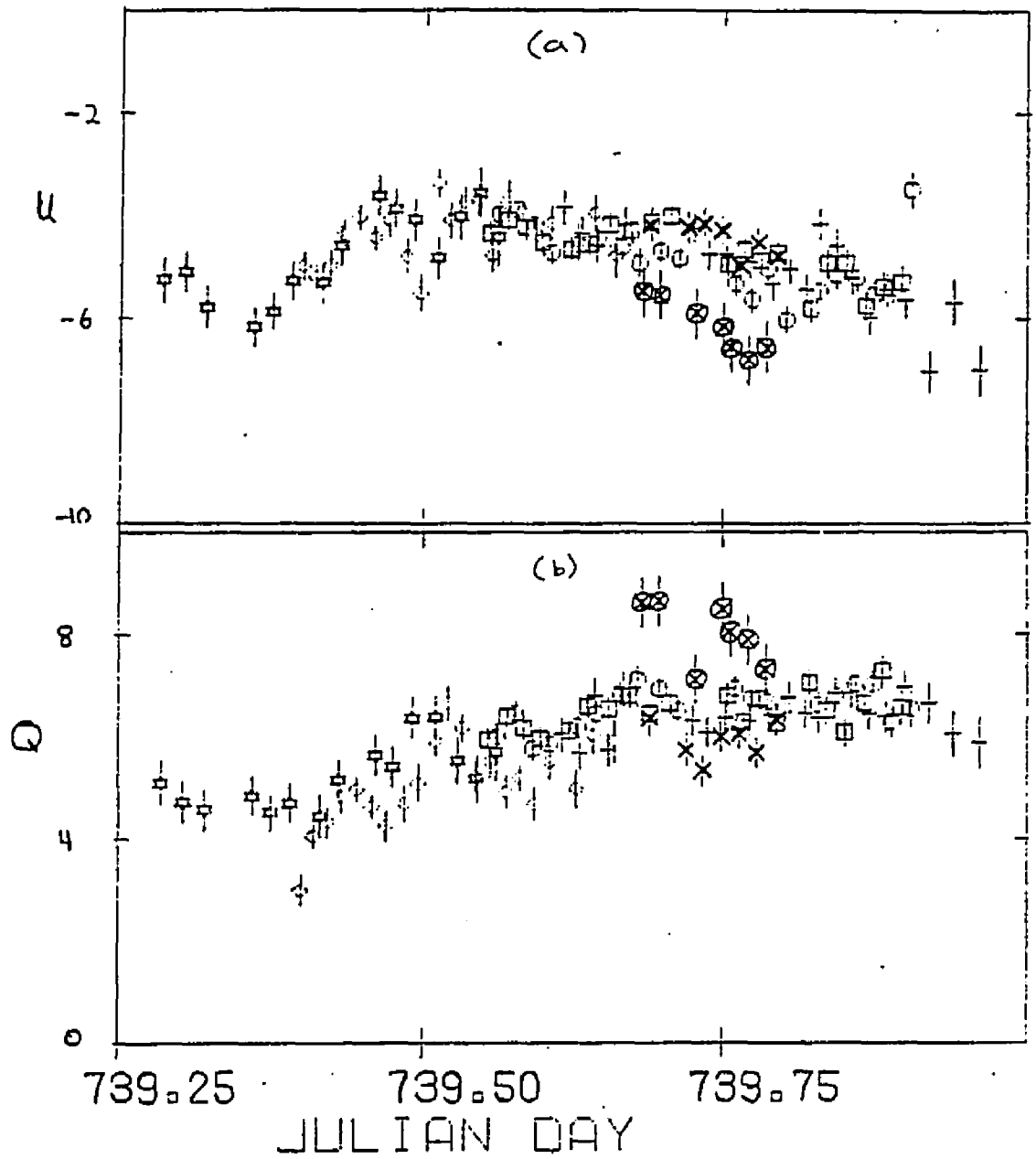

Figure 31. The variability and wavelength dependence of Q and U on day 739 of the BL Lac monitoring program.

Blue ($\lambda \sim 0.45$ μm) measurements are denoted by ⊗ and red ($\lambda \sim 0.85$ m) measurements by X. All other symbols represent broadband optical measurements.

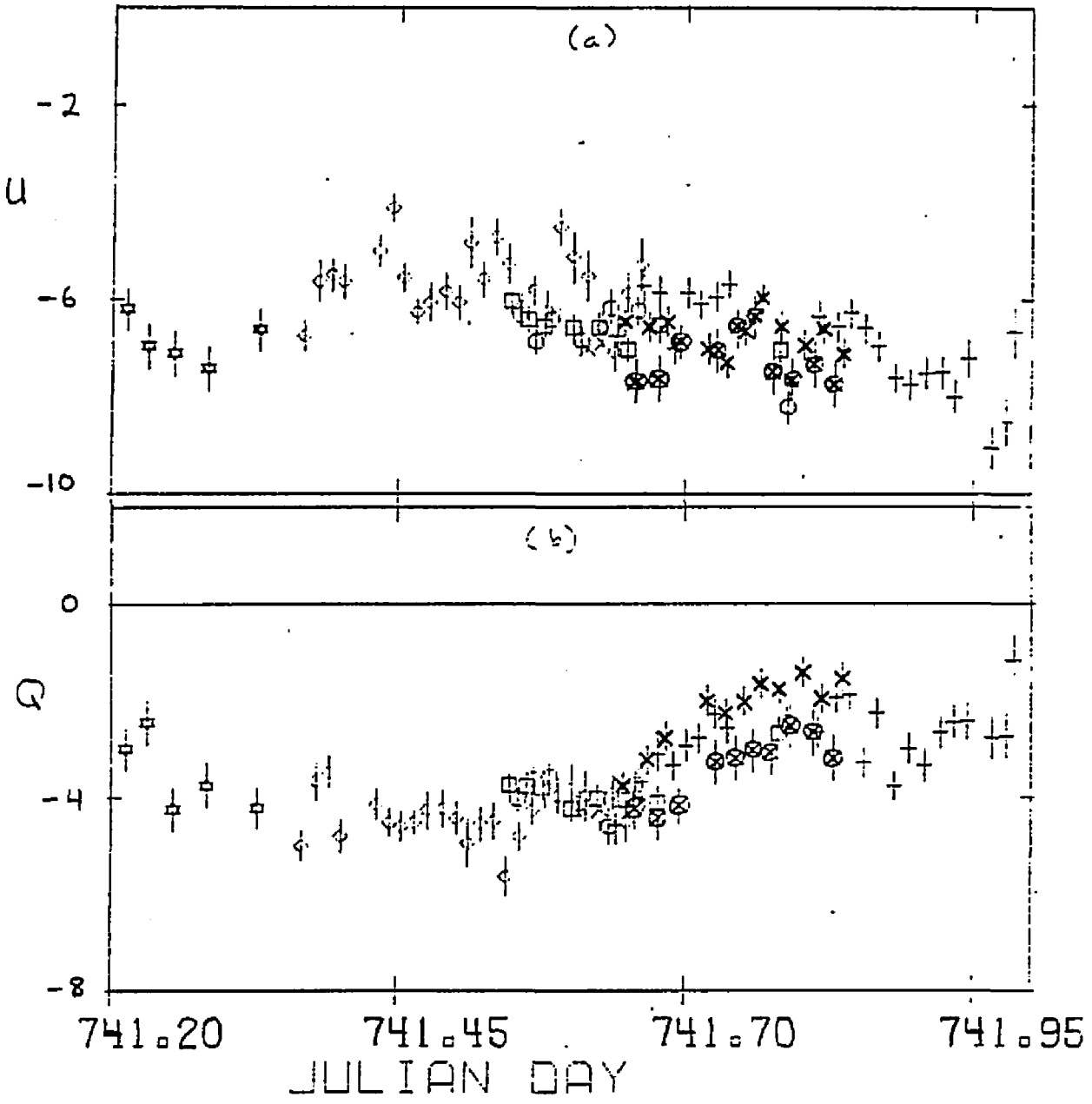

Figure 32. The variability and wavelength dependence of Q and U on day 741 of the BL Lac monitoring program.

Blue ($\lambda \sim 0.45$ μm) measurements are denoted by ⊗ and red ($\lambda \sim 0.85$ μm) measurements by X. All other symbols represent broadband optical measurements.

after substantial variability in both Q and U, the degree of polarization is only slightly higher in the blue bandpass ($P_B/P_R \sim 1.13$), and there is a small but definite position angle rotation of $\sim 5°$.

Thus, we have established that, although the polarizations at all optical/infrared wavelengths track each other during rapid variations, there is some variable wavelength dependence. There are phases when no wavelength dependence is present, when only the percentage polarization varies with wavelength, or when both the degree and position angle of polarization are wavelength dependent. This is the same conclusion as is drawn from our observations of B2 1308+326 and the HPQs.

Another feature of Figures 30 to 32 is that the resolution is high enough to examine the agreement between different observers and any evidence for very rapid variations. It is apparent that, despite the variety of polarimeters used in the program, the systematic differences are minimal. The variations through each day are generally smooth. As stated previously, we find no clear evidence for significant variability on time scales of less than $\sim$1 day.

This intensive monitoring program of BL Lac has produced the following results. Characteristic variations occur on a time scale of $\sim$1 day and more rapid variability does not appear to be present. In the polarization (represented by Q and U), the one day variability is superimposed on a slower ($\sim$ 10 days) large amplitude wave. This morphology has also been observed in prior observing seasons and is characteristic of the object. During the monitoring program, the degree of polarization was low when the object was fainter; further

monitoring is required to determine if this is a general characteristic. We have shown that the most rapid position angle rotations occurred when the degree of polarization was low, suggesting that a (Q,U) representation of the variability is perhaps more meaningful. Occasional wavelength dependence of the polarization is observed, with variable dependence in both the degree and position angle of polarization.

CHAPTER VII

DISCUSSION

The approach of the previous chapters has been to describe the polarimetric characteristics of QSOs and BL Lac objects, to determine the correlations between polarization and other properties of QSOs, and to establish the similarity between HPQs and BL Lac objects. The purpose of this chapter is to discuss the theoretical implications of the observational results we have obtained. The polarimetric characteristics and the properties associated with polarization provide vital clues to understanding the physical nature of QSOs and BL Lac objects.

A. Summary of Observational Results

It is important to briefly summarize the basic observational results which we have established. Perhaps the most fundamental result of the QSO polarization survey is that the great majority of QSOs have very low optical polarization ($P < 2\%$, $\bar{P} \sim 0.6\%$). Although local interstellar polarization is present, the observed polarization of these "normal" low polarization QSOs is primarily intrinsic. About 85% of radio-loud QSOs (from low frequency surveys), and essentially all radio-quiet QSOs are normal low polarization QSOs. There is no difference in the degree of polarization among normal QSOs for

radio-loud or radio-quiet objects. The polarization of normal QSOs is constant over at least a time scale of years (the baseline of our monitoring). There does appear to be some wavelength dependence of the degree of polarization in the sense that, statistically, the polarization increases slightly to the blue; the position angle is wavelength independent. A very important characteristic of the low polarization QSOs is that the optical polarization position angle is preferentially aligned with the position angle of extended double radio structure.

There is a clear break in the distribution of polarization of QSOs at $P \sim 2\text{-}3\%$. If we separate those QSOs which show higher polarization ($P > 3\%$) into a separate class (the HPQs), the polarimetric characteristics appear markedly different from the normal QSOs. Both the degree and position angle of polarization are rapidly variable with typical time scales of a few days. The degree of polarization is only mildly dependent on wavelength; in those few cases where we have observed wavelength dependence, the polarization is higher in the red. Very little rotation of position angle with wavelength is observed; the largest rotation was $\sim 15°$ from 0.4 - 0.8 μm. The polarimetric characteristics of HPQs are very similar to those of BL Lac objects. With the exception of PHL 5200 (an atypical HPQ in many respects), all of the known HPQs are radio-loud QSOs. The occurrence of high polarization is the one polarimetric distinction we have found between radio-loud and radio-quiet QSOs.

The correlation analyses illustrate that the differences between low and high polarization QSOs extend far beyond their polarimetric characteristics. We have presented strong evidence that two basic types of QSOs exist. The general characteristics of the HPQs are: (1) they are compact flat spectrum radio sources, (2) they exhibit rapid large-amplitude photometric variability (i.e. they are OVVs), (3) they have relatively steep smooth optical/infrared continua, and (4) they may show excess X-ray emission relative to the optical flux. In all these respects, the HPQs are very similar to BL Lac objects. On the other hand, normal low polarization QSOs may be either radio-loud or radio-quiet, they exhibit more moderate photometric variability, and they have harder "bumpy" optical continua. These descriptions are general and simplified; exceptions and reservations have been discussed in previous chapters. Although the properties of HPQs and normal QSOs indicate two basic types of QSOs, the two phenomena represented are associated. This is evidenced by the similarities between the two classes in the distribution of redshift, optical luminosity, and the equivalent width of emission lines.

Thus, there are a number of observational characteristics of normal QSOs, HPQs, and BL Lac objects which must be explained by theoretical models. The HPQs provide a crucial link between normal QSOs and BL Lac objects by sharing characteristics of both classes of objects. In the following sections, we address several fundamental questions which are posed by the observational results we have established. For example, what is the mechanism of polarization in

the three types of objects? Why are there two basic types of QSOs? Why do the HPQs have strong emission lines, when their continuum properties are so similar to BL Lac objects? What constraints can be applied to the central "engine" of HPQs or BL Lac objects, and can isotropic incoherent synchrotron processes produce the high luminosities in the small volumes deduced from rapid variability? Is the physical structure fundamentally different for the three kinds of objects, or can the differences be accounted for by our orientation with respect to the same type of structure?

B. Sources of Polarized Optical Emission

1. Highly Polarized QSOs and BL Lac Objects

There is a great deal of data suggesting that the polarized optical/infrared emission of HPQs and BL Lac objects is synchrotron radiation. Both the polarimetric characteristics and the energy distribution of the continuum are readily accounted for by synchrotron processes. Alternative polarizing mechanisms such as scattering are essentially excluded by the high degree of net polarization (up to 35%) sometimes observed in these objects.

For optically thin synchrotron radiation from a uniform magnetic field, the degree of linear polarization is $\sim$75% (Pacholczyk 1970). A nonuniform field produces substantially less net polarization (as is normally observed). The degree and position angle of polarization are also wavelength independent as long as the source remains optically thin and there is no Faraday rotation; some wavelength dependence can be

accounted for by postulating multiple components with different energy distributions and polarization. Finally, if the distribution function of electrons does not vary dramatically within the emission cone (half-angle $\sim \gamma^{-1} = mc^2/E$), the net circular polarization from an ensemble of electrons is zero. Thus, the properties of synchrotron emission can readily account for the observed polarimetric characteristics of HPQs and BL Lac objects.

The optical/infrared continuum energy distribution of highly polarized objects also suggests that synchrotron processes are responsible for the emission. Their continua are generally well approximated by a power law. If the distribution of electron energies is a power law, the synchrotron emission from this ensemble has a power law energy distribution. Such an interpretation is readily justified by analogy to the success of synchrotron theory for explaining the power law radio emission of optically thin extragalactic sources. Although optical/infrared spectral curvature is sometimes observed, the spectra do appear markedly smoother than most normal QSOs. Curvature can be due to superimposed components or high energy electron losses.

A final, more indirect argument that the optical/infrared emission is synchrotron radiation is that extrapolation of the optical spectrum to high frequency radio wavelengths is plausible for many of these objects (e.g. O'Dell et al. 1978). This extrapolation is not exact (e.g. the typical spectral index is apparently higher between 0.3 and 10 μm than between 10 μm and 3 mm) and far-infrared measurements are required to better define the spectrum.

2. Low Polarization QSOs

We have presented substantial evidence that the dominant optical continuum emission of most QSOs is not synchrotron radiation. If synchrotron emission dominated the optical continua of normal QSOs, the low polarizations observed would require that the magnetic field be almost completely randomized. Internal Faraday rotation could depolarize the synchrotron emission. However, if Faraday rotation were the depolarizing mechanism, one would expect the residual polarization to show a strong position angle wavelength dependence (since the rotation is frequency dependent); this characteristic is not observed among low polarization QSOs. Also, the alignment between the position angles of optical polarization and radio structure would be destroyed if Faraday depolarization were significant. In addition to the polarimetric arguments, the energy distributions of normal QSOs provide further evidence that synchrotron radiation is not dominant. The continua of most QSOs are not approximated well by a simple power law energy distribution and often exhibit substantial continuum structure (e.g. Neugebauer et al. 1979, Richstone and Schmidt 1980).

While the statements above argue that synchrotron radiation does not dominate the optical emission of normal QSOs, it is possible that a weak synchrotron component could be present and could be responsible for the small observed polarizations. A dominant unpolarized component in normal QSOs could dilute the high typical polarizations associated with synchrotron radiation. However, it is important to note that the weak synchrotron component postulated in this scenario does not exhibit

the same characteristics as the synchrotron component of HPQs or BL Lac objects. Diluted HPQ-type emission can be ruled out by the lack of polarimetric variability in normal QSOs; the dramatic changes in the degree and position angle of polarization among the HPQs would be detectable in our observations of normal QSOs if HPQ-type emission were present but diluted. Thus, if a weak synchrotron component is present, its polarization is not variable

There is another final point concerning the possibility that the weak constant polarization of normal QSOs is due to diluted synchrotron radiation. If the energy distribution of the synchrotron component is steeper than that of the dominant unpolarized component, one would expect the degree of polarization to increase at longer wavelengths in normal QSOs. This is, in fact, just the opposite of our results for the wavelength dependence of normal QSOs.

It is likely that scattering in an asymmetric geometry is responsible for the low polarizations observed. The amount of polarization resulting from a nonspherical scattering geometry depends on the optical depth of the cloud, the degree of asymmetry, and the viewing angle (Angel 1969). Substantial net polarizations ($2\% < P < 8\%$) can be achieved with intermediate optical depths ($0.5 < \tau < 50$) and asymmetry. Since the QSO polarizations are very low ($P \lesssim 1\%$), the scattering geometry must be nearly spherical, or the optical depth in the ranges $\tau < 0.1$ or $\tau > 50$. It is also important to note that the position angle of polarization is parallel to the minor axis of the

cloud in the optically thin case, while it is parallel to the major axis in the optically thick case.

Two possible scatterers are thermal electrons and dust. If the low polarizations observed are due to scattering, these two mechanisms could be distinguished by accurate measurements of the wavelength dependence of polarization. At optical wavelengths ($h\nu << m_e c^2$), the electron scattering cross-section is independent of wavelength and the degree of polarization should be constant. For scattering by dust, the degree of polarization should rise rapidly to the blue; this behavior is observed in some Seyfert galaxies (Stockman, Angel, and Beaver 1976, Angel et al. 1976, Thompson et al. 1980). The results of two-color polarimetry of low polarization QSOs, discussed in § III.C.2, suggest that the polarization may be slightly higher in the blue. This is well-established in at least one case (PKS 1004+130), although the strong increase to the blue expected from dust scattering is probably not observed. Thus, dust is suggested as a scattering mechanism but additional more accurate wavelength dependence measurements are required. It should be noted that wavelength dependence of polarization can also be explained by a superposition of components with different energy distributions and polarizations.

The preferred alignment between the position angle of optical polarization and the direction of extended radio structure is a key clue to determining the origin of the polarization in normal QSOs. The mechanism which determines the direction of the radio lobes must be related to the mechanism which produces the optical polarization.

Also, this mechanism must operate over long time scales (> 10^7 yr) since the radio lobes are frequently hundreds of kiloparsecs in extent. This alignment must be related to the physical structure of the inner region of QSOs. A plausible scenario is that the optical polarization is produced in a disk scattering geometry, and that the rotational axis of this disk is the same as the direction of the radio lobes. The position angle of polarization would be aligned with the radio lobes if the disk were optically thin. Other scenarios are also possible. It is clear that any theory for the optical polarization of normal QSOs must be able to account for the observed alignment. Also, although this alignment can only be observed in radio-loud extended QSOs, the successul explanation may also apply to the polarization of radio-quiet QSOs, considering the polarimetric and spectroscopic similarities of the two classes.

C. Theoretical Models

In this section, we discuss two basic theoretical models to account for the properties of QSOs which we have established in this paper. The first model, the "isotropic" model, is founded on the concepts that the emission is isotropic and that the minimum variability time scale is indicative of the size of the emission region. In this scenario, it is apparent that the emission region of HPQs and BL Lac objects is much more compact than the emission region of normal QSOs. In the highly polarized objects, we are seeing emission from very close to a compact collapsed object, and the characteristics of the emission

in these objects are representative of the emission from this inner region. The similarities which do exist between HPQs and normal QSOs (e.g. redshift, optical luminosity) suggest that the two types of objects may be fundamentally similar, but either the central "engine" of normal QSOs is much larger or there is a reprocessing cloud around the normal QSOs which is not present in the HPQs. We shall discuss the latter case here. In this scenario, both HPQs and normal QSOs have the same type of central engine (the inner few light-days). We observe this inner region in the HPQs (and BL Lac objects); in normal QSOs, this emission is obscured and reprocessed by a surrounding cloud of material. The basic problems of this model, then, are to establish the feasibility that the enormous luminosities are produced in a volume only light-days across, to determine the mechanism by which the radiation is reprocessed, and to determine why some objects have a reprocessing cloud while others do not.

The second model to be discussed is the "anisotropic" theory. In this model, the same fundamental structure is present in both high and low polarization objects, but the viewing angle with which we observe the object determines the type of object we see. There are two permutations of this model. In the first version, the "nonrelativistic aniostropic" model, the emission at any orientation is not relativistically enhanced but the orientation determines the type of emission we observe. In thesecond permutation, there is enhancement of the emission in a collimated relativistic jet and our orientation with

respect to this jet determines the type of object we observe. In the HPQs and BL Lac objects, we are viewing down the direction of the jet; the emission properties observed are characteristic of the emission from this jet, the observed time scale of variability is shorter than the rest frame time scale, and the luminosity (calculated assuming isotropic emission) is an overestimate of the rest frame luminosity. When viewed off axis, we observe isotropic emission with different emission characteristics, and in this case a normal QSO would be observed.

1. Isotropic Model

The isotropic model is the most straightforward theory to explain the emission properties of normal QSOs, HPQs, and BL Lac objects. The primary difficulty is to explain how the compact (light-days) central engine can produce the tremendous luminosities ($\lesssim 10^{48}$ erg s^{-1}). There are a number of constraints discussed below which can be placed on such a model (e.g. Blandford and Rees 1978).

If one assumes that the emission is isotropic, one can establish that a black hole is likely to be present in the center of these active objects. This can be shown as follows. The Eddington luminosity is that luminosity at which the force of radiation pressure equals the gravitational force. At a distance r from an object of mass M with a luminosity L_{EDD}, the forces are

$$\frac{\sigma_T}{c}\,\frac{L_{EDD}}{4\pi r^2} = \frac{GM\,m_p}{r^2} \quad , \tag{11}$$

where σ_T is the Thompson cross-section and m_p the proton mass. This implies that

$$L_{EDD} = \frac{4\pi G\, m_p\, c}{\sigma_T} M \qquad (12)$$
$$= 1.4 \times 10^{38} \left(\frac{M}{M_\odot}\right) \text{ erg s}^{-1} .$$

If the luminosity exceeds the Eddington luminosity, radiation pressure would blow material away. Thus, we can set the constraint that $L < L_{EDD}$; this implies that

$$M > 7 \times 10^9 \, L_{48} \, M_\odot , \qquad (13)$$

where $L_{48} = L/10^{48}$ erg s^{-1}. (The maximum luminosity observed in QSOs and BL Lac objects is $\sim 10^{48}$ ergs s^{-1}.) We would note that this is not an absolute constraint; it can be violated for brief periods of time. The Schwarzschild radius of an object with mass M is

$$R_s = \frac{2G\,M}{c^2}$$
$$= 3 \times 10^5 \left(\frac{M}{M_\odot}\right) \text{ cm} . \qquad (14)$$

Using condition [13] above,

$$R_s > 2.5 \times 10^{15} \, L_{48} \text{ cm}$$
$$> 0.8 \, L_{48} \text{ light-days} . \qquad (15)$$

Thus, a very luminous QSO ($L_{48} \sim 1$) must have a mass $M \gtrsim 7 \times 10^9 M_\odot$. The Schwarzschild radius of an object with this mass is $\gtrsim 1$ light-day. There are luminous QSOs (e.g. B2 1308+326) which have time scales of variability of about one day. Thus, the dimension of the emitting region deduced from the variability time scale is comparable to the Schwarzchild radius derived from the Eddington limit. This requires that the central object be a black hole. Of course, accretion onto a black hole is a very efficient energy producing mechanism, being able to liberate up to ~35% of the rest mass energy (Lynden-Bell 1978).

We would note that the constraints that $L < L_{EDD}$ and $c\tau > R_s$ are barely satisfied for the most extreme objects. This can be interpreted from alternative perspectives. First, one could say that the observations already exclude the model. The emission region must be larger than the Schwarzschild radius and perhaps the proper constraint should be $c\tau > 5\ R_s$ (e.g. Shields 1977). Extreme QSOs violate this constraint. On the other hand, the Eddington luminosity is not an absolute constraint and may be temporarily exceeded. The fact that the constraints are strained but not severely exceeded could be interpreted as positive evidence that the physical mechanisms described here are actually operating.

It is also of interest to note that the minimum time scale of variability observed in HPQs and BL Lac objects is $\tau \sim 1$ day. This time scale is frequently observed in active objects with a wide range of luminosity (Rieke et al. 1976, Angel et al. 1978, Moore et al. 1980).

This common time scale can be interpreted to imply that the mass of the central black hole is not very different from object to object. The range of luminosity can be accounted for by varying accretion rates.

Now we turn to certain constraints concerning the emission of luminous highly polarized rapidly variable sources such as the HPQs and BL Lac objects. These arguments follow, but do not duplicate, the discussion of Blandford and Rees (1978). We assume that the emission is optically thin synchrotron radiation. The radius of a spherical emitting region is taken to be

$$r \sim c\, t_{var} \sim 2.6 \times 10^{15}\, \tau_D \text{ cm}$$

where τ_D is the time scale of variability measured in days. For simplicity, a characteristic frequency is taken for the optical luminosity, and these quantities are expressed as

$$\nu = 10^{15}\ \nu_{15} \text{ Hz}$$
$$L = 10^{48}\, L_{48} \text{ erg s}^{-1}$$

The dimensionless units are chosen to typify the most extreme observed cases for this model ($L_{48} = 1$, $\tau_D = 1$).

The radiation energy density, u_{rad}, is very high within this volume and energy losses to inverse Compton scattering can be substantial. If half the radiation energy density exceeds the magnetic energy density,

inverse Compton losses exceed synchrotron losses. Thus, a substantial portion of the optical synchrotron photons would be scattered to higher (X-ray) frequencies. Current observations of active sources indicate that the integrated optical/infrared luminosity is comparable to or greater than the X-ray luminosity (§ IV.H). Thus, we require that

$$U_{mag} = \frac{B^2}{8\pi} > \frac{1}{2} U_{rad} \quad . \tag{16}$$

The radiation energy density can be estimated by the energy produced within the volume in a time interval t_{var}.

$$U_{rad} = \frac{L \cdot t_{var}}{\frac{4}{3} \pi r^3}$$

$$\sim 1.2 \times 10^6 \, L_{48} \, \tau_D^{-2} \text{ erg cm}^{-3} \tag{17}$$

Thus, the inverse Compton condition can be expressed as

$$B > 3.9 \times 10^3 \, L_{48}^{\frac{1}{2}} \, \tau_D^{-1} \text{ Gauss.} \tag{18}$$

Obviously, very strong magnetic fields are required in the optical emission region.

The synchrotron cooling time scale, t_s, is significant in that it indicates how long a relativistic electron emits synchrotron radiation. This time scale depends on the magnetic field strength and the Lorentz factor of the electrons. The characteristic Lorentz factor can

be estimated using equation [1] of Burbidge, Jones, and O'Dell (1974) to be

$$\gamma \sim 8.5 \times 10^{-4} \nu^{\frac{1}{2}} B^{-\frac{1}{2}} \quad . \tag{19}$$

Using the lower limit on B derived above, one obtains

$$\gamma < 430 \, \nu_{15}^{\frac{1}{2}} \tau_D^{\frac{1}{2}} L_{48}^{-\frac{1}{4}} \quad . \tag{20}$$

The synchrotron energy loss rate is (Pacholczyk 1970)

$$\dot{E}_s \sim 1.2 \times 10^{-3} B^2 E^2 \quad , \tag{21}$$

where E is the energy of the electrons (γmc^2). Thus, the time scale for synchrotron cooling is

$$t_s \sim \frac{E}{\dot{E}_s} \sim 8.4 \times 10^2 B^{-2} (\gamma mc^2)^{-1} \quad . \tag{22}$$

From the limits on B and γ,

$$t_s \lesssim 0.16 \, L_{48}^{-3/4} \tau_D^{3/2} \nu_{15}^{-\frac{1}{2}} \text{ sec} \, . \tag{23}$$

The cyclotron time scale, t_{cyc}, is the time for cyclotron radiative losses to cool the electrons from mildly relativistic to thermal energies.

$$\dot{E}_c \sim \frac{2}{3} \frac{e^4}{m^3 c^5} E B^2 \tag{24}$$

Therefore,

$$t_{cyc} \sim \frac{E}{\dot{E}_c}$$

$$< 35\, L_{48}^{-1}\, \tau_D^{\,2} \text{ sec} . \qquad (25)$$

The upper limit on the cyclotron cooling time scale is much shorter than the variability time scale. This implies that the electrons, unless frequently accelerated to relativistic energies, are at thermal energies nearly all the time.

This result, that most electrons are at thermal energies, suggests that electron scattering may be significant. If the source were optically thick to electron scattering, the radiation would be depolarized and the variability dampened. Thus, we require that the optical depth to electron scattering, τ_{es}, be less than one.

$$\tau_{es} = \sigma_T\, n_e\, r = c\sigma_T\, n_e\, t_{var} \lesssim 1 \qquad (26)$$

The density of thermal electrons, n_e, can be estimated by the total number of electrons required to produce the observed luminosity divided by the volume. We introduce a free parameter, N, which is the number of times an electron is accelerated to relativistic energies (γmc^2) per crossing time t_{var}, and assume that $N << t_{var}/t_{cyc}$. Thus

$$n_e \sim \frac{L\, t_{var}}{N \gamma mc^2} \left(\frac{4}{3} \pi c^3 t_{var}^3 \right)^{-1} \quad . \tag{27}$$

The constraint derived from the electron scattering optical depth can be expressed as

$$N > 5.8\, L_{48}^{5/4}\, \tau_D^{-3/2}\, \nu_{15}^{-\frac{1}{2}} \quad . \tag{28}$$

This result is much less restrictive than the corresponding value of 440 (for our dimensionless quantities being one) obtained by Blandford and Rees (1978). Their approximation of the optical depth and previous limit on γ are slightly different, but not nearly enough to account for two orders of magnitude in N. The discrepancy arises from our respective estimates of the electron density.

Since strong magnetic fields and a high density of thermal electrons may be present in the source, Faraday rotation of optical emission can also be significant and depolarize the emission. We require that the Faraday rotation, χ_F, across the distance ct_{var} be $\lesssim$ 1 radian. The rotation can be expressed as (Pacholczyk 1970)

$$\chi_F \sim \frac{1}{2} \frac{\omega_p^2\, \omega_g \cos\theta}{\omega^2} \frac{r}{c} \quad . \tag{29}$$

A lower limit for the plasma frequency ω_p can be estimated from equation [27] for the electron density,

$$\omega_p = \left(\frac{4\pi e^2}{m} n_e\right)^{\frac{1}{2}} \qquad (30)$$

$$> 3.3 \times 10^9 L_{48}^{5/8} N^{-\frac{1}{2}} \nu_{15}^{-\frac{1}{4}} \tau_D^{-5/4} \text{ sec.}^{-1} .$$

The gyrofrequency can also be estimated using equation [18] as

$$\omega_g = \frac{eB}{mc}$$

$$> 6.8 \times 10^{10} L_{48}^{\frac{1}{2}} \tau_D^{-1} \text{ sec}^{-1} . \qquad (31)$$

Using these values,

$$1 > \chi_F > 400 L_{48}^{7/4} N^{-1} \nu_{15}^{-5/2} \tau_D^{-5/2}$$

or (32)

$$N > 400 L_{48}^{7/4} \nu_{15}^{-5/2} \tau_D^{-5/2} .$$

This result is also much less restrictive than the corresponding value from Blandford and Rees (1978). The difference can be traced primarily to an order of magnitude discrepancy in the plasma frequency (i.e. two orders of magnitude in the electron density).

The limits on the free parameter N derived from the electron scattering and Faraday rotation conditions require that, in extreme sources (dimensionless parameters of one), there must be numerous reaccelerations of the electrons per crossing time. This recycling of electrons obviously eases problems with this model since it implies that fewer electrons are required within the volume to produce the

observed luminosity. We also note that as N increases, the fraction of electrons which are at thermal energies decreases; we have assumed that essentially all electrons are thermal ($N << t_{var}/t_{cyc}$). Since it is thermal electrons which cause difficulties for this model, rapid recycling ($N \sim t_{var}/t_{cyc}$) can essentially eliminate the electron scattering and Faraday rotation difficulties.

The presence of Faraday rotation in the optical/infrared regime would be very interesting since this condition appears most severe for this model of the central region. We have shown in § III and VI that differential rotation with wavelength is occasionally observed in highly polarized objects. It is impossible with the available data to determine whether this rotation is due to Faraday rotation; at least three very accurate position angle measurements over a wide baseline are required to test the predicted frequency dependence. The observed optical rotations could be caused by superposition of components.

Another predicition of this model is that as the radiation energy density increases relative to the magnetic energy density, inverse Compton losses would be more significant, and the ratio of X-ray to optical emission would increase. There is evidence (§IV.H) that the ratio of X-ray to optical luminosity is higher among the HPQs than normal QSOs; perhaps conditions in the central engines of HPQs are more extreme than in normal QSOs and inverse Compton losses are more significant.

Thus, we have shown that it is possible to circumvent the restrictions encountered in this isotropic optical/infrared synchrotron emission model by rapid recycling of electrons. This model, which is based on the variability time scale being representative of the source dimension, cannot be ruled out.

There are three other basic questions which must be addressed in this model The first question is what mechanism is responsible for depolarizing the central radiation in the normal low polarization QSOs. If there exists a central black hole in QSOs with a surrounding emission region producing radiation like that observed in HPQs and BL Lac objects, this radiation must be reprocessed into emission with low polarization, a harder energy distribution, and more moderate variability for most QSOs. An optically thick cloud of material surrounding the central region would damp the extreme variability of the central region both in the time scale and amplitude of variability. The fact that the polarization of normal QSOs is constant implies that the polarization is not simply diluted polarization from the central region; from this argument as well, the surrounding cloud must have a high optical depth. Katz (1976) has suggested a mechanism by which a hot thermal plasma will harden the optical spectrum by Compton upscattering. This or other mechanisms may be able to produce the harder spectra typically observed in low polarization QSOs. We would note that absorption of soft X-rays by the reprocessing cloud could also produce the correlation between polarization and the ratio of X-ray to optical emission.

One of the problems associated with this reprocessing cloud model is the correlation between the position angles of optical polarization and extended radio structure. As discussed above (§ VII.B.2), this correlation would be explained if the radio lobes were in the direction of the angular momentum vector of a disk, and the disk were slightly asymmetric and optically thin. The physical structure which defines the direction of radio structure may well be related to the reprocessing cloud. However, if such a cloud were optically thin, the central emission would be visible (contrary to observations). An optically thick disk could produce the small polarizations observed (if there is only slight asymmetry), but then the correlation of position angles requires that the radio structure be in directions perpendicular to the angular momentum vector of the disk. There is the possibility that the geometry of the depolarizing cloud is independent of the mechanism which produces the optical polarization and defines the direction of radio structure. For example, a symmetric optically thick reprocessing cloud could be interior to a larger optically thin scattering cloud, with the larger cloud determining the geometry for the optical polarization and radio structure.

Secondly, another question which confronts this model is why some QSO/BL Lac objects are "naked", while others have a reprocessing clouid around the central region. If the reprocessing material were associated with the emission line region of QSOs, one might expect only two classes of objects--the "naked" BL Lac objects where the

central emission is observed and there are no emission lines, and normal QSOs with reprocessed radiation and emission lines. However, the existence of the HPQs, with continuum properties of BL Lac objects and normal QSO emission line strengths, makes this an unsatisfactory explanation. Of course, the reprocessing cloud is not necessarily associated with the emission line region. (We note that spectropolarimetry of low polarization QSOs would indicate whether the reprocessing cloud is interior or exterior to the emission line region.) Thus, it appears that there are three physical components of the structure being discussed here--the central region (C), the reprocessing cloud (R), and the emission line region (E). These components can simply be postulated to exist in different combinations as follows: normal QSOs (C + R + E), HPQs (C + E), and BL Lac objects (C). It seems rather ad hoc to postulate that the type of object is determined by the presence or lack of these components; a more coherent picture of an evolutionary or environmental scheme must be developed.

Finally, the radio properties of HPQs and BL Lac objects, as compared to other QSOs, must also be considered in this model. Why are the highly polarized objects nearly all flat spectrum compact radio sources? Other properties of the highly polarized objects are that they seem more likely to exhibit superluminal variations or low frequency variability; these properties provide strong motivation for relativistic motion within the source (e.g. O'Dell 1978). Why are these radio properties associated with the highly polarized rapidly variable objects?

Motivated by the difficulties associated with this isotropic model for QSOs and BL Lac objects (e.g. the high luminosity and rapid variability, the extreme radio properties, the explanation of different types of surrounding material), alternative models have been proposed by a number of authors. We discuss some of these models below.

2. Anisotropic Models

There are two general anisotropic models which we will discuss. In both scenarios, the crucial feature is that the angle of orientation with which we view an object determines what type of object we observe. In the nonrelativistic anistropic model, there is no relativistic enhancement of the emission, but the orientation with respect to a disk structure determines the type of object observed. In the relativistic anisotropic model, there is a jet in which emitting material has a bulk relativistic motion; our orientation with respect to this jet determines the type of object. In the rapidly variable highly polarized objects, the jet is oriented close to our line-of-sight and the observed emission is characteristic of the emission from the jet.

a. Nonrelativistic Model. This model is similar in many respects to the isotropic theory. Its primary advantage is that it provides an explanation of why some objects are highly polarized while others are not. In this model (e.g. Blandford and Rees 1978), there is a disk-like cloud surrounding the central compact object. When viewed along the axis of this disk, the emission from the central

region is visible and dominates the spectrum. When viewed off axis, the central emission is obscured by the surrounding disk and the observed emission has been reprocessed in the disk. The anisotropy of the emission from the central region implies that the same type of physical structure appears very different from various viewing angles. The fraction of QSOs/BL Lac objects which are highly polarized is understood in terms of the opening angle of the disk structure along the axis.

The problems associated with the central region in the isotropic model (high luminosity, rapid variability, and high polarization) are still applicable to this model. A reprocessing cloud is also required as in the anisotropic model for the low polarization QSOs; this cloud is the disk structure in the nonrelativistic anistropic model. This model can explain the correlation between high optical polarization and compact radio structure if the direction of ejected radio-emitting material is along the axis of the disk.

Thus, the nonrelativistic anistropic model goes one step further than the isotropic model by attributing the difference between the three types of objects to the orientation with which we view the same basic physical structure. Environmental or evolutionary schemes are not required. This model also feasibly addresses the obvious connection between high optical polarization and compact radio sources. The primary difficulties of this model, which does not invoke relativistic enhancement, are the problems imposed by the variability

time scales (both at optical and low frequency radio wavelengths), and the association between high polarization and superluminal radio variations.

b. Relativistic Model. Relativistic jets have been proposed (e.g. Blandford and Rees 1978, Blandford and Königl 1979, Scheuer and Readhead 1979, Marscher 1980) to resolve some of the difficulties discussed above. Both optical and radio synchrotron emission is produced in this jet, which has a bulk relativistic motion (Lorentz factor Γ). This emission is anisotropic, being concentrated in a cone of half-angle Γ^{-1} in the direction of the jet. For the HPQs and BL Lac objects, we are presumably viewing the object within this cone and seeing relativistically enhanced unprocessed emission; in normal QSOs, we are viewing the source off-axis and do not see emission from this jet. Relativistic enhancement of the optical and radio emission greatly eases theoretical difficulties because the rest frame luminosity is lower ($\alpha\ \Gamma^{-2}$) and the rest frame variability time scale is longer ($\alpha\ \Gamma$).

This model has the advantages of the nonrelativistic model in that it invokes orientation as the determining factor of which type of object is observed and can explain the correlation between high optical polarization and compact radio sources. The primary further advantage of this model is that the theoretical difficulties imposed by the variability time scales and high luminosity (calculated by assuming isotropic emission) can be accommodated by adjusting the Lorentz factor of the bulk relativistic motion. While both the

mechanism and the energy requirements for accelerating the material to relativistic velocities must be considered, there is certainly evidence for relativistic motion in the superluminal radio sources such as 3C 279 and 3CR 345.

In evaluating this model, it is useful to consider two components of the optical emission from QSOs. First, there is the isotropic component which includes the emission lines and a relatively steady, low polarization, hard and "bumpy" continuum. The second component is the anisotropic continuum emission from the jet which is highly polarized, rapidly variable, and has a steep power law energy distribution. (The arguments to follow apply to the nonrelativistic model as well where the anisotropic component is the preferentially viewed central region.) There are several predictions of this model which can be examined in light of our results.

If the anisotropic component dominates the continuum of HPQs, there should be little wavelength dependence of the degree of polarization and the spectrum should be straight. Both of these characteristics are generally observed in HPQs. As the strength of the anisotropic component decreases relative to the isotropic component, one would expect the continuum to be concave and have lower polarization in the blue. While there are suggestions of this behavior in some HPQs (e.g. CTA 102), it is not common among HPQs. Thus, one would conclude from these arguments that the anisotropic component dominates the continua of HPQs.

However, there are two very significant results of this work which support the opposite conclusion: that the anistropic component does not dominate the emission of HPQs. First, this model states that we observe both emission components in the HPQs, while only the isotropic component is observed in normal QSOs. This implies that the HPQs should, at least statistically, be more luminous than normal QSOs. However, our results show no correlation between polarization and optical luminosity (§ IV.D). This suggests that the anisotropic component does not dominate the optical continuum of HPQs. Secondly, one would expect the equivalent width of emission lines to be systematically smaller for the HPQs. This also is not supported by our correlation analyses (§ IV.G). Thus, the conclusion drawn from both of these null correlations is that the anisotropic component does not dominate the continua of HPQs.

It is not clear in this model how to reconcile these apparently contradictory results. Certainly, a closer examination of the continuum energy distribution and polarization, and the emission line strengths is necessary to set more quantitative limits on the relative contribution of the anisotropic component in HPQs. A direct test of this model is a program of spectropolarimetric monitoring of individual HPQs. During bright phases, the continuum should be a straight power law which is highly polarized with little wavelength dependence and the equivalent width of emission lines should decrease. During faint phases, the spectrum should show structure similar to that of normal QSOs, a concave continuum, intermediate polarization which is

wavelength-dependent (higher in the red), and stronger (in equivalent width) emission lines. If these characteristics were observed, it would be strong evidence that there is an underlying "normal" QSO present in the HPQs.

An important question relevant to this discussion is whether the HPQs and BL Lac objects represent a continuous distribution of emission line strengths or are two distinct classes of objects. Perhaps BL Lac objects are those objects where the jet is viewed nearly on axis, while the HPQs are an intermediate class where the jet is viewed more obliquely (thus increasing the relative contribution of the isotropic component which includes emission lines). If the difference between normal QSOs, HPQs, and BL Lac objects is strictly the orientation with respect to the jet, there should be a continuous transition in the relative strength of the isotropic component (as reflected in the emission line equivalent width). Although a more quantitative analysis is required, it is not our impression that the emission line strengths of BL Lac objects and HPQs represent a continuous distribution of line-to-continuum ratios. The lines of BL Lac objects appear substantially weaker than those of HPQs. BL Lac objects may represent a different population of objects than the HPQs, although still being jets viewed on axis.

The radio properties of some of the previously known HPQs (e.g., 3C 379, 3CR 345, 3CR 454.3) are a primary motivation for this relativistic jet model. The full sample of HPQs now known provides a crucial test of this model. The presence of extended double radio

structure in HPQs (or BL Lac objects) would imply that the jet is not oriented along the line-of-sight and would be a strong argument against this model. As discussed in § IV.J, while most of the HPQs are compact radio sources, two definite HPQs (3CR 68.1 and PKS 2345-167) may have extended double structure. Three other possible HPQs are double-lobed. There is also at least one BL Lac object, MC 1400+162 (Baldwin et al. 1977, see also Angel and Stockman 1980), which has extended double structure. The HPQ 3CR 68.1 may be an unusual HPQ; photometric variability data are not available and the two polarization measurements show no variability within the errors. It is possible that this object is similar to OI 287, a constant HPQ. However, PKS 2345-167 has shown rapid photometric and polarimetric variability. Further polarization measurements of the double-lobed possible HPQs are also crucial to confirm whether or not they are highly polarized. Radio mapping of HPQs and BL Lac objects with high dynamic range to search for double-lobed structure is an important test of this model. Clear examples of well-separated double-lobed radio sources with the classical optical/infrared properties of HPQs and BL Lac objects would be a strong argument against the jet model.

We would note that Zamorani et al. (1980) have discussed the results of X-ray observations of QSOs in terms of the relativistic jet model. They find that the HPQs in their sample appear to be more luminous at X-ray wavelengths than other QSOs and suggest that this would be expected if the X-ray emission, as well as the radio emission, is relativistically enhanced. Our analysis (§ IV.H) also suggests that

the HPQs may be more luminous than other QSOs in the X-ray regime; however, this does not appear to be true at optical wavelengths (§ IV.D). If these correlations are supported by further observations, this would suggest that the X-ray emission is linked to the radio emission (e.g. the X-rays are produced by inverse Compton scattering of radio photons).

The properties of the low polarization QSOs must also be considered in the context of this model. The general spectroscopic characteristics of normal QSOs can be essentially defined as the properties of the isotropic component. However, the source of the weak constant polarization remains an interesting question. Perhaps the jet produces a net constant polarization when viewed off axis, which is then diluted by the isotropic component. If the polarization arises from synchrotron emission in the jet, the alignment of the position angles of optical polarization and radio structure would require that the average magnetic field in the optically-emitting region of the jet be perpendicular to the direction of the jet. As discussed in § VII.B.2, the problem of the wavelength dependence of polarization in normal QSOs remains in this scenario; if the diluted anisotropic component has a steeper energy distribution than the isotropic component, one would expect the polarization to increase in the red (contrary to observations).

3. Summary of Theoretical Models

The isotropic and anistropic models discussed here offer feasible explanations of the general characteristics of normal QSOs,

HPQs, and BL Lac objects. For clarity, we would like to summarize the theoretical implications of certain key observational results.

In general, the characteristics which we have established for the class of HPQs support the anisotropic model. The strongest support arises from the association between high polarization and extreme radio characteristics such as superluminal expansion and low frequency variability. These radio characteristics are very difficult to explain without invoking relativistic motion (or non-cosmological redshifts). Furthermore, the rapid optical/infrared variability and high luminosity of HPQs certainly strain (but do not exclude) isotropic models of the central emission region. The anisotropic model is also attractive in that it readily explains the existence of two distinct types of QSOs, and the lack of radio-quiet HPQs.

It is tempting in the anisotropic model to attribute the low polarization in normal QSOs to diluted polarized emission from the off-axis jet. It is conceivable that an off-axis jet would produce constant polarization (required by the lack of polarimetric variability in normal QSOs). Also, the alignment between the position angles of optical polarization and extended radio structure could be easily explained in this scenario. However, it is important to note that our results concerning the wavelength dependence of polarization in normal QSOs do not support this interpretation.

There are several crucial results of this work which appear to be inconsistent with each other in the context of the anisotropic model. First, the HPQs have statistically similar optical luminosities and

and emission line equivalent widths to normal QSOs. These results set upper limits to the relative contribution of the anisotropic component. On the other hand, arguments based on the wavelength dependence of polarization and smooth continua of HPQs set lower limits to the anisotropic contribution. The upper and lower limits estimated from these results appear to be contradictory. Further observations are necessary to carefully examine this possible contradication.

There are a number of questions concerning the characteristics of QSOs which are not readily answered in the isotropic model for the optical emission (e.g. the mechanism of rapid electron acceleration, the nature of the reprocessing cloud, the correlations between optical polarization and radio characteristics, the reasons for the presence or absence of the reprocessing cloud). However, these questions do not exclude the model. In fact, certain characteristics of the HPQs may be interpreted as supportive of this model. The similarity of optical luminosities and emission line equivalent widths between HPQs and normal QSOs would be expected in the isotropic model. It is also of interest to note that there appears to be a minimum time scale of optical variability ($\tau \sim 1$ day) among HPQs (and BL Lac objects). In the isotropic model, the minimum time scale is determined by the mass of the central black hole; if this mass were similar among various objects, a common time scale would be expected. In contrast, there is no reason to expect a common minimum time scale in the anisotropic model. Similarly, the fact that the constraints based on Eddington

luminosity arguments (i.e., $L < L_{EDD}$ and $c\tau > R_s$) are not severely exceeded may be interpreted as evidence that the mechanisms described are operating.

Although a great deal of our discussion has focused on the properties of highly polarized objects, our results concerning the polarization of normal QSOs are crucial to examining the structure of these objects (which represent the vast majority of QSOs). The lack of polarimetric variability in normal QSOs implies that the polarization is not diluted HPQ-type emission. The apparent increase in polarization at shorter wavelengths suggests that the polarization is due to dust scattering, rather than electron scattering or diluted synchrotron emission. Finally, the alignment between the position angles of optical polarization and extended radio structure demands that the inner structure of QSOs have a long memory, and it sets a key constraint on any model for the mechanism which produces the optical polarization and which defines the direction of radio lobes.

D. Suggestions for Future Observational Studies

The observations reported in this paper represent a major step forward in describing the polarimetric properties of QSOs and BL Lac objects. There are numerous further observations which are suggested in the course of the discussion of these results. We emphasize optical polarimetric projects which complement the present polarization survey or bear directly on tests of the models we have discussed.

The most pressing polarization survey of QSOs which should be made is to observe all QSOs in a well-defined complete flux-limited sample. The bright QSO survey is not a complete sample and it is difficult to draw firm conclusions regarding the correlations of polarization with either redshift or luminosity. Both optically-selected and radio-selected samples should be observed.

Whether or not a complete sample is observed, it is important to survey the polarization of additional radio-quiet QSOs. We have concluded that the radio-quiet QSOs are not highly polarized (with the exception of PHL 5200). However, this conclusion is based on a sample of 50 QSOs and, even though PHL 5200 is an atypical HPQ, it is highly polarized. It is clear from the present survey that high polarization is much more common among radio-loud QSOs. However, radio-quiet QSOs represent the majority of QSOs and the discovery of radio-quiet highly polarized (rapidly variable) QSOs would have a profound impact on theoretical models.

The present polarization survey also contains relatively few high redshift QSOs. Although there is no apparent correlation between polarization and redshift in our sample, high redshift QSOs are not well sampled. An excess or deficiency of HPQs at high redshifts would suggest that high polarization is associated with an evolutionary phase of the QSO or host environment.

The anisotropic models suggest another important polarization survey. For each BL Lac object or HPQ where we are viewing the object

on-axis, there should be a large number of objects of lower luminosity viewed off-axis. Elliptical galaxies have been detected around some BL Lac objects (e.g. Miller, French, and Hawley 1978). Perhaps misdirected BL Lac objects lie in the nuclei of other elliptical galaxies, but the nonthermal emission is dominated by normal starlgiht. An efficient probe to search for nonthermal nuclear emission is high accuracy polarimetric measurements of the nuclei of elliptical galaxies. Multi-aperture and wavelength dependence measurements are necessary to establish whether the origin of any polarization is non-thermal nuclear emission.

There are two follow-up projects which are crucial to determining the nature of polarization in normal QSOs. The first is to establish more accurate limits to the polarimetric variability. Our conclusion that the polarization is constant (within the accuracy of our observations) is a central point for several theoretical arguments. While we can rule out strong (HPQ-type) variability, more accurate measurements are required to determine the extent of mild variability. High-accuracy polarimetric monitoring, particularly through brightness variations, is necessary. Secondly, spectropolarimetry of the low polarization QSOs can distinguish between various origins of the weak polarization and can determine whether the reprocessing cloud is interior or exterior to the emission line region. By extending the measurements into the infrared, the origin of the break in the spectrum of many QSOs near 1 μm (e.g. Neugebauer et al. 1979) can also be explored. If the

infrared polarization were higher than the optical polarization, this may be evidence of a steep nonthermal component similar to that in the HPQs.

One major result of this work is that there is now a large sample of HPQs available for further observational tests. It is clear that observations of the class of HPQs are crucial to understanding the nature of both the QSO and BL Lac phenomena. We discuss below several projects related to the present sample of HPQs.

First, it is becoming increasingly evident that the emission properties of QSOs and BL Lac objects in all wavelength regimes are related to each other; a coherent picture which unifies results from all regions of the spectrum is crucial. Because of their variability, the HPQs are excellent candidates for simultaneous multi-frequency flux and polarization monitoring in order to determine the relationship between the emission in various regimes. The radio characteristics of the HPQs are of particular importance. The spectra of many of the new HPQs is not well known, particularly at high frequencies. Interferometer mapping at both VLA and VLBI resolutions is required. For example, if the radio structure of a classical HPQ were well-separated double lobes, this would be a strong argument against the relativistic jet model. Or perhaps, the position angle of any extended radio structure is aligned with a preferred position angle of optical polarization, such as is observed in the low polarization QSOs; this would suggest that a common mechanism is operating in both types of objects.

Further observations of the HPQs can be used to better test the correlations between polarization and other properties of HPQs. It is important to establish whether all HPQs are OVVS, either by archival plates or current photometric monitoring. A control sample of low polarization QSOs is also necessary to establish whether there is a one-to-one correspondence between high polarization and strong photometric variability. Spectrophotometry of the new HPQs would determine the extent to which the HPQs exhibit steep smooth optical/infrared continua. Perhaps more important, spectrophotometry can test two crucial null correlations--the lack of correlation between high polarization and emission line equivalent width or optical luminosity. The present results argue against the anisotropic model. However, as stated, the variability of the HPQs introduces uncertainty into our analyses. It is vital to measure the emission line equivalent widths over a range of brightness, and to compare the results to normal QSOs.

A powerful and direct test of the anisotropic model is spectropolarimetry of the HPQs. One obtains not only the brightness, energy distribution, and emission line strengths, but also the strength and wavelength dependence of the polarization. As discussed in § VII.C.2.b, if there is a typical normal QSO underlying the highly polarized component (as expected for the HPQs in the anisotropic model), there are specific predictions for the behavior of all these quantities as the continuum brightness varies. A program of spectropolarimetric monitoring of several HPQs, particularly during faint phases, can readily test the relativistic jet model.

REFERENCES

Allen, C. W., 1973, Astrophysical Quantities, London: Athlone Press.

Aller, H. D., and J. E. Ledden, 1978, Pittsburgh Conference on BL Lac Objects, ed. A. M. Wolfe, p. 53, Pittsburgh: Univ. of Pittsburgh.

Altschuler, D. R., and J. F. C. Wardle, 1976, Mem. R.A.S., 82, 1.

Anderson, B., and W. Donaldson, 1967, M.N.R.A.S., 137, 81.

Angel, J. R. P., 1969, Ap. J., 158, 219.

Angel, J. R. P. et al., 1978, Pittsburgh Conference on BL Lac Objects ed. A. M. Wolfe, p. 117, Pittsburgh: Univ. of Pittsburgh.

Angel, J. R. P., H. S. Stockman, N. J. Woölf, E. A. Beaver, and P. G. Martin, 1976, Ap. J. (Letters), 206, L5.

Angel, J. R. P., and J. D. Landstreet, 1970, Ap. J. (Letters), 160, L147.

Angel, J. R. P., and R. L. Moore, 1980, Ann. N.Y. Acad. Sci., 336, 55.

Angel, J. R. P., and H. S. Stockman, 1980, Ann. Rev. Astr. Ap., 8, 321.

Angione, R. J., 1971, A. J., 76, 25.

Angione, R. J., 1973, A. J., 78, 353.

Appenzeller, I., and W. A. Hiltner, 1967, Ap. J. (Letters), 149, L17.

Arp, H., W. L. W. Sargent, A. G. Willis, and C. E. Oosterbaan, 1979, Ap. J., 230, 68.

Baldwin, J. A., 1975, Ap. J., 201, 26.

Baldwin, J. A. et al., 1977, Ap. J., 215, 408.

Barbieri, C., and L. A. Erculiani, 1968, Mem. S.A.I., 39, 421.

Battistini, P., A. Bracessi, and L. Formiggini, 1974, Astr. Ap., 35, 93.

Bertaud, C., et al., 1969, Astr. Ap., 3, 436.

Blandford, R.D., and A. Königl, 1979, Ap. J., 232, 34.

Blandford, R. D., and M. J. Rees, 1978, Pittsburgh Conference on BL Lac Objects, ed. A. M. Wolfe, p. 328, Pittsburgh: Univ. of Pittsburgh.

Boksenberg, A., R. F. Carswell, and J. B. Oke, 1976, Ap. J. (Letters), 206, L121.

Bond, H. E., R. G. Kron, and H. Spinrad, 1977, Ap. J., 213, 1.

Burbidge, G. R., A. H. Crowne, and H. E. Smith, 1977, Ap. J. Suppl., 33, 113.

Burbidge, G. R., T. W. Jones, and S. L. O'Dell, 1974, Ap. J., 193, 43.

Burstein, D., and C. Heiles, 1978, Ap. J., 225, 40.

Cohen, M. H. et al., 1977, Nature, 268, 405.

Condon, J. J., 1978, Pittsburgh Conference on BL Lac Objects, ed. A. M. Wolfe, p. 21, Pittsburgh: Univ. of Pittsburgh.

Condon, J. J., J. E. Ledden, S. L. O'Dell, and B. Dennison, 1979, A.J., 84, 1.

Conway, R. G., B. J. Burn, and J. P. Vallee, 1977, Astr. Ap. Supl., 27, 155.

Davis, R. J., D. Stannard, and R. G. Conway, 1977, Nature, 267, 596.

Eachus, L. J., and W. Liller, 1975, Ap. J. (Letters), 200, L61.

Fanti, C., R. Fanti, L. Formiggini, C. Lari and L. Padrielli, 1977, Astr. Ap. Suppl., 28, 351.

Folsom, G. H., A. G. Smith, R. L. Hackney, K. R. Hackney, and R. J. Leacock, 1971, Ap. J. (Letters), 169, L131.

Gaskell, C. M., 1978, Bull. A.A.S., 10, 662.

Gopal-Krishna, and R. A. Sramek, 1980, Astr. Ap., in press.

Gottlieb, E. W., and W. Liller, 1976, IAU Circ. No. 2939.

Gottlieb, E. W., and W. Liller, 1978, Ap. J. (Letters), 222, L1.

Grandi, S., and W. G. Tifft, 1974, Publ.A.S.P., 86, 873.

Green, R. F., 1976, Publ. A.S.P., 88, 665.

Hawley, S. A., J. S. Miller, and R. J. Weymann, 1977, Ap. J., 213, 632.

Hewitt, A., and G. Burbidge, 1980, Ap. J. Suppl., in press.

Hiltner, W. A., 1956, Ap. J. Suppl., 2, No. 24, 389.

Hogg, D. E., 1969, Ap. J., 155, 1099.

Holmberg, E. B., 1974, Astr. Ap., 35, 121.

Hunstead, R. W., 1972, Astr. Letters, 12, 193.

Jackisch, G., 1971, Astr. Nach., 292, 271.

Jauncey, D. L., A. E. Wright, B. A. Peterson, and J. J. Condon, 1978, Ap. J. (Letters), 221, L109.

Jones, T. W., L. Rudnick, F. N. Owen, J. J. Puschell, D. J. Ennis, and M. W. Werner, 1980, preprint.

Katz, J. I., 1976, Ap. J., 206, 910.

Kikuchi, S., Y. Mikami, M. Konno, and M. Inoue, 1976, Publ. A.S.J., 28, 117.

Kinman, T. D., 1967, Ap. J. (Letters), 148, L53.

Kinman, T. D., 1976, Ap. J., 205, 1.

Kinman, T. D., 1977, Nature, 267, 798.

Kinman, T. D., J. Bolton, R. Clark, and A. Sandage, 1967, Ap. J., 147, 848.

Kinman, T. D., E. Lamla, and C. A. Wirtanen, 1966, Ap. J., 146, 964.

Kinman, T. D., E. Lamla, T. Ciurla, E. Harlan, and C. A. Wirtanen, 1968, Ap. J., 152, 357.

Knacke, R. F., R. W. Capps, and M. Johns, 1976, Ap. J. (Letters), 210, L69.

Knacke, R. F., R. W. Capps and M. Johns, 1979, Nature, 280, 215.

Ku, W. H.-M., and D. J. Helfand, 1980, preprint.

Landstreet, J. D., and J. R. P. Angel, 1972; Ap. J. (Letters), 174, L127.

Liller, W., 1969, Ap. J., 155, 1113.

Liller, M. H., and W. Liller, 1975, Ap. J. (Letters), 199, L133.

Lindgren, B. W., C. W. McElrath, and D. A. Berry, 1978, Introduction to Probability and Statistics, New York: Macmillan.

Lü, P. K., 1972, A. J., 77, 829.

Lucy, L. B., 1974, A. J., 79, 745.

Lynden-Bell, D., 1978, Phys. Scripta, 17, 185.

Lynds, R., and D. Wills, 1972, Ap. J., 172, 531.

MacDonald, G. H., and G. K. Miley, 1971, Ap. J., 164, 23.

Mackay, C. D., 1969, M.N.R.A.S., 145, 31.

Markannen, T., 1978, Astr. Ap., 74, 201.

Marscher, A. P., 1980, Ap. J., 235, 386.

Matthews, T. A., and A. R. Sandage, 1963, Ap. J., 138, 30.

Maza, J., 1979, Polarization of Seyfert Galaxies and Related Objects, Ph.D. thesis, Univ. of Toronto.

McGimsey, B. Q., A. G. Smith, R. L. Scott, R. J. Leacock, P. L. Edwards, R. L. Hackney, and K. R. Hackney, 1975, A. J., 80, 895.

Miley, G. K., and A. P. Hartsuijker, 1978, Astr. Ap. Suppl., 34, 129.

Miller, H. R., 1977, Astr. Ap., 54, 537.

Miller, J. S., and H. B. French, 1978, Pittsburgh Conference on BL Lac Objects, ed. A. M. Wolfe, p. 228, Pittsburgh: Univ. of Pittsburgh.

Miller, J. S., H. B. French, and S. A. Hawley, 1978, Pittsburgh Conference on BL Lac Objects, ed. A. M. Wolfe, p. 176, Pittsburgh: Univ. of Pittsburgh.

Moore, R. L., 1981, in prep.

Moore, R. L. et al., 1980, Ap. J., 235, 717.

Moore, R. L. et al., 1981, in prep.

Moore, R. L., and H. S. Stockman, 1981, Ap. J., scheduled Jan 1 issue.

Moore, R. L., J. F. C. Wardle, and J. R. P. Angel, 1981, in prep.

Netzer, H., B. J. Wills, A. K. Uomoto, P. M. Rybski, and R. G. Tull, 1979, Ap. J. (Letters), 232, L155.

Neugebauer, G., J. B. Oke, E. E. Becklin, and K. Matthews, 1979, Ap. J., 230, 79.

Nordsieck, K. H., 1976, Ap. J., 209, 653.

O'Dell, S. L., J. J. Puschell, and W. A. Stein, 1977, Ap. J., 213, 351.

O'Dell, S. L., et al., 1978, Ap. J., 224, 22.

Oke, J. B., 1966, Ap. J., 145, 668.

Oke, J. B., 1967, Ap. J., 147, 901.

Oke, J. B., G. Neugebauer, and E. E. Becklin, 1970, Ap. J., 159, 341.

Owen, F. N., R. W. Porcas, S. L. Mufson, and T. J. Moffett, 1978, A. J., 83, 685.

Pacholczyk, A. G., 1970, Radio Astrophysics, San Francisco: Freeman.

Peach, J. V., 1969, Nature, 222, 439.

Penston, M. V., and R. D. Cannon, 1970, R.O.B., 159, 85.

Pollock, J. T., A. J. Pica, A. G. Smith, R. J. Leacock, P. L. Edwards, R. L. Scott, 1979, A.J., 84, 1658.

Puschell, J. J., and W. A. Stein, 1980, Ap. J., 237, 331.

Puschell, J. J., et al., 1979, Ap. J. (Letters), 227, L11.

Racine, R., 1970, Ap. J., 158, L99.

Richstone, D. O., and M. Schmidt, 1980, Ap. J., 235, 361.

Rieke, G. H., G. L. Grasdalen, T. D. Kinman, P. Hintzen, B. J. Wills, and D. Wills, 1976, Nature, 260, 754.

Rieke, G. H., M. J. Lebofsky, J. C. Kemp, G. V. Coyne, and S. Tapia, 1977, Ap. J. (Letters), 218, L37.

Rieke, G. H., and M. J. Lebofsky, 1979, Ann. Rev. Astr. Ap., 17, 477.

Sandage, A., 1966, Ap. J. (Letters), 144, 1234.

Sandage, A., 1973, Ap. J., 183, 711.

Scheuer, P. A. G., and A. C. S. Readhead, 1979, Nature, 277, 182.

Scheuer, P. A. G., and P. J. S. Williams, 1968, Ann. Rev. Astr. Ap., 6, 321.

Schmidt, M., 1968, Ap. J., 151, 393.

Schmidt, M., 1976, Ap. J. (Letters), 209, L55.

Scott, R. L., et al., 1976, A. J., 81, 7.

Shields, G., 1977, Astr. Letters, 18, 119.

Smith, H. E., 1978, Pittsburgh Conference on BL Lac Objects, ed. A. M. Wolfe, p. 211, Pittsburgh: Univ. of Pittsburgh.

Smith, H. E., et al. 1977, Ap. J., 215, 427.

Smith, H. E., and H. Spinrad, 1980, Ap. J., 236, 419.

Smith, M. G.,and A. E. Wright, 1980, preprint.

Sramek, R. A., and D. W. Weedman, 1978, Ap. J., 221, 468.

Sramek, R. A., and D. W. Weedman, 1980, Ap. J., 238, 435.

Stein, W. A., 1978, Pittsburgh Conference on BL Lac Objects, ed. A. M. Wolfe, p. 1, Pittsburgh: Univ. of Pittsburgh.

Stein, W. A., S. L. O'Dell, and P. A. Strittmatter, 1976, Ann. Rev. Astr. Ap., 14, 173.

Stockman, H. S., 1978, Pittsburgh Conference on BL Lac Objects, ed. A. M. Wolfe, p. 149, Pittsburgh: Univ. of Pittsburgh.

Stockman, H. S., and J. R. P. Angel, 1978, Ap. J. (Letters), 220, L67.

Stockman, H. S., J. R. P. Angel, and E. A. Beaver, 1976, Bull. A.A.S., 8, 495.

Stockman, H. S., J. R. P. Angel, and R. G. Hier, 1980, Ap. J., in press.

Stockman, H. S., J. R. P. Angel, and G. K. Miley, 1979, Ap. J. (Letters), 227, L55.

Strittmatter, P. A., K. Serkowski, R. Carswell, W. A. Stein, K. M. Merrill, and E. M. Burbidge, 1972, Ap. J. (Letters), 175, L7.

Tananbaum, H., et al., 1979, Ap. J. (Letters), 234. L9.

Tapia, S., E. R. Craine, M. R. Gearhart, E. Pacht, and J. Kraus, 1977, Ap. J. (Letters), 215. L71.

Thompson, I., J. D. Landstreet, H. S. Stockman, J. R. P. Angel and E. A. Beaver, 1980, M.N.R.A.S., 192, 53.

Tritton, K. P., and R. A. Selmes, 1971, M. N.R.A.S., 153, 453.

Usher, P. D., 1975, Ap. J. (Letters), 198, L57.

Visvanathan, N., 1968, Ap. J. (Letters), 153, L19.

Visvanathan, N., 1969, Ap. J. (Letters), 155, L133.

Visvanathan, N., 1973, Ap. J., 179, 1.

Wampler, E. J., 1967a, Publ. A.S.P., 79, 210.

Wampler, E. J., 1967b, Ap. J., 147, 1.

Wampler, E. J., 1968, Ap. J., 153, 19.

Wampler, E. J., and J. B. Oke, 1967, Ap. J., 148, 695.

Wardle, J. F. C., 1977, Nature, 269, 563.

Wardle, J. F. C., 1978, Pittsburgh Conference on BL Lac Objects, ed. A. M. Wolfe, p. 39, Pittsburgh: Univ. of Pittsburgh.

Wardle, J. F. C. and G. K. Miley, 1974, Astr. Ap., 30, 305.

Weistrop, D., 1973a, Nature Phys. Sci., 241, 157.

Weistrop, D., 1973b, Astr. Ap., 23, 215.

Weistrop, D., and S. Goldsmith, 1973, Astr. Letters, 14, 225.

Whiteoak, J. B., 1966, Zs. f. Ap., 64, 181.

Wilkinson, P. N., P. J. Richards, and T. N. Bowden, 1974, M.N.R.A.S., 168, 515.

Wolfe, A. M., 1978, ed. Pittsburgh Conference on BL Lac Objects, Pittsburgh: Univ. of Pittsburgh.

Zamorani, G., et al., 1980, preprint.

Zotov, N.V., and S. Tapia, 1979, Ap. J. (Letters), 229, L5.